Physiology and Evolution of Methylamine Metabolism across Methylobacterium extorquens strains

Physiology and evolution of methylamine metabolism across *Methylobacterium extorquens* strains

A dissertation presented

by

Dipti Dinkar Nayak

to

The Department of Organismic and Evolutionary Biology

in partial fulfillment of the requirements

for the degree of

Doctor of Philosophy

in the subject of

Biology

Harvard University

Cambridge, Massachusetts

August 2014

Dissertation Advisor: Professor Christopher J. Marx Dipti Dinkar Nayak

Physiology and evolution of methylamine metabolism across *Methylobacterium extorquens* strains

Abstract

The interplay between physiology and evolution in microorganisms is extremely relevant from the stand-point of human health, the environment, and biotechnology; yet microbial physiology and microbial evolution largely continue to grow as disjoint fields of research. The goal of this dissertation was to use experimental evolution to study methylamine metabolism in *Methylobacterium extorquens* species. Methylotrophs like the *M. extorquens* species grow on reduced single carbon compounds and are the largest biological sink for methane. *M. extorquens* AM1, the model system for the study of aerobic methylotrophy, has an unstable genome and severe growth defects as a result of laboratory domestication. First, I describe the genomic, genetic, and phenotypic characterization of a new model system for the study of aerobic methylotrophy: *M. extorquens* PA1. This strain has a stable genome, was recently isolated from a known ecological niche, and is closely related to AM1. Whereas PA1 grew 10-50% faster than AM1on most substrates, it was five-fold slower on methylamine. The PA1 genome encodes a poorly characterized but ecologically relevant *N*-methylglutamate pathway whereas AM1 also encodes the well-characterized methylamine dehydrogenase for methylamine oxidation. I characterized the genetics of the *N*-methylglutamate pathway in PA1 to resolve a linear topology that requires the formation of two, unique amino acid intermediates during methylamine oxidation. I also showed that methylamine metabolism via the *N*-methylglutamate pathway routes carbon flux in a manner completely different from previous instances of methylotrophy. Next, I evolved replicate populations of PA1 on methylamine for 150 generations. Based on the empirical heuristic that the initial fitness is negatively correlated to the rate of adaptation, it was expected that the fitness gain would be rapid. However, methylamine fitness did not improve at all; adaptive constraints led to evolutionary recalcitrance despite low initial fitness. These adaptive constraints were alleviated by the horizontal gene transfer of an alternate, functionally degenerate metabolic module. Finally, I uncovered ecologically distinct roles for two functionally

degenerate routes for methylamine oxidation pathways in the AM1 genome; the highly expressed, efficient route is primarily used for growth and the tightly regulated, energetically expensive route is used for assimilating nitrogen in methylamine-limiting environments.

Table of Contents

Acknowledgements

This dissertation, all the steps leading up to it and beyond, would not be possible without the support of friends, mentors, and family. First, I owe a debt of gratitude to Chris for welcoming me into his research group; for giving me the intellectual freedom to pursue a completely new research thread; and for the words of encouragement at opportune moments. Chris' razor sharp intellect and scientific creativity combined with an addictive enthusiasm for research is awe-inspiring. He has been an outstanding mentor over the years and it was a joy to be a graduate student in the Marx lab. I would also like to specifically thank a few members of the Marx lab; Deepa Agashe and Will Harcombe for long and meandering yet extremely illuminating scientific discussions and Sean Carroll for being a sounding board on all matters C_1 related and for working as a partner-in-crime on the betaine project. A big thank you to everyone else in the Marx lab for reading manuscripts, patiently sitting through and critiquing practice talks, sharing technical knowhow, and being awesome!

Colleen Cavanaugh deserves a special mention. The first time I met her, we spent three hours animatedly discussing the wonderful, curious world of methylotrophy. I admire her passion for microbiology and really appreciate the regular doses of positive reinforcement from her end; those kind words have meant a lot. I am grateful to all the faculty members (Martin Polz, Graham Walker, Peter Girguis, and especially Michael Desai) who have taken the time to read this dissertation, my thesis proposal, and served as a part of my thesis committee over the last few years; their feedback, support and encouragement was invaluable. I'd also like to thank my collaborators, Yousif Shamoo and Milya Davileva at Rice University and Marty Ytreberg at University of Idaho for their time and energy; I've learnt a lot from these collaborations. A big thank you to Chris Preheim for running the OEB graduate program like a well-oiled machine, as well as to Nikki Hughes, Krista Carmichael, and Becky Chetham for administrative support through the years.

Heather, Roxie, Kiana, Liz, Didem and Laura, having all of you around made grad school so much fun. Thank you all being such wonderfully quirky people and for the support and laughter through these past five years. Aditi and Nithya, thank you for your friendship through the years, and for travelling far and wide to spend time together. I cannot even fathom what I'd be doing now if wasn't for the sage advice that the two of you have given me over the last fifteen years. I am grateful to have extremely kind and encouraging in-laws, and a wonderful, caring family. I will always be indebted to my maternal grandparents for being such an integral part of my childhood and for defying gender stereotypes; she is one of the most progressive, fearless, and independent women I've met and he is the most gentle, patient soul I know. I am so glad to have Mahesh as a sibling; I've always admired his quick witted humor and cheerful disposition and am extremely proud of his accomplishments. My husband Aditya is an inspiration. It has and will always be reassuring to have his dazzling intellect, pragmatic perspective, distinct sense of humor, and unconditional love at my side; I, too, look forward to our journey together. Finally, I am so fortunate to have two brilliant, forward-thinking individuals, Suman and Dinkar, as parents; they are the sole reason I have made it this far.

Chapter 1

Introduction

"*Most basically, natural selection converts accident into apparent design, randomness into organized pattern"*- Julian Huxley, Evolution in Action.

The interplay between physiology and evolution is, arguably, the single-most important factor that governs the diverse metabolic and other physiological features observed in microorganisms (Falkowski et al. 2008; T. Ferenci 2007). More than a century of research in microbial physiology has resulted in sophisticated tools for the genetic manipulation of various bacteria (Holloway et al,. 1979; Simon et al. 1983; Sonenshein et al. 1993; Hopwood 1999; Marx and Lidstrom 2002) and archaea (Pritchett et al. 2004; Allers and Mevarech 2005; Wagner et al. 2009); and the discovery and characterization of thousands of enzymes and proteins involved in metabolism, transport, cell division, virulence, and many other traits (Tatusov et al. 1997; Marakova et al. 1999; Bateman et al. 2000; Haft et al. 2003). However, one-third of the genes in *E. coli* K12 - conceivably, the best characterized bacterial strain - remain functionally unannotated (Vogel and Chothia 2006); the evolutionary processes and constraints that have shaped many of the functionally annotated traits are also largely unknown.

Microbial evolution is a relatively new field; the advent of experimental evolution (Elena and Lenski 2003) i.e. evolution of microorganisms in a controlled laboratory environment has spurred a 'post-modern synthesis' in the field of evolutionary biology in the last couple of decades (Lenski et al. 1991; Rainey and Travisano 1998; Kassen 2002; Perron et al. 2006; Mahajan et al. 2006; Lee et al. 2009; Lang et al. 2013). Laboratory evolution with microorganisms has opened up experimental avenues to rigorously test concepts in evolution and population genetics like the DFE or the Distribution of Fitness Effects (Frenkel et al. 2014; Delaney et al. in prep), the prevalence of epistasis or non-additive interactions (Chou et al. 2011; Khan et al. 2011; Kryazhimskiy et al. 2014), the role of mutation-selection balance (Taddei et al. 1997; Elena and Lenski 1997) i.e. clonal interference (Miralles et al. 1999; Kao and Sherlock 2008; Lang et al. 2013) in evolution of asexual populations; concepts which were otherwise restricted to theoretical speculation and observational studies (S. Wright 1932; R. A. Fisher 1958; S. J. Gould 1977; M. Kimura 1977; Gould and Lewontin 1979; Fay et al. 2002). Over the course of experimental evolution,

adaptive mutations that rise and fix in populations often point to novel aspects of physiology (Beaumont et al. 2009; Ratcliff et al. 2012). Often, these adaptive mutations are in conserved genes of unknown/hypothetical function (Chou et al. 2009; Michener et al. in submission; Nayak et al. in prep) and provide an ideal framework to probe the function of these proteins. However, apart from their impact on fitness and growth rate in the selective environment, the physiological underpinnings of these adaptive mutations are rarely explored. On the whole, despite being fundamentally interconnected, microbial physiology and microbial evolution continue to grow as disjoint fields.

The overarching goal of various chapters in this thesis was to create an evolutionary framework to probe microbial physiology. The primary mechanism for addressing this goal was to develop and implement experimental evolution as a forward genetic screen.

In terms its application as a forward genetic screen and throughout this thesis, the phrase 'experimental evolution' explicitly refers to the propagation of replicate populations in batch culture. Each population is initiated by a distinct colony of an isogenic ancestor and propagated by serial transfer in well-defined minimal media (Lenski et al. 1991). Under such conditions, selection primarily acts on growth rate; mutants that grow faster have higher competitive fitness (Lenski et al. 1991; Lee et al. 2009). The physiological basis of adaptation can be uncovered by sequencing the genome of the evolved isolates (Barrick et al. 2009). Experimental evolution has several advantages over traditional genetic screens like transposon- or chemical induced mutagenesis as listed below (also reviewed in Marx, 2011):

- Experimental evolution does not require the organism to be genetically tractable since mutations are uncovered by sequencing the genome. Therefore, experimental evolution can be used as a genetic screen in a much wider breadth of microorganisms.
- Experimental evolution can screen the entire mutational spectrum at once. Separate experiments do not need to be designed to separately screen for null mutations and gain-of-function mutations that give rise to a particular phenotype of interest.

- Experimental evolution is not restricted to non-essential genes (Barrick et al. 2009) unlike transposon mutagenesis; the screen most commonly used by bacterial geneticists.
- Unlike chemical mutagenesis, experimental evolution does have any inherently strong mutational bias apart from that of the organism itself. Therefore, adaptive mutations that arise in experimentally evolved populations are more likely to be observed in Nature.
- Multiple generations can amplify the effect of smaller fitness improvement. In contrast, traditional genetic screens require careful screening of tens of thousands of individual colonies. Multiple genotypes with a particular phenotype of interest can also be uncovered from replicate populations.
- Beneficial, but extremely rare, mutations are more likely to be observed due to the prolonged duration of the experiment (Blount et al. 2012).
- If a particular phenotype of interest requires multiple mutations simultaneously, such mutants are more likely to be enriched by experimental evolution as well (Lee and Palssøn 2010).
- Experimental evolution can be used to screen for genes which impact growth in a complex or variable environment; for instance, during growth on multiple substrates simultaneously or switching between substrates.

The use of experimental evolution as a genetic screen does have a few drawbacks as well. It is difficult to screen for mutations with a deleterious impact on an organismal phenotype using experimental evolution. Clonal interference or competition between beneficial mutations that simultaneously arise in different individuals (Lang et al. 2013; Kao and Sherlock 2008) eliminates a large fraction of genotypes with a desired phenotype of interest (Lee and Marx 2013). However, these genotypes can be uncovered by meta-sequencing the mixed population at different time points over the course of evolution (Kao and Sherlock 2008; Chubiz et al. 2012; Herron and Doebeli 2013). Also, experimental evolution selects for the 'fittest' or the fastest growing genotypes; since enrichment is directly tied to growth, genotypes with growth defects relative to others that also give rise to a phenotype of interest will not be detected. But, given the novel paradigm experimental evolution brings to microbial physiology- the ability to investigate

mutations that improve rather the deteriorate growth in a given environment- it is surely a promising technique for studying microbial physiology in this genome sequencing era.

Over the course of this thesis, experimental evolution was implemented as a genetic screen to study methylamine metabolism in methylotrophs that belong to the *Methylobacterium extorquens* species. Methylotrophs are a polyphyletic group (Boucher et al. 2003) of microorganisms that can grow on reduced single carbon (C_1) compounds, like methanol and methylamine, as the sole source of carbon and energy (C. Anthony 1982). Methylotrophs are abundant in many ecosystems (Chistoserdova 2011; Swan et al. 2011) and are the largest biological sink for methane on our planet (Oremland et al. 1982). Due to the ease of isolation and cultivation, fast and reproducible growth under laboratory conditions, the Alphaproteobacterium, *Methylobacterium extorquens* AM1 (referred to as AM1 henceforth) has emerged as the model system for the study of aerobic methylotrophy in the last few decades (Chistoserdova et al. 2003). By now, almost all methylotrophy-specific metabolic reactions in AM1 are well-characterized (Chistoserdova et al. 2003; Chistoserdova, 2009) (Figure 1.1). C_1 compounds like methanol are oxidized by a dedicated periplasmic dehydrogenase to produce free formaldehyde (Nunn and Lidstrom 1986; Chistoserdov et al. 1991). Free formaldehyde enters the cytoplasmic space where it gets oxidized further to formate by a tetrahydromethanopterin (H_4MPT) –dependent formaldehyde oxidation pathway (Marx et al. 2003(H_4MPT); Chistoserdova et al. 2003). Formate serves as the branch point for metabolism (Crowther et al. 2008; Marx et al. 2005): a small fraction gets oxidized further to CO_2 via a panel of formate dehydrogenases (Chistoserdova et al. 2007) and the rest gets assimilated (along with one-third of the CO_2 produced) to components of biomass via the tetrahydrofolate (H_4F) dependent C_1 transfer pathway (E. H. Maden 2000; Marx et al. 2003 (FtfL); Chistoserdova et al. 2003), the serine cycle (Chistoserdova and Lidstrom 1994; Chistoserdova et al. 2003) and the ethyl-malonyl CoA pathway (Peyraud et al. 2009).

Metagenomes and metatranscriptomes form aquatic ecosystems (Chistoserdova 2011; Swan et al. 2011), suggest that environmentally abundant, ecologically relevant, methylotrophs use completely

different metabolic modules for methylotrophy than those characterized in AM1. In various chapters of this thesis, I have used a combination of traditional genetics and experimental evolution to uncover the physiology and evolution of a poorly characterized, environmentally relevant module used for methylamine oxidation in naturally occurring methylotrophs. In the first two chapters, I describe the characterization of a new methylotroph that was recently isolated from the environment (*Methylobacterium extorquens* PA1) and a new pathway for methylamine utilization (*N*-methylglutamate pathway). Subsequent chapters use experimental evolution to uncover that the rate of adaptation in strains constrained by the *N*-methylglutamate pathway for methylamine oxidation is not dependent on the initial fitness but on the genotype and establish ecologically distinct roles for functionally degenerate routes for methylamine oxidation (including *N*-methylglutamate pathway and the well-established methylamine dehydrogeanse).

M. extorquens PA1 as an alternate model system for experimental evolution

Despite being extremely well-characterized from the perspective of methylotrophy, the genome of AM1 posed a few major challenges for developing and implementing experimental evolution as a forward genetic screen. Five replicons of varying sizes (Vuilleumier et al. 2009; Marx et al. 2012) and 174 partial or complete insertion sequence (IS) elements across 39 IS families (Vuilleumier et al. 2009; Robinson et al. 2012) in the AM1 genome contribute to significant genomic plasticity and drastically increase the rate of spurious recombination during reverse genetic manipulations (Skovran et al. 2011) and lead to large, beneficial deletions during experimental evolution (Lee and Marx 2012). These deletions are not physiologically pertinent to the selective environment and confound the use of experimental evolution as a genetic screen. Also, recent work (Carroll et al. 2014) has demonstrated that the current laboratory strain of AM1, which has been 'domesticated' since the 1950s, grows up to 25% slower than the 'archival' version; aspects of physiology in AM1 may no longer be hold for natural methylotrophs. Therefore, we sought to find and characterize another strain of the *M. extorquens* species that is more ecologically relevant and amenable to using experimental evolution as a forward genetic

screen. In the second chapter of this thesis, we describe the genomic, genetic, and phenotypic characterization of *M. extorquens* PA1 (referred to as PA1 henceforth), which was recently isolated from the phyllosphere of *Arabidopsis* (Knief et al. 2010), and propose the use of this strain as a new/alternate model system for the study of aerobic methylotrophy. PA1 is 100% identical to AM1 at the 16S rRNA level (Marx et al. 2012, Knief et al. 2010) but has a single chromosome with only 20 intact IS elements in its genome. By constructing knockout mutants in methylotrophy-specific modules, quantifying their phenotype on a large suite of C_1- and multi-C compounds, and comparing it to those established for AM1, we showed that, with a few exceptions (which will be discussed subsequently), the large body of knowledge in AM1 can be transferred to PA1 which, by virtue of a more streamlined and stable genome, is better suited for experimental evolution.

Physiological characterization of the *N*-methylglutamate pathway for methylamine oxidation

The most striking difference between strains AM1 and PA1, in terms of methylotrophic metabolism, is that AM1 has a doubling time (t_D) of 3-4 hours (Delaney et al. 2013) while PA1has a t_D of ~18 hours during growth on methylamine. On other methylotrophic substrates, the growth rates of these strains differ by 10-15%. The stark contrast in methylamine growth rates can be attributed to the metabolic module used for the primary oxidation of methylamine in each strain. Whereas PA1only possesses the poorly characterized *N*-methylglutamate (NMG) pathway (Shaw et al,. 1966; Latypova et al. 2010; Martinez-Gomez et al. 2013; Gruffaz et al. 2014) for methylamine oxidation, AM1 also encodes the well-characterized methylamine dehydrogenase (MaDH)(Chistoserdov et al. 1991). Methylamine plays an important role in the global nitrogen and carbon budget (Oremland et al. 1982; Ge et al. 2011) and recent metagenomic studies (Chistoserdova, 2011) have revealed the import and abundance of the NMG pathway in aquatic environments.

In the third chapter of this thesis, I characterized the genetics and physiology of the NMG pathway for methylamine oxidation in PA1. By coupling traditional genetics (Marx 2008) with

quantitative phenotypic assays using an extremely accurate growth measurement platform (Delaney et al. 2013) we showed that the NMG pathway has a linear topology rather than the branched topology proposed previously (Latypova et al. 2010). So far, all C_1 substrates tested in *Methylobacterium* species, absolutely require the H_4F-dependent C_1 transfer pathway for assimilation or dissimilation (Vannelli et al. 1999; Marx et al. 2003 (FtFL); Marx et al. 2005; Crowther et al. 2008). The H_4F-dependent C_1 transfer pathway was not essential and the C_1 flux flows in a completely novel manner during methylamine growth using the NMG pathway; C_1 units are assimilated directly into the serine cycle and dissimilated directly by the H_4MPT pathway and the branch point of metabolism shifts to either formaldehyde or methylene tetrahydrofolate ($CH_2=H_4F$). Apart from the physiological details of the NMG pathway, the results in this chapter also suggest that metabolic modules in a particular cell can be used in distinct configurations to route carbon flux in different ways depending upon the growth substrate in question.

The role of Horizontal Gene Transfer (HGT) in adaptive evolution of methylotrophs

The distribution of methylamine fitness across the *M. extorquens* species is approximately bimodal; strains that encode the methylamine dehydrogeanse are at least five fold more fit than strains that use the NMG pathway for methylamine oxidation. Laboratory evolution studies the span a large cross section of organisms and environments have established an empirical rule-of-thumb in microbial evolution; the rate of adaptation is negatively correlated with the initial fitness of an organism (Bennett et al. 1992; Travisano et al. 1995; Lee et al. 2009; Lee and Marx 2013) and mostly independent of the initial genotype (Kryazhimskiy et al. 2014). We evolved three replicate populations of *M. extorquens* PA1 on methylamine as the sole carbon and energy source; given the distance from the fitness optima, it was expected that the fitness gain on methylamine would be rapid.

In the fourth chapter, we describe the unexpected outcome of methylamine evolution in PA1. Despite 150 generations of evolution and adaptation, as indicated by genetic parallelism (Woods et al. 2006) across replicate lines, the growth rate as well as the competitive fitness on methylamine for any of

the evolved populations or isolates was not significantly different than that of the founding ancestor. This result directly counters the recently proposed concept (Kryazhimskiy et al. 2014) that the rate of adaption is primarily dependent on the initial fitness of an organism in an environment; in a novel or sub-optimal environment, physiology can pose severe constraints that slow down the rate of adaptation independent of the initial fitness. In parallel, we also simulated a horizontal gene transfer (HGT) by transforming a low copy plasmid with the *mau* gene cluster, encoding methylamine dehydrogeanse and ancillary proteins (Chistoserdov et al. 1991), in the PA1 genome. The growth rate and competitive fitness of the resulting transconjugant on methylamine was significantly greater than PA1 and comparable to or even greater than AM1. This result alluded to the important role of HGT as an evolutionary force in nature; when a novel environment poses constraints that lead to 'evolutionary recalcitrance', HGT can speed up the rate of adaptation drastically. To the best of our knowledge, this is the first study to quantify and compare the effect of HGT relative to mutations on the rate of adaptation in asexual, haploid, microbial populations.

Evolutionary physiology of functionally redundant pathways in methylotrophs

Despite 150 generations of laboratory evolution, PA1 did not grow any faster on methylamine. Therefore we evolved AM1 to use the NMG pathway, instead of MaDH, for primary oxidation during methylamine growth. In the fifth chapter of this thesis, we delineate novel physiological adaptations in experimentally evolved mutants of AM1 that grow on methylamine using the NMG pathway.

AMI encodes the NMG pathway too, but in the absence of MaDH strains have extremely low competitive fitness on methylamine; much lower than PA1, in fact. Why does AM1 not tap into its genomic potential and use the NMG pathway for methylamine growth? To uncover the physiological constraints that prevent the actualization of this functional degeneracy, we evolved two distinct genotypes with extremely low methylamine fitness, but an intact NMG pathway, on methylamine as the sole source of carbon and energy. In contrast to the PA1 evolution experiment, methylamine fitness of the AM1 mutants increased rapidly (by 20-100 fold) and genome sequencing revealed three major constraints

associated with using the NMG pathway for methylamine growth: 1) antagonism with methylamine dehydrogeanse, 2) low expression and 3) growth inhibition by a sharp rise in cytoplasmic pH due to ammonia buildup. A novel physiological solution for mitigating the rise in cytoplasmic pH was observed in each evolved population: 1) constitutive expression of the *kefB* proton pore (Booth et al. 2003) independent of the glutathione binding domain and 2) conversion of cytoplasmic ammonia to urea and subsequent excretion. These observations led to the conclusion that AM1 cells solely use the highly expressed methylamine dehydrogenase for primary oxidation during growth on high concentrations of methylamine as a carbon source and switch to the energetically expensive NMG pathway for primary oxidation perhaps while using limiting concentrations of methylamine as a nitrogen source. We suspect that trade-offs between the kinetic parameters of these two methylamine oxidation pathways across an environmentally relevant concentration gradient of methylamine selects for this functional redundancy in AM1. In addition to the chapters outlined above, I have contributed to the following topics of research as well:

- Used experimental evolution as a genetic screen in PA1 to uncover a functional role for proteins with the DUF (Domain of Unknown Function) 336 in the cellular response to formaldehyde buildup. This work has contributed significantly to to resolve the long-standing metabolic paradox surrounding formaldehyde growth in methylotrophs.
- Developed and implemented a high-throughput method for traditional transposon mutagenesis to uncover a new metabolic pathway for betaine (*N*-*N*-*N*-trimethyl glycine) oxidation in methylotrophs.
- Engineered strains of PA1 to use the RuMP (Ribulose Monophosphate) pathway (Ward et al. 2004) in place of the native pathway for C_1 assimilation and/or C_1 dissimilation and experimentally evolved these engineered strains on methanol. Evolved isolates with higher yields than the ancestor hold great promise for biotechnological purposes.

References

1. **Falkowski P. G., T. Fenchel, and E.F. Delong.** 2008. The microbial engines that drive Earth's biogeochemical cycles. Science **320:**1034-1039.

2. **Ferenci T.** 2007. Bacterial physiology, regulation, and mutational adaptation in a chemostat environment. Advances in Microbial Physiology **53:**169-229.

3. **Holloway B. W., V. Krishnapillai, and A. F. Morgan.** 1979. Chromosomal genetics of *Pseudomonas.* Microbiol. Rev. **43:**73-102.

4. **Simon R., U. Priefer, and A. Puhler.** 1983. A broad host range mobilization system for *in vivo* genetic engineering: Transposon mutagenesis in Gram Negative bacteria. Nature Biotech. **1:**784-791.

5. **Sonenshein A. L., J. A. Hoch, and R. Losick.** 1993. *Bacillus subtilis* and other gram-positive bacteria: biochemistry, physiology, and molecular genetics. American Society of Microbiology Press, Washington D.C.

6. **Hopwood D. A.** 1999. Forty years of genetics with *Streptomyces*: from *in vivo* through *in vitro* to *in silico*. Microbiology. **145:**2183-2202.

7. **Marx C. J., and M. E. Lidstrom.** 2002. Broad-host-range *cre-lox* system for antibiotic marker recycling in Gram-Negative bacteria. BioTechniques. **33:**1062-1067.

8. **Pritchett M. A., J. K. Zhang, and W. W. Metcalf.** 2004. Development of a markerless genetic exchange method for *Methanosarcina acetivorans* C2A and its use in construction of new genetic tools for methanogenic archaea. Appl. Environ. Microbiol. **70:**1425-1433.

9. **Allers T., and Mevarech M.** 2005. Archaeal genetics – the third way. Nature Rev. Genetics. **6:** 58-73.

10. **Wagner M., S. Berkner, M. Ajon, A. J. M. Driessen, G. Lipps, and S-J. Albers.** 2009. Expanding and understanding the genetic toolbox of the hyperthermophilic genus *Sulfolobus.* Biochem. Soc. Trans. **37:**97-101.

11. **Tatusov R. L., E. V. Koonin, and D. J. Lipman.** 1997. A genomic perspective on protein families. Science. **24:**631-637.

12. **Marakova K. S., L. Aravind, M. Y. Galperin, N. V. Grishin, R L. Tatusov, Y. I. Wolf and E V. Koonin.** 1999. Comparative genomics of the Archaea (Euryarchaeota): Evolution of conserved protein families, the stable core, and the variable shell. Genome Res. **9:**608-628.

13. **Bateman A., E. Birney, R. Durbin, S. R. Eddy, K. L. Howe, and E. L. L. Sonnhammer.** 2000. The Pfam protein families database. Nucl. Acids Res. **28:**263-266.

14. **Haft D. H., J. D. Selengut, and O. White.** 2003. The TIGRFAMs database. Nucl. Acids Res. **31:**371-373.

15. **Vogel C., and C. Chotia.** 2006. Protein family expansions and biological complexity. PloS Comput. Biol. **2:**e48.

16. **Elena S. F., and R. E Lenski.** 2003. Microbial genetics: Evolution experiments with microorganisms: the dynamics and genetic basis of adaptation. Nature Rev. Genetics. **4:**457-469.

17. **Lenski R. E., M. R. Rose, S. C. Simpson, and S. C. Tadler.** 1991. Long-term experimental evolution in *Escherichia coli.* I. Adaptation and divergence during 2,000 generations. Am. Naturalist. **138:**1315-1341.

18. **Rainey P. B., and M. Travisano.** 1998. Adaptive radiation in a heterogeneous environment. Nature. **394:**69-72.

19. **Kassen R.** 2002. The experimental evolution of specialists, generalists, and the maintenance of diversity. J. of Evol. Biol. **15:**173-190.

20. **Perron G. G., M. Zasloff, and G. Bell.** 2006. Experimental evolution of resistance of an antimicrobial peptide. Proc. R. Soc. B. **273:**251-256.

21. **Maharjan R. S. Seeto, L. Notley-McRobb, and T. Ferenci.** 2006. Clonal adaptive radiation in a constant environment. Science. **313:**514-517.

22. **Lee M-C., H-H. Chou, and C. J. Marx.** 2009. Asymmetric, bimodal trade-offs during adaptation of *Methylobacterium* to distinct growth substrates. Evolution. **63:**2816-2830.

23. **Ratcliff W. C., R. F. Denison, M. Borrello, and M. Travisano.** 2012. Experimental evolution of multicellularity. PNAS. **109:**1595-1600.

24. **Chou H-H, J. Berthet J, and C. J. Marx.** 2009. Fast growth increases the selective advantage of a mutation arising recurrently during evolution under metal limitation. PLoS Genetics. **5:** e1000652.
25. **Lang G. I., D. P. Rice, M. J. Hickman, E. Sodergren, G. M. Weinstock, D. Botstein, and M. M. Desai.** 2013. Pervasive genetic hitchhiking and clonal interference in forty evolving yeast populations. Nature. **500:**571-574.

26. **Frenkel E.M., B. H. Good, and M. M. Desai.** 2014. The fate of mutant lineages and the distribution of fitness effects of beneficial mutations in laboratory budding yeast populations. Genetics. **196:**1217-1226.

27. **Chou H-H., H-C. Chiu, N. F. Delaney, D. Segre, and C. J. Marx.** 2011. Diminishing returns epistasis among beneficial mutations decelerates adaptation. Science. **332:**1190-1192.

28. **Khan A. I., D. M. Dinh, D. Schneider, R. E. Lenski, and T. F. Cooper.** 2011. Negative epistasis between beneficial mutations in an evolving bacterial population. Science. **332:**1193-1196.

29. **Kryazhimskiy S., D. P. Rice, E. Jerison, and M. M. Desai.** 2014. Global epistasis makes adaptation predictable despite sequence-level stochasticity. Science. **344:** 1519-1522.

30. **Taddei F., M. Radman, J. Maynard-Smith, B. Toupance, P. H. Gouyon and B. Godelle.** 1997. Role of mutator alleles in adaptive evolution. Nature. **387:**700-702.
31. **Elena S. F., and R. E. Lenski.** 1997. Test of synergistic interactions among deleterious mutations in bacteria. Nature. **390:**395-398.

32. **Miralles R., P. J. Gerrish, A. Moya, and S. F. Elena.** 1999. Clonal interference and the evolution of RNA viruses. Science. **285:**1745-1747.

33. **Kao K. C., and G. Sherlock.** 2008. Molecular characterization of clonal interference during adaptive evolution in asexual population of *Saccharomyces cerevisiae.* Nature Genetics. **40:** 1499-1504.

34. **Wright S.** 1932. The role of mutation, inbreeding, crossbreeding and selection in evolution. Sixth International Congress on Genetics. **1:**356-366.

35. **Gould S. J., and R. C. Lewontin.** 1979. The spandrels of San Marco and the Panglossian paradigm: A critique of the adaptationist programme. Proc. R. Soc. Lond. B. **205:**581-598.

36. **Gould S. J., and N. Eldredge.** 1977. Punctuated equilibria: the tempo and mode of evolution reconsidered. Paleobiology. **3:**115-151.

37. **Fisher R. A.** 1958. The genetical theory of natural selection. Рипол Классик.

38. **Kimura M.** 1977. Preponderance of synonymous changes as evidence for the neutral theory of molecular evolution. Nature. **267:**275-276

39. **Fay J. C., G. J. Wyckoff, and C.-I Wu.** 2002. Testing the neutral theory of molecular evolution with genomic data from *Drosophila.* Nature. **415:**1024-1026.

40. **Beaumont H. J. E., J. Gallie, C. Kost, G. C. Ferguson, and P. B. Rainey.** 2009. Experimental evolution of bet hedging. Nature. **462:**90-93.

41. **Barrick J. E., D. S. Yu, S. H. Yoon, H. Jeong, T. K. Oh, D. Schneider, R. E. Lenski, and J. F. Kim.** 2009. Genome evolution and adaptation in a long-term experiment with *Escherichia coli.* Nature. **461:**1243-1247.

42. **Marx C. J.** 2011. Evolution as an experimental tool in microbiology: 'Bacterium, improve thyself!' Environmental Microbiology Reports. **3:**12-14.

43. **Blount Z. D., J. E. Barrick, C. J. Davidson, and R. E. Lenski.** 2012. Genomic analysis of a key innovation in an experimental *Escherichia coli* population. Nature. **489:**513.518.

44. **Lee D. H., and B. O. Palssøn.** 2010. Adaptive evolution of *Escherichia coli* K-12 MG1655 during growth on a nonnative carbon source, L-1, 2-propanediol. Appl. Environ. Microbiol. **76:** 4158-4168.

45. **Lee M.-C., and C. J. Marx.** 2013. Synchronous waves of failed soft sweeps in the laboratory: remarkably rampant clonal interference of alleles at a single locus. Genetics. **193:**943-952.

46. **Chubiz L. M., M.-C. Lee, N. F. Delaney, and C. J. Marx.** 2012. FREQ-Seq: A rapid, cost-effective, sequencing-based method to determine allele frequencies directly from mixed populations. PLoS ONE. **7:**e47959.

47. **Herron M. D., and M. Doebeli.** 2013. Parallel evolutionary dynamics of adaptive diversification in *Escherichia coli.* PloS Biology. **11:**e1001490.

48. **Boucher Y., C. J. Doudy, R. T. Papke, D. A. Walsh, M. E. R. Boudreau, C. L. Nesbø, R. J. Case, and W. F. Doolittle.** 2003. Lateral gene transfer and the origin of prokaryotic groups. Ann. Rev. Genet. **37:**283-328.

49. **Anthony C.** 1982. The biochemistry of methylotrophs. Academic Press Ltd., London.

50. **Oremland R. S., L. M. Marsh, and S. Polcin.** 1982. Methane production and simultaneous sulphate reduction in anoxic, salt marsh sediments. Nature **296:**143-145.

51. **Chistoserdova L.**, **S. W. Chen, A. Lapidus, and M. E. Lidstrom.** 2003. Methylotrophy in *Methylobacterium extorquens* AM1 from a genomic point of view. J. Bacteriol. **185:**2980-2987.

52. **Vuilleumier S., L. Chistoserdova, M-C. Lee, F. Bringel, et al.** 2009. *Methylobacterium* genome sequences: a reference blueprint to investigate microbial metabolism of C_1 compounds from natural and industrial sources. PLoS One. **4:**e5584.

53. **Marx C. J., F. Bringel, L. Chistoserdova, et al.** 2012. Complete genome sequences of six strains of the genus *Methylobacterium*. J. Bacteriol.**194:**4746-4748.

54. **Chistoserdova L.**, **M. G. Kalyuzhnaya, and M. E. Lidstrom.** 2009. The expanding world of methylotrophic metabolism. Annu. Rev. Microbiol. **63:**477-499.

55. **Nunn D. N., and M. E. Lidstrom.** 1986. Isolation and complementation analysis of 10 methanol oxidation mutant classes and identification of the methanol dehydrogenase structural gene of *Methylobacterium* sp. strain AM1. J. Bacteriol. **166:**581-590.

56. **Chistoserdov A. Y., Y.D. Tsygankov, and M. E. Lidstrom.** 1991. Genetic organization of methylamine utilization genes from *Methylobacterium extorquens* AM1. J. Bacteriol. **173:**5901-5908.

57. **Marx C. J., L. Chistoserdova, and M. E. Lidstrom.** 2003. Formaldehyde-detoxifying role of the tetrahydromethanopterin-linked pathway in *Methylobacterium extorquens* AM1. J. Bacteriol.**185:**7160-7168.

58. **Marx C. J., S. J. Van Dien, and M. E. Lidstrom.** 2005. Flux analysis uncovers key role of functional redundancy in formaldehyde metabolism, PloS Biol. **3:**e16.

59. **Crowther G. J., G. Kosaly, and M. E. Lidstrom.** 2008. Formate as the main branch point for methylotrophic metabolism in *Methylobacterium extorquens* AM1. J. Bacteriol. **190:**5057-5062.

60. **Chistoserdova L., G. J. Crowther, J. A. Vorholt, E. Skovran, J. C. Portais, and M. E. Lidstrom.** 2007. Identification of a fourth formate dehydrogenase in *Methylobacterium extorquens* AM1 and confirmation of the essential role of formate oxidation in methylotrophy. J. Bacteriol. **189:**9076-9081.

61. **Marx C. J., M. Laukel, J. A. Vorholt, and M. E. Lidstrom.** 2003. Purification of the formate-tetrahydrofolate ligase from *Methylobacterium extorquens* AM1 and demonstration of its requirement for methylotrophic growth. J. Bacteriol. **185:**7169-7175.
62. **Maden E.H.** 2000.Tetrahydrofolate and tetrahydromethanopterin compared: functionally distinct carriers in C_1 metabolism. Biochem. J. **350:** 609-629.

63. **Chistoserdova L., and M. E. Lidstrom.** 1994. Genetics of the serine cycle in *Methylobacterium extorquens* AM1: cloning, sequence, mutation and physiological effect of *glyA*, the gene for serine hydroxymethyltransferase. **176:** 6759-6762.

64. **Peyraud R., P. Kiefer, P. Christen, S. Massou, J. C. Portais, and J. A. Vorholt.** 2009. Demonstration of the ethylmalonyl-CoA pathway by using 13C metabolomics. PNAS. **106:** 4846-4851.

65. **L. Chistoserdova.** 2011. Methylotrophy in a lake: from metagenomics to single-organism physiology. Appl. Environ. Microbiol. **77:**4705-4711.

66. **Swan B. K., M-M. Garcia, C. M. Preston, A. Sczyrba, T. Woyke, D. Lamy, T. Reinthaler, N. J. Poulton, E. D. P. Masland, M. L. Gomez, M. E. Sieracki, E. F. DeLong, G. J. Herndl, and R. Stepanauskas.** 2011. Potential for chemolithoautotrophy among ubiquitous bacterial lineages in the dark ocean. Science. **333:**1296-1300.

67. **Robinson D. G., M-C. Lee, and C. J. Marx.** 2012. OASIS: an automated program for global investigation of bacterial and archaeal insertion sequences. Nucleic Acids Res. **40:**e174.

68. **Skovran E., A. D. Palmer, A. M. Rountree, N. M. Good, and M. E. Lidstrom.** 2011. XoxF is required for expression of methanol dehydrogenase in *Methylobacterium extorquens* AM1. J. Bacteriol. **193:**6032-6038.

69. **Carroll S. M., K. S. Xue, and C. J. Marx.**2014. Laboratory divergence of *Methylobacterium extorquens* AM1 through unintended domestication and past selection for antibiotic resistance. BMC Microbiol. **14:** 2.

70. **Lee M-C., and C. J. Marx.** 2012. Repeated, selection-driven genome reduction of accessory genes in experimental populations. PLoS Genetics. **8:**e1002651.

71. **Knief C., L. Frances, and J. A. Vorholt.** 2010. Competitiveness of diverse *Methylobacterium* strains in the phyllosphere of *Arabidopsis thaliana* and identification of representative models, including *M. extorquens* PA1. Microb. Ecol. **60:**440-452.

72. **Delaney N. F., M. E. Kaczmarek, L. M. Ward, P. K. Swanson, M-C. Lee, and C. J. Marx.**2013. Development of an optimized medium, strain, and high-throughput culturing methods for *Methylobacterium extorquens*. PLoS One. **8:**e62957.

73. **Shaw W.V., L. Tsai, and R. R. Stadtman.** 1966. The enzymatic synthesis of *N*-methylglutamic acid. J. Biol. Chem. **241:**935-945.

74. **Latypova E., S. Yang, Y. S. Wang, T. Wang, T. A. Chavkin, M. Hackett, H. Schafer, and M. G. Kalyuzhnaya.** 2010. Genetics of the glutamate-mediated methylamine utilization pathway in the facultative methylotrophic beta-proteobacteria *Methyloversatilis universalis* FAM5. Mol. Microbiol. **75:**426-439.

75. **Martinez-Gomez N. C., S. Nguyen, and M. E Lidstrom.** 2013. Elucidation of the role of methylene-tetrahydromethanopterin dehydrogenase MtdA in the tetrahydromethanopterin-dependent oxidation pathway in *Methylobacterium extorquens* AM1. J. Bacteriol.**195:**2359-2367.

76. **Gruffaz C., E.E. L. Muller, Y. Louhichi-Jelail, Y. R. Nelli, G. Guichard, and F. Bringel.** 2014. Genes of the *N*-methylglutamate pathway are essential for growth of *Methylobacterium extorquens* DM4 on monomethylamine. Appl. Environ. Microbiol. **80:**3541-3550.

77. **Ge X., A. S. Wexler, and S.L. Clegg.** 2011. Atmospheric amines- Part I. A review. Atmospheric Environment **45:**524-546.

78. **Marx C. J.** 2008. Development of a broad-host-range *sacB*-based vector for unmarked allelic exchange. BMC Res. Notes. **1:**1.

79. **Delaney N. F., J. I. Rojas Echenique, and C. J. Marx.** 2013. Clarity: an open-source manager for laboratory automation. J. Lab Autom.**18:**171-177.

80. **Vannelli T., M. Messmer, A. Studer, S. Vuilleumier, and T. Leisinger.** 1999. A corrinoid-dependent catabolic pathway for growth of a *Methylobacterium* strain with chloromethane. PNAS **96:**4615-4620.

81. **Bennett A. F., R. E. Lenski, and J. E. Miller.** 1992. Evolutionary adaptation to temperature. I. Fitness response of *Escherichia coli* to changes in its thermal environment. Evolution. **46:** 16-30.

82. **Travisano M., J. A. Mongold, A. F. Bennett, and R. E. Lenski.** 1995. Experimental tests of the role of adaptation, chance, and history in evolution. Science. **267:** 87-90.

83. **Woods R., D. Schneider, C. L. Winkworth, M. A. Riley, and R. E. Lenski.** 2006. Tests of parallel molecular evolution in a long-term evolution experiment with *Escherichia coli*. PNAS. **103:** 9107-9112.

84. **Vorholt J. A., C. J. Marx, M. E. Lidstrom, and R. K. Thauer.** 2000. Novel formaldehyde-activating enzyme in *Methylobacterium extorquens* AM1. **182:**6645-6650.

85. **Booth I. R., G. P. Ferguson, S. Miller, C. Li, B. Gunasekara, and S. Kinghorn.** 2003. Bacterial production of methylglyoxal: a survival strategy or death by misadventure? Biochem. Soc. Trans. **31:**1406-1408.

86. **Ward N., Ø. Larson, J. Sakwa, L. Bruseth, *et al.*** 2004. Genomic insights into methanotrophy: The complete genome sequence of *Methylococcus capsulatus* (Bath).

Chapter 2

Genetic and phenotypic comparison of methylotrophy

in *Methylobacterium extorquens* strains PA1 and AM1

Genetic and phenotypic comparison of methylotrophy between *Methylobacterium extorquens* strains PA1 and AM1

Running title: A new model system for the study of aerobic methylotrophy

Dipti D. Nayak[1] and Christopher J. Marx[1, 2,3,4]

[1]Organismic and Evolutionary Biology, Harvard University, Cambridge, MA, USA, [2]Faculty of Arts and Sciences Center for Systems Biology, Harvard University, Cambridge, MA, USA. [3]Department of Biological Sciences, University of Idaho, Moscow, ID, USA. [4]Institute for Bioinformatics and Evolutionary Studies, University of Idaho, Moscow, ID, USA.

#Corresponding author: Christopher J. Marx, cmarx@uidaho.edu

Abstract

Methylobacterium extorquens AM1, a strain serendipitously isolated half a century ago, has become the best-characterized model system for the study of aerobic methylotrophy (the ability to grow on reduced single carbon compounds). However, with 5 replicons, 174 insertion sequence (IS) elements in the genome and a long history of domestication in the laboratory, genetic and genomic analysis of *M. extorquens* AM1 face several challenges. On the other hand, a recently isolated strain - *M.extorquens* PA1- is closely related to *M. extorquens* AM1 (100% 16S rRNA identity) and contains a streamlined genome with a single replicon and only 20 IS elements. In this paper we report four primary findings regarding methylotrophy in PA1. First, with a few notable exceptions, the repertoire of methylotrophy genes between PA1 and AM1 is extremely similar. Second, PA1 grows faster with higher yields compared to AM1 on C_1 and multi-C substrates in minimal media, but AM1 grows faster in rich medium. Third, deletion mutants in PA1 throughout methylotrophy modules have the same C_1 growth phenotypes observed in AM1. Finally, the precision of our growth assays revealed several unexpected growth phenotypes for various knockout mutants that serve as leads for future work in understanding their basis and generality across *Methylobacterium* strains.

Introduction

Methylotrophy is the ability of microorganisms to grow on reduced single-carbon (C_1) compounds like CH_4 (methane) or CH_3OH (methanol) as a sole carbon and energy source (Peel and Quayle 1961; Large and Quayle 1963; Johnson and Quayle 1964; C. Anthony 1982). *Methylobacterium extorquens* AM1 (Peel and Quayle 1961) is a facultative methylotroph that belongs to the *Rhizobiales* family of the Alpha-proteobacteria. Since *M. extorquens* AM1 is genetically tractable (Marx and Lidstrom 2001; Marx and Lidstrom 2002; Marx et al. 2003a; Marx and Lidstrom 2004; C. J. Marx 2008; Choi et al. 2006; Kaczmarczyk et al. 2013), has fast, roughly comparable growth rates on C_1 compounds (t_D~3-4 h on methanol and methylamine) and multi-carbon compounds (t_D~2.5 -3 h on succinate) (Delaney et al. 2013;

Lee et al. 2009), it has emerged as the model system for the study of aerobic methylotrophy (Chistoserdova et al. 2003; Chistoserdova et al. 2009). There are three specific aspects of the genome architecture and physiology of AM1 that pose challenges (Vuilleumier et al. 2009; Lee and Marx 2012; Robinson et al. 2012; Chou et al. 2009; Chou and Marx 2012; Lee and Marx 2013; Carroll and Marx 2013; Carroll et al. 2014). First, the AM1 genome has five replicons of varying sizes (Vuilleumier et al. 2009). One of the replicons in the AM1 genome is a 1.3 Mb megaplasmid that contains many insertion sequence (IS) elements; recombination events mediated by IS elements often lead to large, beneficial deletions (Lee and Marx 2012). Hence, experiments designed to study a variety of questions have and will commonly result in this particular change of large benefit (Lee and Marx 2012). Second, the 174 intact or partial IS elements across 39 IS families present in the AM1 genome (Vuilleumier et al. 2009; Robinson et al. 2012) are responsible for a significant amount of genome plasticity which has often been observed during genetic manipulations and evolution experiments with AM1 (Chou et al. 2009; Chou and Marx 2012; Lee and Marx 2013; Carroll and Marx 2013). Such high rates of IS insertion/recombination in AM1 leads to spurious recombination events across the genome during reverse genetic manipulations (Nayak, Carroll, and Marx; unpublished) and skews the mutational spectrum during experimental evolution (Lee and Marx 2012). Third, the current strain of AM1 has been domesticated in laboratory conditions since the late 1950s (Peel and Quayle 1961; Large and Quayle 1963; Johnson and Quayle 1964) and has changed significantly ever since (Carroll et al. 2014). A notable difference is that the 'modern' strain (C. J. Marx 2008) grows ~25% worse than an archival version under a wide variety of conditions. These results indicate that aspects of physiology uncovered in the modern AM1 may be hard to extrapolate to other environmentally relevant methylotrophs.

Of late, an increasing number of studies have been conducted with several members of the *M. extorquens* species and genome sequence data is now available for six strains (Vuilleumier et al. 2009; Marx et al. 2012). Despite 16S rRNA sequence similarity, these strains vary significantly in terms of their metabolic breadth, genetic tractability, ecological niche and genomic composition (Marx et al. 2012). We

considered whether one of these six sequenced strains might overcome the challenges posed by AM1 and finally narrowed in on *M. extorquens* PA1 (hereafter PA1) as it has the most streamlined genome, with a single 5.47 Mb chromosome, that contains only 20 intact IS elements. These features can make the design and implementation of genetic screens more efficient, and prevent beneficial elimination of extra-chromosomal elements or IS-mediated events from dominating the spectrum of beneficial mutations. Recent isolation of PA1 from the leaves of *Arabidopsis thaliana* (Knief et al. 2010), and immediate cryopreservation obviate concerns associated with domestication of the 'modern' AM1 strain and provide a clear link to a known ecological niche.

There are some clear advantages of the genome composition and culturing history of PA1 over AM1. In order to ascertain how well the decades of characterization of methylotrophy in AM1 will apply directly to PA1, we identified the shared repertoire of methylotrophy genes and performed a broad genetic analysis of the role of various methylotrophy-specific modules in PA1 (Figure 2.1). In AM1, reduced C_1 compounds like methanol or methylamine are oxidized by dedicated periplasmic dehydrogenases to generate formaldehyde. Once in the cytoplasm, formaldehyde is oxidized to formate via a tetrahydromethanopterin (H_4MPT) dependent pathway (Chistoserdova et al. 1998; Marx et al. 2003b). Formate is then either oxidized to CO_2 via a panel of formate dehydrogenases (Chistoserdova et al. 2007), or is assimilated into biomass via a tetrahydrofolate (H_4F) dependent pathway (Marx et al. 2003c; Marx et al. 2005; Crowther et al. 2008; E. H. Maden 2000). The C_1 unit from methylene-H_4F (an intermediate of the H_4F pathway) and one third of the CO_2 produced is assimilated into biomass via the serine cycle (Chistoserdova et al. 2003).

A quantitative comparison of growth rates and yield showed that *M. extorquens* PA1 grew faster, with higher yield, than *M. extorquens* AM1 on single- and multi-carbon compounds in minimal media, whereas *M. extorquens* AM1 grew faster than *M. extorquens* PA1 in rich medium.

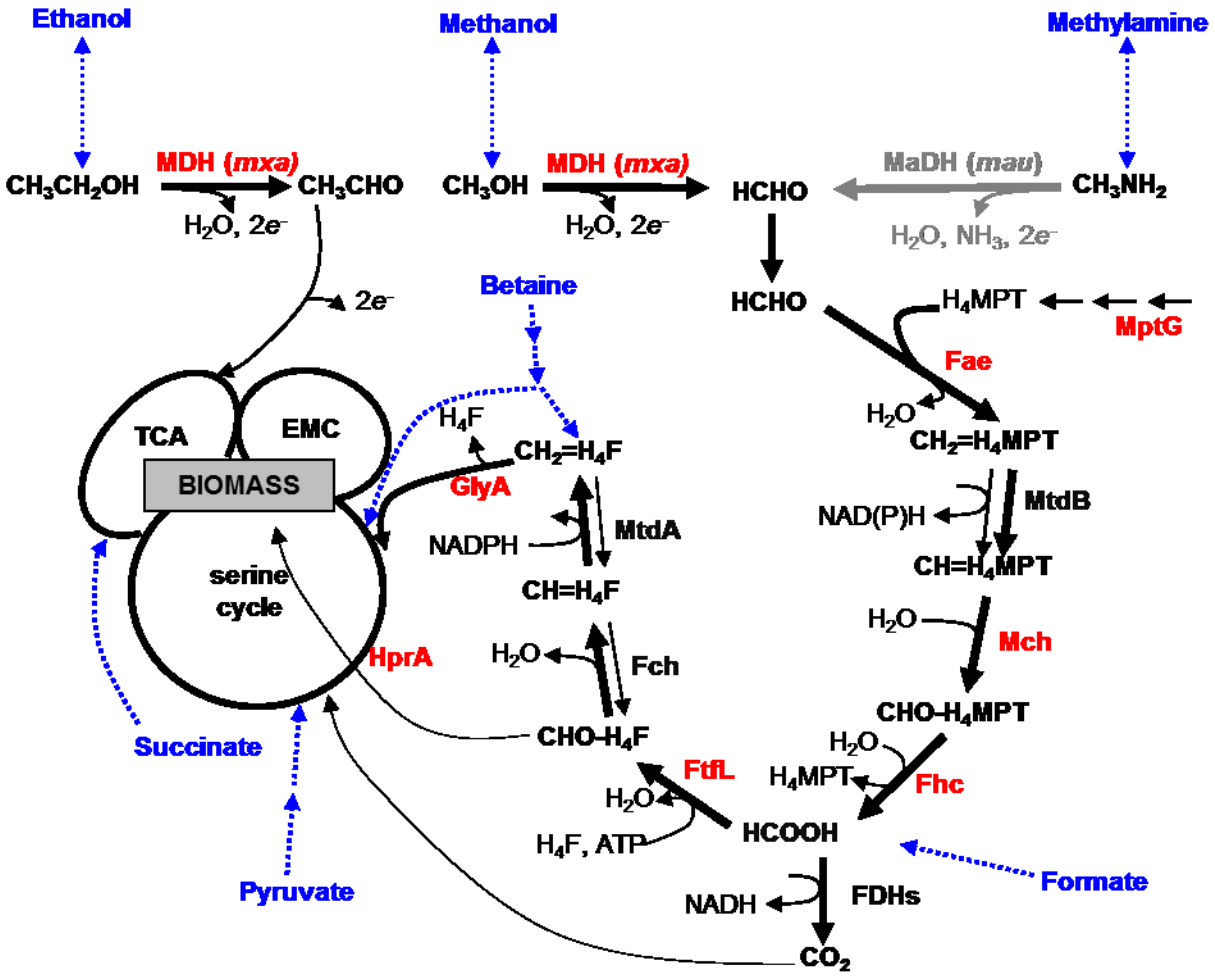

Figure 2.1.: The methylotrophy specific metabolic network in in *M. extorquens* AM1. All methylotrophy-specific genes, except for the *mau* cluster (gray), are present and >95% identical in *M. extorquens* PA1. *M. extorquens* AM1 and *M. extorquens* PA1 were grown on various C_1 and multi-C substrates (blue) for this study. Genes highlighted in red were deleted in *M. extorquens* PA1 to uncover that the metabolic network involved in methylotrophy in *M. extorquens* PA1 is identical to *M. extorquens* AM1. FDH: Formate Dehydrogeanse, TCA: Tricarboxylic acid Cycle and EMC: Ethyl-malonyl CoA Pathway.

Analysis of the growth phenotypes of a large suite of *M. extorquens* PA1 knockout mutants in various methylotrophy-specific modules revealed that the metabolic network functions as established for *M. extorquens* AM1. Our analysis demonstrated that the vast body of knowledge for *M. extorquens* AM1 is largely transferable to *M. extorquens* PA1: an alternate model system for the study of aerobic

methylotrophy in the future. Additionally, our quantitative physiological analysis has unveiled novel phenotypes for methylotrophy-specific genes that generate leads to uncover poorly understood aspects of regulation in future work.

Materials and Methods

Bacterial Strains and Growth Conditions

Strains relevant to this study included the following: the Δ*cel* mutant of the pink-pigmented 'wildtype' stock of AM1 (CM2720) and the Δ*cel* mutant of the pink-pigmented 'wildtype' stock of PA1 (CM2730) used for growth comparisons are described elsewhere (Delaney et al. 2013a). Standard growth conditions utilized a modified version of Hypho minimal medium consisting of: 100 mL phosphate salts solution (25.3 g of K_2HPO_4 plus 22.5 g Na_2HPO_4 in 1L deionized water), 100 mL sulfate salts solution (5 g of $(NH_4)_2SO_4$ and 2 g of $MgSO_4 \cdot 7\ H_2O$ in 1L deionized water), 799 mL of deionized water, and 1 mL of trace metal solution (Agashe et al. 2013). All components were autoclaved separately before mixing under sterile conditions. Filter-sterilized carbon sources were added just prior to inoculation in liquid minimal media with a final concentration of 15 mM methanol, 3.5 mM sodium succinate, 15 mM methylamine hydrochloride, 7.5 mM ethanol, 5 mM sodium succinate, 15 mM glycine betaine, 7.5 mM methanol and 1.25 mM succinate, or Difco nutrient broth. Difco nutrient broth (Becton, Dickson, and Company, Franklin Lakes, NJ) was prepared according to the manufacturer's guidelines.

Growth Rate Measurements

Cells were acclimated and grown in 48-well microtiter plates (CoStar-3548) in an incubation tower (Liconic USA LTX44 with custom fabricated cassettes) shaking at 650 rpm, in a room that was constantly maintained at 30 ºC and 80% humidity, (Delaney et al. 2013b), containing Hypho medium with the appropriate carbon source to a volume of 640 μL. All growth regimes consisted of three cycles consisting of inoculation, acclimation, and growth measurement. All strains were stored in vials at -80 °C in 10% DMSO; growth was initiated by transferring 10 μL freezer stock into 10 mL of Hypho medium with 3.5

mM succinate. Upon reaching stationary phase (~2 days), cultures were transferred 1:64 into fresh medium with the carbon source to be tested, allowed to reach saturation in this acclimation phase, and diluted 1:64 again into fresh medium for the measured (experimental) growth. The increase in OD_{600} for strains grown in 48-well microtiter plates was measured using an automated, robotic culturing and monitoring system (Delaney et al. 2013b). A series of robotic instruments (including a shovel, a transfer station, and a twister arm), all controlled by an open-source control program, Clarity (Delaney et al. 2013b), were used to move the 48-well plates from the incubation tower (Liconic USA LTX44 with custom fabricated cassettes) to a Perkin-Elmer Victor2 plate reader for optical density (OD_{600}) measurements. The dynamics and specific growth rate of cultures were calculated from the log-linear growth phase using an open source, custom-designed growth analysis software called CurveFitter available at http://www.evolvedmicrobe.com/CurveFitter/ . Growth rates reported for each strain and condition are the mean plus SEM calculated from triplicate biological replicates, unless otherwise noted.

Generation of Mutant Strains

M. extorquens PA1 deletion mutants lacking the *mxa* operon, *fae*, *mptG*, *ftfL*, *glyA*, or *hprA* (Figure 2.1, Table 2.1) were generated on the genetic background of CM2730 using the allelic exchange vector pCM433 (C. J. Marx 2008). The double deletion mutants lacking *mptG* and *mch* or *fhcBACD* were generated on the genetic background of CM3803 (Δ*mptG* in CM2730) using the allelic exchange vector pCM433 (C. J. Marx 2008). A region upstream and downstream of each of these genes or operons of ~0.5 kb was amplified using PCR. The forward primer for the upstream flank was designed to have a 30 bp long sequence at the 5' end homologous to the sequence upstream of the *Not*I cut site in pCM433. The reverse primer for the upstream flank was designed to have a 30 bp sequence at the 5' end homologous to the first 30 bp of the downstream flank. The reverse primer for the downstream flank was designed to have a 30 bp long sequence at the 5' end homologous to the sequence downstream of the *Not*I cut site in pCM433. The PCR products representing the upstream and downstream flank were ligated on the pCM433 vector cut with *Not*I using the Gibson assembly protocol described elsewhere (Gibson et al.

2009). Cloning the upstream and downstream flanks for *fae*, *ftfL, glyA, mptG,* the *mxa* operon, *fhc*BACD*, mch,* and *hprA* in pCM433 resulted in pDN50, pDN56, pDN66, pDN68, pDN94, pDN108, pDN109, and pDN125, respectively. Mutant strains of *M. extorquens* PA1 were made by introducing the appropriate donor constructs through conjugation by a tri-parental mating between the competent *E.coli* NEB 10β (New England Biolabs, Ipswich, MA) containing the donor construct, an *E. coli* strain containing the conjugative plasmid pRK2073, and PA1 as described elsewhere (C. J. Marx 2008). All mutant strains were confirmed by diagnostic PCR analysis and validated by Sanger sequencing the mutant locus. All strains and plasmids used and generated for this study are listed in Table 2.1.

Results and Discussion

Comparison of methylotrophy genes in PA1 versus AM1

As a first step to compare methylotrophy in PA1 and AM1, we considered the content, similarity and organization of C_1 genes in each genome. Apart from 100% identity at the16S rRNA locus (25), the two strains also share 95.9% ITS (Internal Transcribed Spacer) 1 sequence identity, each has five *rrn* operons, and their GC contents are quite close (68.2% versus 68.5%). Of the 5333 coding sequences in the PA1 genome, 4260 are shared with AM1 (amino acid identity > 30%). Of the 90 genes known to be involved in methylotrophy, 62 have >99% identity and the remaining 28 have at least 95% identity at the amino acid level between AM1 and PA1 (Table S1.1, Appendix 1). This repertoire includes the genes involved in methanol oxidation, the H_4MPT- and H_4F-dependent C_1-transfer pathways, the four formate dehydrogenases, and genes of the serine cycle (Figure 2.1). The arrangement of genes is extremely similar between the main chromosome of AM1 and PA1 (Figure S1.1, Appendix 1).

Table 2.1: *M.extorquens* strains and plasmids used in this study

Strain or plasmid	Description	Reference
Strains		
CM2720	Δ*cel M.extorquens* AM1	Delaney et al.. 2013
CM2730	Δ*cel M.extorquens* PA1	Delaney et al. 2013
CM3753	Δ*fae* in CM2730	This study
CM3773	Δ*ftfL* in CM2730	This study
CM3799	Δ*glyA* in CM2730	This study
CM3803	Δ*mptG* in CM2730	This study
CM3849	Δ*mxa* operon in CM2730	This study
CM4122	Δ*hprA* in CM2730	This study
CM3889	Δ*fhcBACD*, Δ*mptG* in CM2730	This study
CM3891	Δ*mch*, Δ*mptG* in CM2730	This study
Plasmids		
pCM433	Allelic exchange vector (Tet^R, Suc^S)	C. J. Marx 2008
pDN50	pCM433 with Δ*fae* upstream and downsteam flanks	This study
pDN56	pCM433 with Δ*ftfL*upstream and downsteam flanks	This study
pDN66	pCM433 with Δ*glyA* upstream and downsteam flanks	This study
pDN68	pCM433 with Δ*mptG* upstream and downsteam flanks	This study
pDN94	pCM433 with Δ*mxa* operon upstream and downsteam flanks	This study
pDN125	pCM433 with Δ*hprA* upstream and downsteam flanks	This study
pDN108	pCM433 with Δ*fhcBACD* upstream and downsteam flanks	This study
pDN109	pCM433 with Δ*mch* upstream and downsteam flanks	This study
pRK2073	Conjugative helper plasmid (Str^R)	Figurski and Helinski 1979

There is one major difference: the cluster of genes encoding methylamine dehydrogenase (*mau)* is missing in PA1. The *mau* cluster in AM1 and *M. extorquens* CM4 is flanked by IS elements, and is also missing in another sequenced strain, *M. extorquens* DM4. These data further support the hypothesis that the *mau* cluster was acquired by horizontal gene transfer (Vuilleumier et al. 2009; Marx et al. 2012).

Phenotypic comparison of growth on C_1 and multi-C substrates for PA1 versus AM1

Even though methylotrophy-specific genes are shared are extremely similar between PA1 and AM1, it does not necessarily translate into quantitatively similar growth phenotypes on C_1 compounds or multi-C substrates. In order to rigorously compare the growth capabilities of the two strains, we took advantage of the recent development of an automated, robotic platform for high-throughput, quantitative measurements of *M. extorquens* growth (Delaney et al. 2013a, Delaney et al. 2013b). No significant difference in cell shape, cell size and biomass/ OD_{600} ratio was observed between PA1 and AM1 (Table S2, Appendix 1) hence maximum OD_{600} during growth was used as a proxy for yield. Additionally, for all phenotypic analyses we used strains of PA1 and AM1 that lacked the *cel* locus for cellulose biosynthesis. The Δ*cel* manipulation prevents 'clumping' of cells in 48-well plates, thereby made growth measurements more accurate and consistent (Delaney et al. 2013a). With a few notable exceptions, PA1 grew faster, with significantly higher yields, than AM1 on C_1 and multi-C substrates (Figure 2.2a and 2.2b). For C_1 substrates like methanol and formate, PA1 grew 10-15% faster, with 50-75% higher yield on them, than AM1. A stark difference in growth was observed on ethanol. An increase in OD_{600} (Figure 2.2b) after ~ 48 hours of incubation indicated that AM1 does grow on ethanol, however we were unable to reliably estimate the growth rate since it was below the detection limit (t_D ~17.5 h) of our growth measurement platform. In contrast, PA1 grew with a t_D 4.39± 0.05 h (mean ± 95% C.I. (Confidence Interval) of the mean of three biological replicates) on ethanol. At a genomic level, such a striking difference in ethanol growth rates might be due to specific genes downstream of primary oxidation, such as an aldehyde dehydrogeanse (Mext_1295), that are present in PA1 but absent in AM1. On multi-C organic acids, PA1 grew faster than AM1 by 5-25% with 12-25% higher yield.

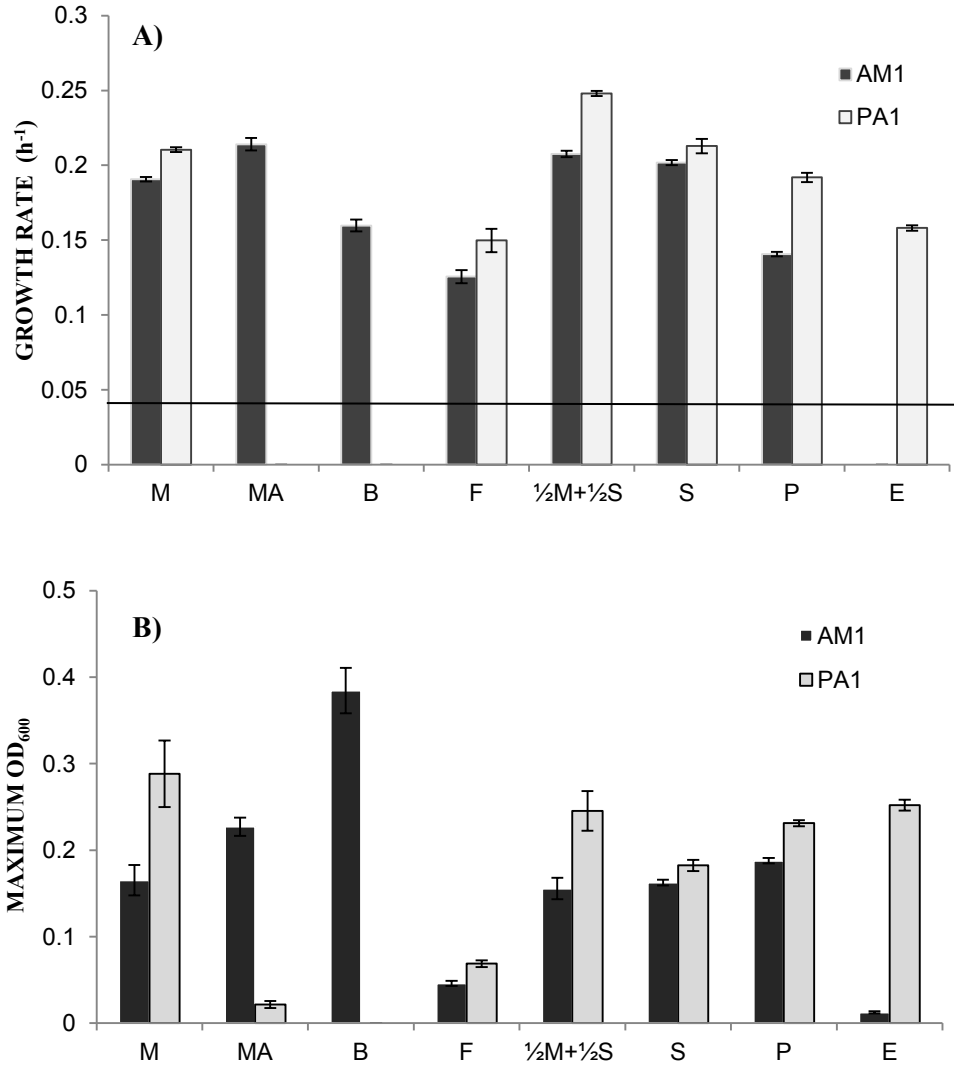

Figure 2.2: A) Quantitative comparison of growth rates and **B)** maximum OD_{600} for the Δ*cel* 'wild-type' strain of AM1 (filled) versus the Δ*cel* 'wild-type' strain of PA1 (open) on C_1 substrates (M, 15 mM methanol; MA, 15 mM methylamine; F, 15 mM formate), the joint C_1 and multi-C substrate betaine (B, 15 mM), multi-carbon substrates (S, 3.5 mM succinate; P, 5 mM pyruvate; E, 7.5 mM ethanol) and a combination of C_1 and multi-carbon substrates (½M+½S, 1.75 mM succinate and 7.5 mM methanol). The line indicates the approximate detection limit of our automated growth rate measurement device of 0.04 hr^{-1}. Growth rates for PA1 on MA or B and for AM1 on E were below this detection limit. Error bars represent the 95% C.I. of the average of three biological replicates.

In contrast to the results above, AM1 grew faster than PA1 on two C_1 substrates: methylamine and betaine (*N, N, N*- tri-methyl glycine). A small but significant increase in OD_{600} (Figure 2.2b) indicated that PA1 can grow on methylamine, but the growth rate was extremely slow and below the detection limit of our growth measurement platform. In PA1, slow methylamine growth was corroborated by the lack of methylamine dehydrogeanse (*mau)* operon, and was consistent with the growth rates known for other organisms dependent upon the *N*-methylglutamate pathway for methylamine utilization (Martinez-Gomez et al. 2013; Gruffaz et al. 2014). Specific proteins involved in betaine transport and utilization have not been discovered in AM1, so we can speculate that these genes may be missing or insufficiently active in PA1. AM1 also grew faster than PA1 on Nutrient Broth. Growth in Nutrient Broth did not have the typical log-linear dynamics that display a consistent, quantifiable growth rate (Figure S1.2, Appendix 1) because: a) Nutrient Broth is a composite of many different growth substrates and b) Nutrient Broth is not buffered so the pH of the media changes drastically over the course of growth. However, given that AM1 reached stationary phase much before PA1, it was evident that AM1 grew significantly faster than PA1 (Figure S1.2, Appendix 1). As previously hypothesized (Carroll et al. 2014), faster growth of AM1 on Nutrient Broth may stem from 'laboratory adaptation' since AM1 was stored on agar slants (Stieglitz and Mateles 1973) in the refrigerator for prolonged periods of time prior to cryopreservation. These conditions could have led to cryptic nutrient cycling of a wide variety of compounds, perhaps even lysed cell material, by surviving lineages (Carroll et al. 2014).

Genetic characterization of methylotrophy in PA1

In order to probe the architecture of the metabolic network involved in methylotrophy in PA1 (Figure 2.1) and ascertain how similar it is to that described for AM1, we deleted from the Δ*cel* PA1 strain (referred to as WT from here on) key genes involved each methylotrophy-specific module and examined the resulting growth phenotypes on C_1, multi-C, and a combination of C_1 and multi-C substrates (Table S1.3-S1.8, Appendix 1).

Methanol oxidation: There are 15 methanol oxidation genes at a single locus in AM1 as well PA1.In AM1, 14 of these genes are co-transcribed (Zhang and Lidstrom 2003), including those encoding the large and small subunit (MxaFI) of methanol dehydrogenase (Nunn and Lidstrom 1986) and ancillary proteins involved in transport, assembly and electron transfer (Chistoserdova et al. 2003). Deleting the *mxa* operon in PA1 led a to a drastic growth defect on methanol (Figure 2.3) demonstrating that MDH is, the primary enzyme involved in methanol oxidation in PA1, too. The Δ*mxa* mutant of PA1 had a severe growth defect on ethanol as well (Figure 2.3 and 2.4; Table S1.6-S1.8, Appendix 1). This observation supported a previous hypothesis, based on *in vitro* studies (Goodwin and Anthony 1998), that MDH in *M. extorquens* species can catalyze the oxidation of ethanol *in vivo* as well. Slow growth (as indicated by an increase in yield in Figure 2.4; Table S1.6-S1.8; Appendix 1) for the Δ*mxa* mutant on methanol and ethanol indicated that alternate, physiologically relevant alcohol dehydrogenase(s) for each of these substrates also exist in the PA1 genome.

Formaldehyde oxidation: Genetic and biochemical analyses have determined that the tetrahydromethanopterin (H_4MPT) dependent pathway is the sole route for the oxidation of formaldehyde to formate in AM1 (Marx et al. 2003a; Marx et al. 2003b; Marx et al. 2005) (Figure 2.1). In order to determine if the H_4MPT dependent pathway is required for formaldehyde oxidation in PA1, we individually deleted two key genes of this pathway: *mptG* (encoding ribofuranosylaminobenzene 5'-phosphate synthase that catalyzes the first step of the H_4MPT biosynthesis pathway (Rasche et al. 2004)) and *fae* (encoding the formaldehyde-activating enzyme that catalyzes the condensation of formaldehyde and H_4MPT (Vorholt et al. 2000)). Deleting either *mptG* or *fae* in PA1 abolished growth on methanol as well as a combination of methanol and succinate (Figure 2.3). Like in AM1, we suspect PA1 mutants lacking theH_4MPT pathway were sensitive to methanol because of the toxic effects of formaldehyde buildup (Marx et al. 2003b). Additionally, we noted that these two mutants grew slower (without any yield defect) on multi-C compounds and the Δ*mptG* mutant had a more severe growth-rate defect than the Δ*fae* mutant (Figure 2.3; Table S1.3-S1.5, Appendix 1).

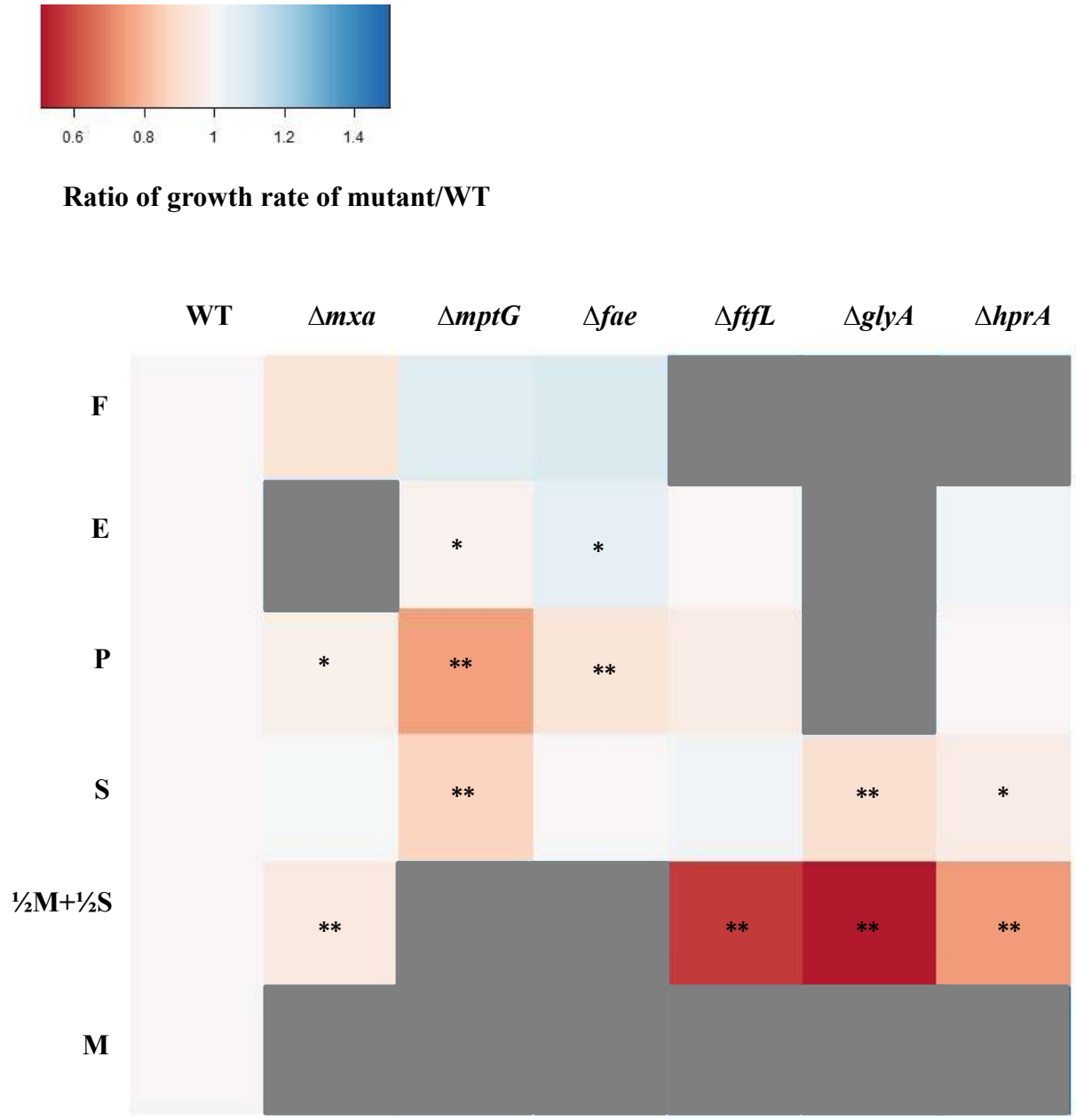

Figure 2.3: Heat map depicting the ratio of growth rate of knockout mutants of PA1 relative to the growth rate of the Δ*cel* wild-type strain on C_1 or multi-C substrates (same concentrations as in Figure 2.2). Undetectable growth is indicated by grey. A significant difference (determined by comparing the mean growth rate of three biological replicates using the t-test) in growth rate with a p-value <0.05 is indicated by a * and a p-value <0.001 is indicated by **.

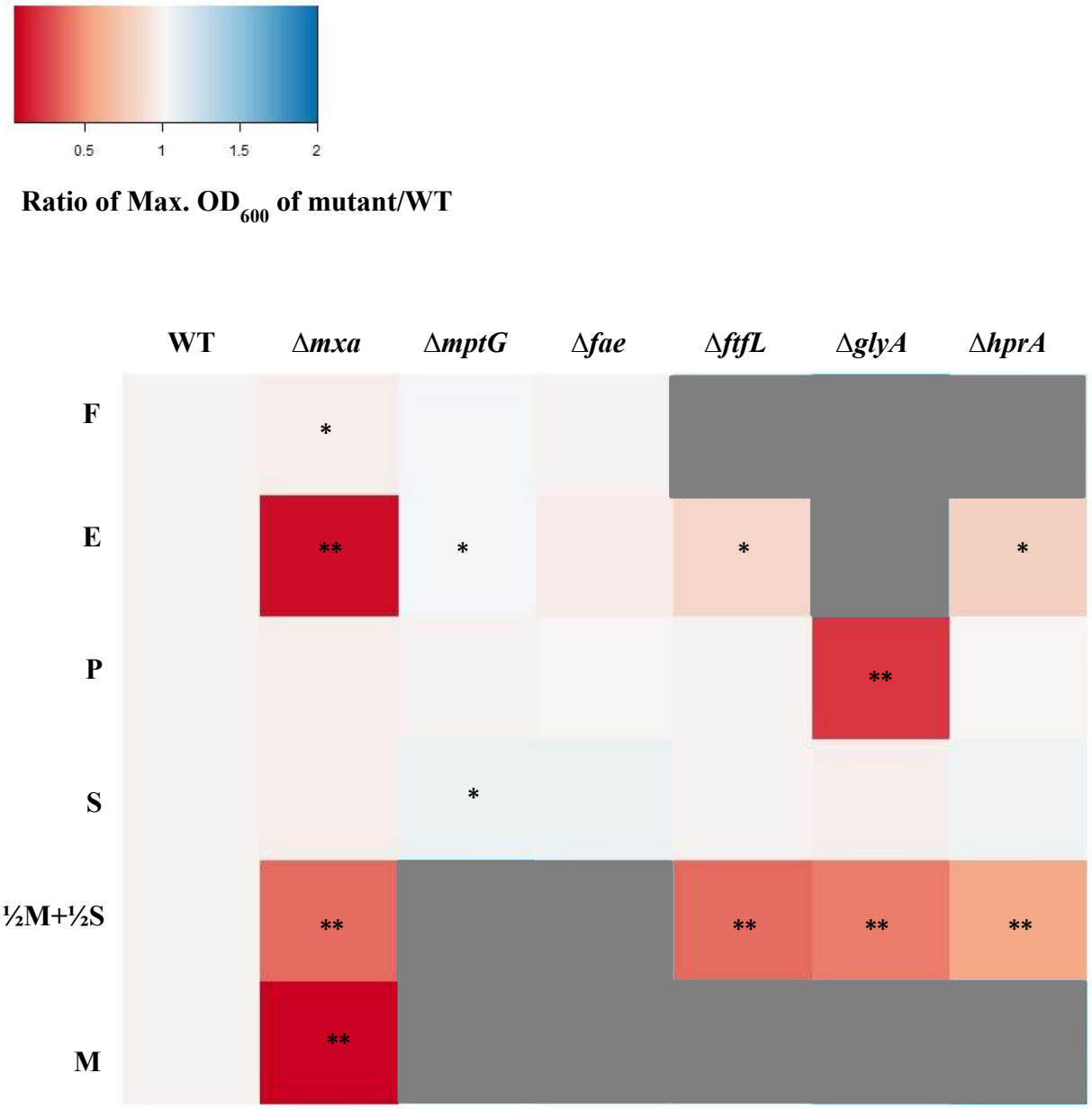

Figure 2.4: Heat map depicting the ratio of maximum OD_{600} of knockout mutants of PA1 relative to the maximum OD_{600} of the Δ*cel* wild-type strain on several C_1 or multi-C substrates (same concentrations as in Figure 2.2). Maximum OD_{600} values below 0.01 are indicated by grey. A significant difference in maximum OD_{600} (determined by comparing the mean growth rate of three biological replicates using the t-test) with a p-value < 0.05 is indicated by a * and a p-value <0.001 is indicated by **.

For example, on pyruvate, the Δ*mptG* mutant grew 25% slower ($p<0.001$; Student's two-sided t-test with n=3) and the Δ*fae* mutant grew 7% slower ($p<0.01$) than WT. These results are consistent with, and build upon, previous work in AM1 that qualitatively demonstrated that the Δ*mptG* mutant has a growth defect on succinate (Marx et al. 2003b). Furthermore, ethanol growth was not abolished in formaldehyde oxidation mutants, suggesting that the overlap between methanol and ethanol growth includes just primary oxidation but not any further oxidation steps (Table S1.3-S1.8, Appendix 1).

As observed in AM1 (Marx et al. 2003b), deletions in the genes encoding the final two enzymes of the H_4MPT pathway, *mch* and *fhc* (Pomper et al. 1999; Pomper and Vorholt 2001; Pomper et al. 2002), could only be generated in strains already lacking H_4MPT biosynthesis due to a lesion in *mptG* (Rasche et al. 2004). This result is consistent with the hypothesis (Marx et al. 2003b) that a late block in the H_4MPT mediated formaldehyde oxidation pathway leads to the accumulation of either methylene- or methenyl-H_4MPT, which may be either be directly toxic and/or lead to a regulatory response halting growth.

Formate assimilation: In order to establish the role of the H_4F mediated C_1 transfer pathway during methylotrophy in PA1, we deleted *ftfL* (encoding formate-H_4F ligase) (Marx et al. 2003c) and assayed the phenotype of the resulting strain on a panel of substrates (Figure 2.3 and Figure 2.4; Table S1.3-S1.8, Appendix 1). The Δ*ftfL* mutant in PA1 could not grow on methanol or formate because of a lesion in the first dedicated step toward assimilation of C_1 compounds (Marx et al. 2005; Crowther et al. 2008) (Figure 2.3). Since carbon from multi-C can be shunted into biomass and rescue the inability to assimilate methanol, we observed that the Δ*ftfL* mutant could grow on a combination of methanol and succinate (Marx et al. 2003c). However, the Δ*ftfL* PA1 mutant, unlike the Δ*ftfL* AM1 mutant (Carroll et al. 2013), did not have a significant growth rate or yield advantage on multi-C compounds (Table S1.3-S1.5, Appendix 1).

Serine cycle: Carbon from C_1 substrates is converted to various components of biomass through the serine cycle in AM1 (C. Anthony 1982; Chistoserdova et al. 2003). To determine whether the serine cycle plays a key role during C_1 assimilation in PA1 as well, we deleted *glyA* (serine hydroxyl

methyltransferase), and *hprA* (hydroxypyruvate reductase) (Figure 2.1) (Chistoserdova et al. 2003). As in AM1, neither mutant could grow on any C_1 substrates (Figure 2.3). While the Δ*hprA* strain had WT-like growth characteristics on multi-C compounds, the Δ*glyA* mutant exhibited several unexpected phenotypes: a complete inability to grow on ethanol, extremely slow growth on pyruvate and a 10% decrease ($p<0.01$) in growth rate on succinate compared to WT (Figure 2.3 and Figure 2.4; Table S1.3-S1.8, Appendix 1). These results suggest that alternative pathway(s) used to generate C_1-H_4F intermediates during multi-C growth, such as glycine cleavage (G. Kikuchi 1973), only partially rescue growth in the Δ*glyA* strain. Future work will be required to understand why the magnitude of growth defects on ethanol, pyruvate, and succinate varies for the Δ*glyA* mutant.

Growth on the combination of C_1- and multi-C substrates: The major goal of this study was a comprehensive comparison of the metabolic network involved in C_1- and multi-C metabolism in PA1 to that established for AM1. In addition, however, we also uncovered a number of unexpected growth phenotypes, especially on the combination of C_1- and multi-C substrates. In contrast to a previous study (Peyraud et al. 2012), which showed that AM1 grows on a combination of succinate and methanol at the same rate as succinate or methanol, PA1 grew 16% faster, with a 35% increase in yield, on a combination of methanol and succinate, compared to succinate alone (Figure 2.5a and 2.5b). Just like AM1, however, PA1 grew on a combination of methanol and succinate without the typical diauxic growth patterns. Since growth on succinate is energy-limited and growth on methanol is reducing-power limited (Peyraud et al. 2012; Skovran et al. 2010), it is likely that growth and yield on methanol and succinate is greater because the combination compensates for limitations posed by each substrate in isolation. Having determined the growth characteristics of mutants in methylotrophy-specific modules on either just C_1 or multi-C compounds, we proposed straightforward hypotheses for phenotypes during growth on the combination of C_1 and multi-C substrates.

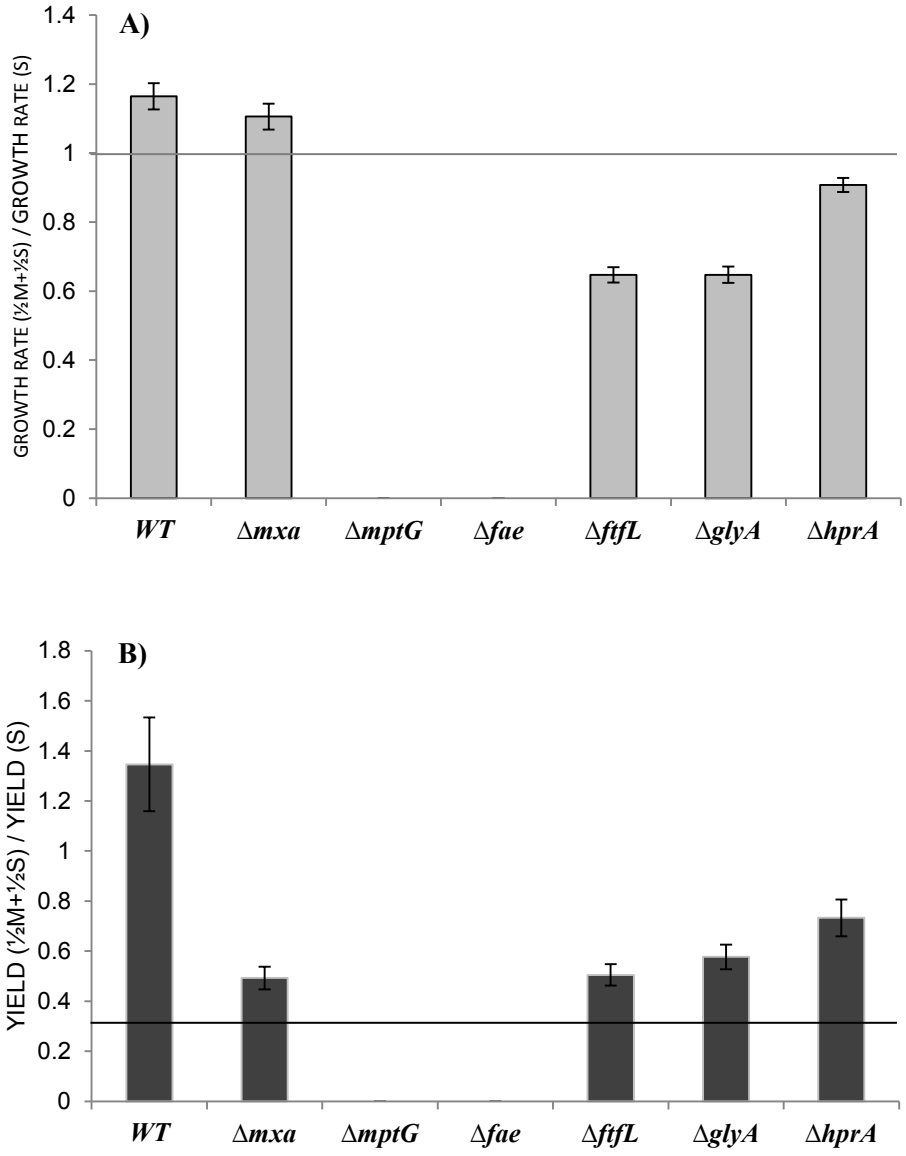

Figure 2.5: A) Ratio of growth rates, of the Δ*cel* 'wildtype' strain of PA1 and various knockout mutants, on a combination of ½M+½S (7.5 mM methanol + 1.75 mM succinate) versus S (3.5 mM succinate). The dotted line depicts the expected ratio for growth rate, if no methanol was oxidized in a combination of M+S**. B)** Ratio of yield (measured as the maximum OD_{600} value during growth), for the Δ*cel* 'wildtype' strain of PA1 and various knockout mutants, on M+S versus S. The dotted line depicts expected ratio for yields, if no methanol was assimilated in a combination of M+S. For all data error bars represent the 95% C.I. of the average ratio of three biological replicates grown in each condition.

Since the Δ*mxa* mutant was incapable of methanol growth, we anticipated that its growth rate on a combination of methanol and succinate would be the same as that on succinate, but with 50% lower yield since the combination contains half the concentration of succinate and methanol. While the observed yield on the combination matched the expected value, the Δ*mxa* mutant grew 11% faster ($p<0.001$) on the combination than in succinate alone (Figure 2.5a and 2.5b). One possibility is that methanol is either being sensed or oxidized by the XoxFI system -a MxaFI homolog that has been suggested to play a regulatory role in *M. extorquens* (Skovran et al. 2011, Schmidt et al. 2010). Next, we hypothesized that the C_1 assimilation mutants (i.e., Δ*ftfL,* Δ*glyA,* and Δ*hprA* mutants) might be able to grow faster on a combination of methanol and succinate because these mutants are capable of completely oxidizing methanol to generate reducing power. The ability to generate additional reducing power from methanol might also result in a proportional increase in the yield. Although yields on the combination of methanol and succinate were significantly elevated for the Δ*glyA* and Δ*hprA* strains, growth rate was compromised relative to succinate growth (Δ*ftfL* and Δ*glyA* by 35% and Δ*hprA* by 9%; Figure 2.5a). This partial methanol sensitivity, though not as severe as seen for H_4MPT mutants, may be due to build-up of (potentially toxic) C_1 intermediates and/or a regulatory mismatch between C_1 dissimilation and succinate assimilation. Future work will be required to understand the basis for these effects, and to determine whether they hold for other strains of *Methylobacterium*.

Conclusions

Aerobic methylotrophy is well studied in *M. extorquens* AM1; however, it also has a long history of laboratory domestication, and a bulky, flexible genome containing a large number of IS elements that pose challenges for both traditional genetic screens and selection for improved growth during laboratory evolution. *M. extorquens* PA1, a closely related strain, was recently isolated from the environment and overcomes these hurdles due to a streamlined, stable genome. Since extremely closely-related strains sometimes occupy distinct niches (Shapiro et al. 2012) and have distinct metabolic capabilities, we felt it was critical to compare the growth of PA1 and AM1 on a range of substrates in order to establish just

how much confidence one should have in transferring knowledge gained from the long-studied AM1 to the newer option of PA1. With the exception of a couple of C_1 substrates (methylamine, betaine) and nutrient broth, PA1 grew significantly faster, with significantly higher yields, than AM1. In general, growth rates and yield for AM1 might be slower due to mutations that occurred over the course of its 'laboratory domestication'. Notably, there are two non-synonymous substitutions in the *rpoB* gene, encoding one of the subunits of the RNA polymerase holoenzyme, which lead to rifamycin/rifampicin resistance. These substitutions involved in rifampicin/rifamycin resistance were recently shown to lead to slow growth (Carroll et al. 2014). The stark difference in growth rate and yield on substrates like betaine, methylamine, and ethanol between the two strains might reflect adaptation/s to unique ecological niches by each of these strains prior to isolation, such as via recent gain or loss of certain metabolic genes (Coleman et al. 2006) or differential regulation (Coleman et al. 2006). Although we present a case for PA1 being a more tractable system overall, these differences in substrate use would specifically make PA1 a better system in which to study ethanol metabolism, whereas betaine metabolism may be better addressed in AM1.

Our genetic analysis of methylotrophy in PA1 establishes that the roles of the various methylotrophy specific modules during C_1 growth are the same as described in AM1. In addition, owing to the quantitative nature of our analyses, several knockout mutants also revealed unexpected phenotypes on multi-C compounds as well as a combination of C_1 and multi-C compounds. These phenotypes point towards yet-undiscovered aspects of metabolism in these facultative methylotrophs in terms of regulation that allows cells to switch between C_1 metabolism and multi-C growth, as well as to establish balanced growth on multiple substrates simultaneously.

References

1. Peel D, Quayle JR (1961) Microbial growth on C_1 compounds. 1. Isolation and characterization of *Pseudomonas* AM1. Biochem J. 81: 465-469.

2. Large PJ, Quayle JR (1963) Microbial growth on C_1 compounds. 5. Enzyme activities in extracts of *Pseudomonas* AM1. Biochem J. 87: 386-396.

3. Johnson PA, Quayle JR (1964) Microbial growth on C_1 compounds. 6. Oxidation of methanol, formaldehyde, and formate by methanol-growth *Pseudomonas* AM1. Biochem J. 93: 281-290.

4. Anthony C (1982) The biochemistry of methylotrophs. Academic Press Ltd., London.

5. Marx CJ, Lidstrom ME (2001) Development of improved versatile broad host-range vectors for use in methylotrophs and other Gram-negative bacteria. Microbiology. 147: 2065-2075.

6. Marx CJ, Lidstrom ME (2002) Broad-host-range *cre-lox* system for antibiotic marker recycling in Gram-negative bacteria. Biotechniques. 33: 1062-1067.

7. Marx CJ, O'Brien BN, Breezee J, Lidstrom ME (2003) Novel methylotrophy genes of *Methylobacterium extorquens* AM1 identified by using transposon mutagenesis including a putative dihydromethanopterin reductase. J. Bacteriol. 185: 669-673.

8. Marx CJ, Lidstrom ME (2004) Development of an insertional expression vector system for *Methylobacterium extorquens* AM1 and generation of null mutants lacking *mtdA* and/or *fch*. Microbiology. 150: 9-19.

9. Marx CJ (2008) Development of a broad-host-range *sacB*-based vector for unmarked allelic exchange. BMC Res. Notes. 1: 1.

10. Choi YJ, Morel L, Bourque D, Mullick A, Massie B, Miguez CB (2006) Bestowing inducibility on the cloned methanol dehydrogenase promoter (P_{mxaF}) of *Methylobacterium extorquens* by applying regulatory elements of *Pseudomonas putida* F1. Appl. Environ. Microbiol. 72: 7723-7729.

11. Chubiz LM, Purswani J, Carroll SM, Marx CJ (2013) A novel pair of inducible expression vectors for use in *Methylobacterium extorquens*. BMC Res. Notes. 6: 183.

12. Kaczmarczyk A, Vorholt JA, Francez-Charlot A (2013) Cumate-inducible gene expression system for sphingomonads and other Alphaproteobacteria. Appl. Environ. Microbiol. 79: 6795-6802.

13. Delaney NF, Kaczmarek ME, Ward LM, Swanson PK, Lee M-C, Marx CJ (2013) Development of an optimized medium, strain, and high-throughput culturing methods for *Methylobacterium extorquens*. PLoS One. 8: e62957.

14. Lee M-C, Chou H-H, Marx CJ (2009) Asymmetric, bimodal trade-offs during adaptation of *Methylobacterium* to different growth substrates. Evolution. 63: 2816-2830.

15. Chistoserdova L, Chen SW, Lapidus A, Lidstrom ME (2003) Methylotrophy in *Methylobacterium extorquens* AM1 from a genomic point of view. J. Bacteriol. 185:2980-2987.

16. Chistoserdova L, Kalyuzhnaya MG, Lidstrom ME (2009) The expanding world of methylotrophic metabolism. Annu. Rev. Microbiol. 63: 477-499.

17. Vuilleumier S, Chistoserdova L, Lee M-C et al. (2009) *Methylobacterium* genome sequences: a reference blueprint to investigate microbial metabolism of C_1 compounds from natural and industrial sources. PLoS One. 4: e5584.

18. Lee M-C, Marx CJ (2012) Repeated, selection-driven genome reduction of accessory genes in experimental populations. PLoS Genetics. 8: e1002651.

19. Robinson DG, Lee M-C, Marx CJ (2012) OASIS: an automated program for global investigation of bacterial and archaeal insertion sequences. Nucleic Acids Res. 40: e174.

20. Chou H-H, Berthet J, Marx CJ (2009) Fast growth increases the selective advantage of a mutation arising recurrently during evolution under metal limitation. PLoS Genetics. 5: e1000652.

21. Chou H-H, Marx CJ (2012) Optimization of gene expression through divergent mutational paths. Cell Rep. 1: 133-140.

22. Lee M-C, Marx CJ (2013) Synchronous waves of failed soft sweeps in the laboratory: remarkably rampant clonal interference of alleles at a single locus. Genetics. 193: 943-952.

23. Carroll SM, Marx CJ (2013) Evolution after introduction of a novel metabolic pathway consistently leads to restoration of wild-type physiology. PloS Genet. 9: e1003427.

24. Carroll SM, Xue KS, Marx CJ (2014) Laboratory divergence of *Methylobacterium extorquens* AM1 through unintended domestication and past selection for antibiotic resistance. BMC Microbiol. 14: 2.

25. Marx CJ, Bringel F, Chistoserdova L et al. (2012) Complete genome sequences of six strains of the genus *Methylobacterium*. J. Bacteriol. 194: 4746-4748.

26. Knief C, Frances L, Vorholt JA (2010) Competitiveness of diverse *Methylobacterium* strains in the phyllosphere of *Arabidopsis thaliana* and identification of representative models, including *M. extorquens* PA1. Microb. Ecol. 60: 440-452.

27. Chistoserdova L, Vorholt JA, Thauer RK, Lidstrom ME (1998) C1 transfer enzymes and coenzymes linking methylotrophic bacteria and methanogenic archaea. Science. 281: 99-102.

28. Marx CJ, Chistoserdova L, Lidstrom ME (2003) Formaldehyde-detoxifying role of the tetrahydromethanopterin-linked pathway in *Methylobacterium extorquens* AM1. J. Bacteriol. 185: 7160-7168.

29. Chistoserdova L, Crowther GJ, Vorholt JA, Skovran E, Portais J-C, Lidstrom ME (2007) Identification of a fourth formate dehydrogenase in *Methylobacterium extorquens* AM1 and confirmation of the essential role of formate oxidation in methylotrophy. J. Bacteriol. 189: 9076-9081.

30. Marx CJ, Laukel M, Vorholt JA, Lidstrom ME (2003) Purification of the formate-tetrahydrofolate ligase from *Methylobacterium extorquens* AM1 and demonstration of its requirement for methylotrophic growth. J. Bacteriol. 185: 7169-7175.

31. Marx CJ, Van Dien SJ, Lidstrom ME (2005) Flux analysis uncovers key role of functional redundancy in formaldehyde metabolism, PloS Biol. 3: e16.

32. Crowther GJ, Kosaly G, Lidstrom ME (2008) Formate as the main branch point for methylotrophic metabolism in *Methylobacterium extorquens* AM1. J. Bacteriol. 190: 5057-5062.

33. Maden EH (2000) Tetrahydrofolate and tetrahydromethanopterin compared: functionally distinct carriers in C_1 metabolism. Biochem. J. 350: 609-629.

34. Delaney NF, Rojas Echenique JI, Marx CJ (2013) Clarity: an open-source manager for laboratory automation. J. Lab Autom. 18: 171-177.

35. Martinez-Gomez NC, Nguyen S, Lidstrom ME (2013) Elucidation of the role of methylene-tetrahydromethanopterin dehydrogenase MtdA in the tetrahydromethanopterin-dependent oxidation pathway in *Methylobacterium extorquens* AM1. J. Bacteriol.195:2359-2367.

36. Gruffaz C, Muller EEL, Louhichi-Jelail Y, Nelli YR, Guichard G, Bringel F (2014) Genes of the N-methylglutamate pathway are essential for growth of *Methylobacterium extorquens* DM4 on monomethylamine. Appl. Environ. Microbiol. 80:3541-3550.

37. Stieglitz B, Mateles RI (1973) Methanol metabolism in pseudomonad C. J. Bacteriol. 114: 390-398.

38. Zhang M, Lidstrom ME (2003) Promoters and transcripts for genes involved in methanol oxidation in *Methylobacterium extorquens* AM1. Microbiology. 149: 1033-1040.

39. Nunn DN, Lidstrom ME(1986) Isolation and complementation analysis of 10 methanol oxidation mutant classes and identification of the methanol dehydrogenase structural gene of *Methylobacterium* sp. strain AM1. J. Bacteriol. 166: 581-590.

40. Goodwin PM, Anthony C (1998) The biochemistry, physiology, and genetics of PQQ and PQQ-containing enzymes. Adv. Microb. Physiol. 40: 1-80.

41. Rasche ME, Havemann SA, Rosenzvaig M (2004) Characterization of two methanopterin biosynthesis mutants of *Methylobacterium extorquens* AM1 by use of a tetrahydromethanopterin bioassay. J. Bacteriol. 186: 1565-1570.

42. Vorholt JA, Marx CJ, Lidstrom ME, Thauer RK (2000) Novel formaldehyde-activating enzyme in *Methylobacterium extorquens* AM1. 182: 6645-6650.

43. Pomper BK, Vorholt JA, Chistoserdova L, Lidstrom ME, Thauer RK (1999) A methenyl tetrahydromethanopterin cyclohydrolase and a methenyl tetrahydrofolate cyclohydrolase in *Methylobacterium extorquens* AM1. Eur. J. Biochem. 261: 475-480.

44. Pomper BK, Vorholt JA (2001) Characterization of the formyltransferase from *Methylobacterium extorquens* AM1. Eur. J. Biochem. 268: 4769-4675.

45. Pomper BK, Saurel O, Milon A, Vorholt JA (2002) Generation of formate by the formyltransferase/hydrolase (Fhc) complex in *Methylobacterium extorquens* AM1.FEBS Lett. 523: 133-137.

46. Carroll SM, Lee M-C, Marx CJ (2013) Sign epistasis limits evolutionary trade-offs at the confluence of single- and multi-carbon metabolism in *Methylobacterium extorquens* AM1. Evolution. 68: 760-771

47. Kikuchi G (1973) The glycine cleavage system: composition, reaction mechanism, and physiological significance. Mol. Cell Biochem. 1: 169-187.

48. Peyraud R, Kiefer P, Christen P, Portais J-C, Vorholt JA (2012) Co-consumption of methanol and succinate by *Methylobacterium extroquens* AM1. PLoS ONE.7: e48271.

49. Skovran E, Crowther GJ, Guo X, Yang S, Lidstrom ME (2010) A systems biology approach to uncover cellular strategies used by *Methylobacterium extorquens* AM1 during the switch from multi- to single-carbon growth. PloS One. 5: e14091.

50. Skovran E, Palmer AD, Rountree AM, Good NM, Lidstrom ME (2011) XoxF is required for expression of methanol dehydrogenase in *Methylobacterium extorquens* AM1. J. Bacteriol. 193: 6032-6038.

51. Schmidt S, Christen P, Kiefer P, Vorholt JA (2010) Functional investigation of methanol dehydrogenase-like protein XoxF in *Methylobacterium extorquens* AM1. Microbiology. 156: 2575-2586.

52. Shapiro BJ, Friedman J, Cordero OX et al. (2012) Population genomics of early events in the ecological differentiation of bacteria. Science.336: 48-51.

53. Coleman ML, Sullivan MB, Martiny AC et al. (2006) Genomic islands and the ecology and evolution of *Prochlorococcus.* Science. 311: 1768-1770.

54. Agashe D, Martinez-Gomez NC, Drummond DA, Marx CJ (2013) Good codons, bad transcript: large reductions in gene expression and fitness arising from synonymous mutations in a key enzyme. Mol. Biol. Evol. 30: 549-560.

55. Gibson DG, Young L, Chuang RY et al. (2009) Enzymatic assembly of DNA molecules up to several hundred kilobases. Nat. Methods. 6: 343-345.

56. Figurski DH, Helinski DR (1979) Replication of an origin-containing derivative of plasmid RK2 dependent on a plasmid function provided *in trans*. PNAS.76: 1648-1652.

Chapter 3

Methylamine utilization via a linear *N*-methylglutamate pathway

in *Methylobacterium extorquens* PA1 does not require

the tetrahydrofolate-dependent C_1 transfer pathway

Methylamine utilization via a linear *N*-methylglutamate pathway in *Methylobacterium extorquens* PA1 does not require the tetrahydrofolate-dependent C_1 transfer pathway

Running title: Methylotrophic growth using a novel topology of C_1 pathways

Dipti D. Nayak[1] and Christopher J. Marx[1, 2, 3, 4, *]

[1]Organismic and Evolutionary Biology, Harvard University, Cambridge, MA, USA, [2]Faculty of Arts and Sciences Center for Systems Biology, Harvard University, Cambridge, MA, USA, [3]Biological Sciences, University of Idaho, Moscow, ID, USA, [4]Institute for Bioinformatics and Evolutionary Studies, University of Idaho, Moscow, ID, USA.

* Corresponding author: Biological Sciences, University of Idaho, Moscow, ID 83843, USA. Tel.: + 1 208 885 8594; Fax: + 1 208 885 7905; E-mail: cmarx@uidaho.edu

Abstract

Methylotrophs grow on reduced single carbon compounds like methylamine as the sole source of carbon and energy. In *Methylobacterium extorquens* AM1, the best-studied aerobic methylotroph, a periplasmic methylamine dehydrogenase that catalyzes the primary oxidation of methylamine to formaldehyde has been examined in great detail. However, recent metagenomic data from natural ecosystems is revealing the abundance and importance of lesser-known routes such as the *N*-methylglutamate pathway for methylamine oxidation. In this paper we use *M. extorquens* PA1, a strain closely related to *M. extorquens* AM1 but lacking the methylamine dehydrogenase, to dissect the genetics and physiology of the ecologically relevant *N*-methylglutamate pathway for methylamine oxidation. Phenotypic analyses of null mutants in genes encoding enzymes of the *N*-methylglutamate pathway strongly support a linear topology for the pathway in *M.extorquens* PA1. Furthermore, analysis of *M. extorquens* PA1 mutants with lesions in methylotrophy-specific dissimilatory and assimilatory modules suggested that, compared to other C_1-substrates, methylamine use via the *N*-methylglutamate pathway results in a shift of the branch point for C_1 metabolism from formate to formaldehyde and/or methylene tetrahydrofolate (CH_2=H_4F). Due to this shift, the C_1 flux emerging from the *N*-methylglutamate pathway is routed through the pre-existing metabolic network in a novel fashion where a complete H_4F-mediated pathway for C_1 assimilation is no longer needed. Additionally, we present genetic evidence that formaldehyde-activating enzyme (FAE) homologs might be involved in methylotrophy. Null mutants revealed that FAE and FAE2 influence growth rate and FAE3 influences yield during growth of *M. extorquens* PA1 on methylamine.

Introduction

Methylated amines are a large group of biologically, industrially, and environmentally relevant compounds. The simplest methylated amine, (mono-) methylamine (MA), is produced by anaerobic bacteria that decarboxylate nitrogenous organic matter in the gastrointestinal tract or animal waste, and decompose methylated osmolytes such as glycine betaine in the marine environment (Ge et al. 2011;

Oremland et al. 1982). In addition, a growing fraction of MA is also being released during the degradation of nitrogen containing herbicides and pesticides (Chen et al. 2010a), biomass combustion (Ge et al. 2011), and industrial processes such as fish processing. MA also plays an important role in the global carbon and nitrogen budget (Oremland et al. 1982; Neff et al. 2002). However, MA does not accumulate in aerobic environments (Neff et al. 2002) because it gets rapidly consumed by methylotrophs, that oxidize reduced single-carbon or C_1 substrates to produce biomass and CO_2 (C. Anthony 1982), and serves as a nitrogen source for several classes of aerobic microorganisms (Chen et al. 2010b; Y. Chen 2012).

There are three well-characterized enzymes/pathways used by methylotrophs to oxidize MA. In many gram-negative methylotrophs, such as *Methylobacterium extorquens* AM1 (hereafter AM1), MA is oxidized by a periplasmic dehydrogeanse (MaDH) (Eady and Large 1962; Chistoserdov et al. 1991) to formaldehyde. Methylamine oxidase, a Cu-containing enzyme present in Gram-positive methylotrophs (Van Iersel et al. 1986) and methylotrophic yeast (Cai et al. 1994) oxidizes MA to formaldehyde (Dooley et al. 1990) in a single step as well. In contrast, the *N*-methylglutamate (NMG) pathway, originally described in *Pseudomonas* spp. (now *Aminobacter* sp. (Shaw et al. 1966)), is a complex, multi-step pathway in which the methyl group from MA is transferred to glutamate to form two novel amino acid derivatives - NMG and γ-glutamylmethylamide (GMA) - which are then oxidized to release formaldehyde (Bamforth and O'Connor 1979). The NMG pathway involves at least three unique enzymes: *N*-methylglutamate synthase, *N*-methylglutamate dehydrogenase, and γ-glutamylmethylamide synthetase (Chen et al. 2010a; Latypova et al. 2010; Martinez-Gomez et al. 2013; Gruffaz et al. 2014). While the enzymes involved in the NMG pathway were purified and characterized over three decades ago (Hersh et al. 1971; Pollock and Hersh 1973; Bamforth and Large 1977a; Bamforth and Large 1977b; Kung and Wagner 1969; Boulton et al. 1979), the genes were discovered very recently (Chen et al. 2010a; Latypova et al. 2010; Gruffaz et al. 2014). Genes encoding the enzymes of the NMG pathway are often clustered in a ~10 kb genomic region (Figure 3.1).

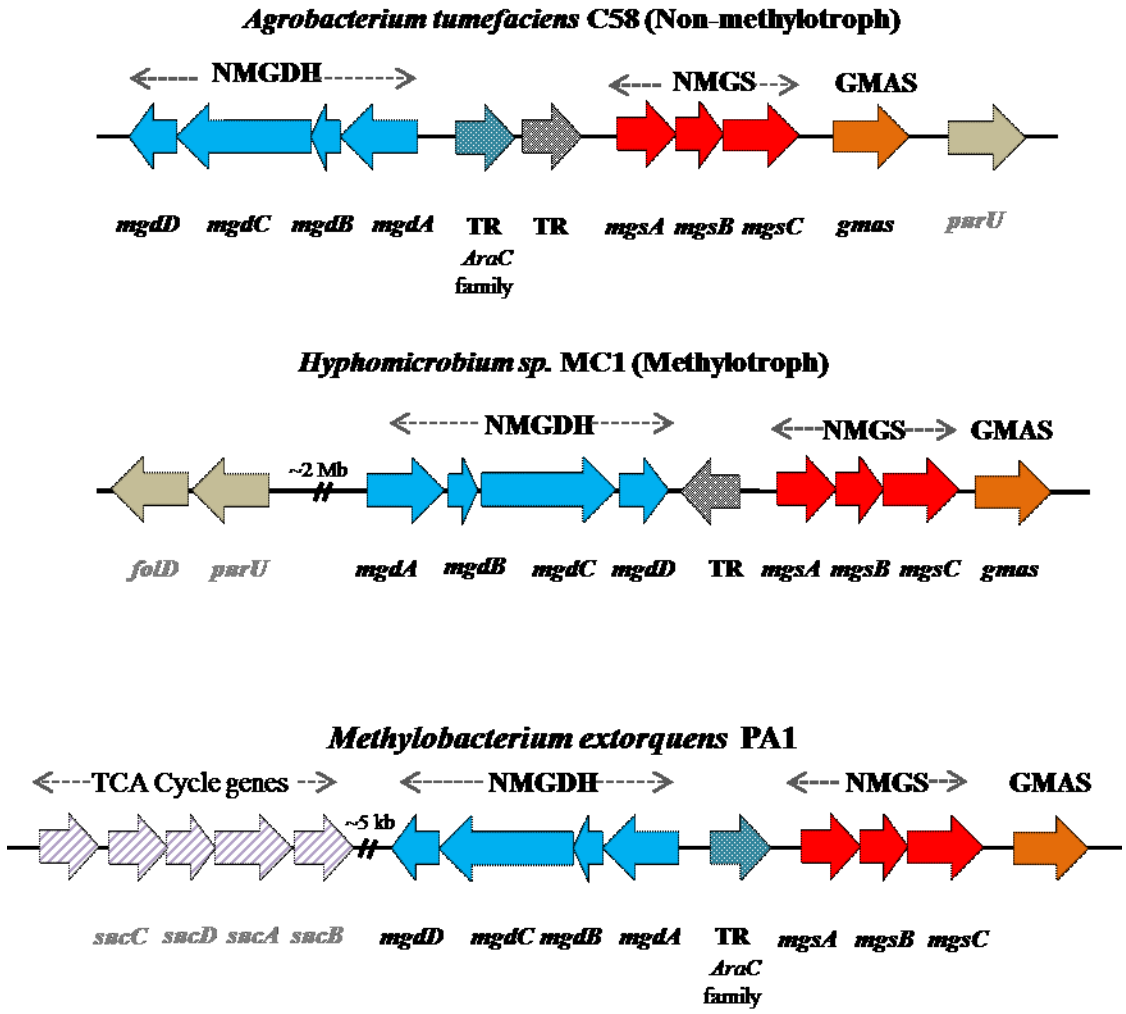

Figure 3.1: Arrangement of genes encoding the *N*-methylglutamate pathway on the chromosome of non-methylotrophic proteobacteria (like *Agrobacterium tumefaciens*) and methylotrophic proteobacteria (like *Hyphomicrobium sp.* MC1 and *Methylobacterium extroquens* PA1). Blue: genes encoding the four subunits of *N*-methylglutamate dehydrogenase (*mgdABCD)*, red: genes encoding the three subunits of *N*-methylglutamate synthase *(mgsABC)*, and orange: a single gene encoding the γ-glutamylmethylamide synthetase (*gmaS)*.

NMGDH: *N*-methylglutamate dehydrogenase, NMGS: *N*-methylglutamate synthase, GMAS: γ-glutamylmethylamide synthetase, TR: Transcriptional regulator, *purU:* formyl-tetrahydrofolate hydrolase, *folD*: bi-functional methylene tetrahydrofolate dehydrogeanse and methenyl tetrahydrofolate cyclohydrolase, and TCA: Tri-carboxylic acid cycle.

A sarcosine oxidase-like group of four genes encode the *N*-methylglutamate dehydrogeanse (*mgdABCD),* a glutamate synthase-like group of three genes encode the *N*-methylglutamate synthase (*mgsABC)* and a glutamine synthetase-like gene encodes the γ-glutamylmethylamide synthetase (*gmaS)*. Since the discovery of the NMG pathway gene cluster, sequence based analysis has revealed that the NMG pathway is present in a large fraction of methylotrophs (even those containing MADH) as well as non-methylotrophs where it serves to extract the nitrogen from MA (Chen et al. 2010b).

Recent genetic analyses of the NMG pathway have produced somewhat contradictory results in terms of its topology. A study using *Methyloversatilis universalis* FAM5 (a facultative methylotroph of the Betaproteobacteria) (Latypova et al. 2010) showed that the enzyme γ-glutamylmethylamide synthetase was not essential for MA growth using the NMG pathway. This observation supported a branched topology for the NMG pathway (Figure 3.2a): MA flux gets partitioned to NMG (via *N*-methylglutamate synthase) and GMA (via γ-glutamylmethylamide synthetase) and each of these amino acid derivatives, independently, get oxidized to formaldehyde. However, in *Methylocella silvestris* BL2 (a facultative methanotroph of the Alphaproteobacteria) (Chen et al. 2010a) and very recently, *Methylobacterium extroquens* DM4 (hereafter DM4) (Gruffaz et al. 2014), γ-glutamylmethylamide synthetase was shown to be essential for MA growth. These studies supported a linear topology for the NMG pathway (Figure 3.2b) where GMA, not MA, is the true substrate for *N*-methylglutamate synthase (Pollock and Hersh 1971) and *N*-methylglutamate dehydrogenase is the sole enzyme involved in dissimilation. A linear topology for the NMG pathway was further corroborated by the absence of an additional GMA dissimilating enzyme in many NMG pathway-containing methylotrophs (Chen et al. 2010a).

Additionally, uncertainty surrounding the end-product of methylamine oxidation via the NMG pathway has occluded our understanding of how the NMG pathway feeds into the C_1 assimilatory and dissimilatory modules. For a long time, it was assumed that methylamine oxidation mediated by the NMG pathway led to the production of formaldehyde (Bamforth and Large 1977a).

Figure 3.2: A) A branched version of the *N*-methylglutamate pathway*:* each of the two degenerate branches, in two enzymatic steps, oxidizes methylamine to formaldehyde. In gray, an additional enzyme required for γ-glutamylmethylamide dissimilation in a branched version of the *N*-methylglutamate pathway is indicated. This enzyme has not been found in *M. extorquens* species yet. **B)** A linear version of the *N*-methylglutamate pathway: a single branch with three enzymes mediates the oxidation of methylamine to formaldehyde. **C)** Optical Density (OD_{600}) versus time plots for three replicate cultures of i) the Δ*cel* 'wildtype' strain of *M. extroquens* PA1 (black) ii) the Δ*mgsABC* mutant (red), iii) the Δ*gmas* mutant (orange) and iv) the Δ*mgsABC*-Δ*gmas* double mutant (purple) in nitrogen-free media with 3.5 mM succinate and 7.66 mM methylamine. **D)** The topology of the *N*-methylglutamate pathway in *M. extroquens* PA1 is linear; *N*-methylglutamate synthase is capable of synthesizing *N*-methylglutamate from γ-glutamylmethylamide (black arrow) as well as methylamine (gray arrow) albeit only in the Δ*gmas* mutant.

NMGDH: *N*-methylglutamate dehydrogenase, MGS: *N*-methylglutamate synthase, GMAS: γ-glutamylmethylamide synthetase, NMG: *N*-methylglutamate, GMA: γ-glutamylmethylamide

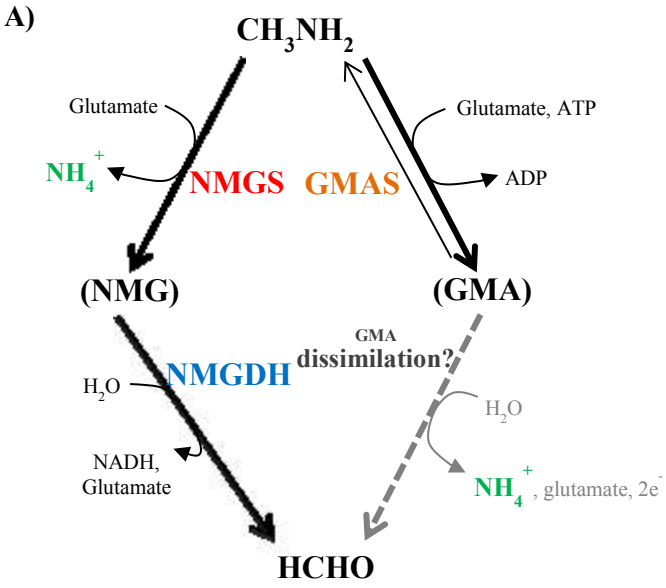
A)
CH_3NH_2
Glutamate
NH_4^+
NMGS
GMAS
Glutamate, ATP
ADP
(NMG)
(GMA)
GMA dissimilation?
H_2O
NMGDH
NADH, Glutamate
H_2O
NH_4^+, glutamate, $2e^-$
HCHO

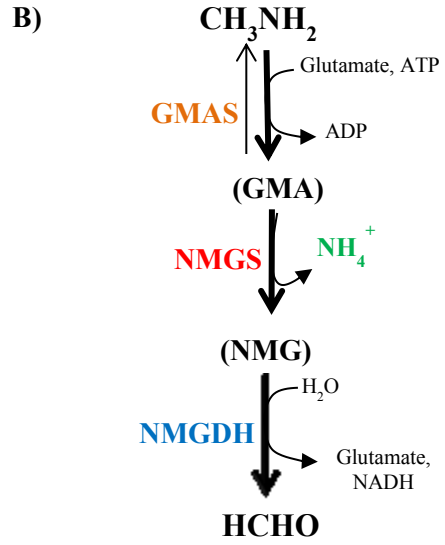
B)
CH_3NH_2
GMAS
Glutamate, ATP
ADP
(GMA)
NMGS
NH_4^+
(NMG)
H_2O
NMGDH
Glutamate, NADH
HCHO

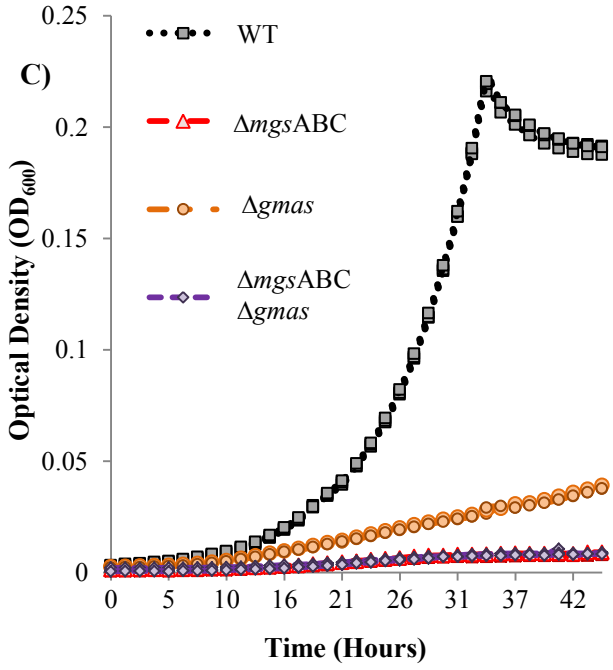
C)
0.25
0.2
0.15
0.1
0.05
0
Optical Density (OD_{600})
WT
Δ*mgs*ABC
Δ*gmas*
Δ*mgs*ABC Δ*gmas*
0
5
10
16
21
26
31
37
42
Time (Hours)

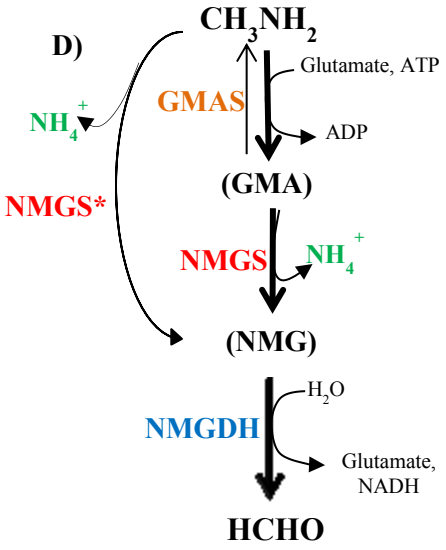
D)
CH_3NH_2
NH_4^+
GMAS
Glutamate, ATP
ADP
(GMA)
NMGS*
NMGS
NH_4^+
(NMG)
H_2O
NMGDH
Glutamate, NADH
HCHO

Then, as observed during methanol growth in *M. extorquens* species (Nayak and Marx 2014), the tetrahydromethanopterin (H_4MPT)-dependent formaldehyde oxidation pathway (Marx et al. 2003a) would serve as the primary dissimilatory module. Formate, thus produced, would be incorporated into biomass through the H_4F-dependent C_1 assimilation pathway (Marx et al. 2003b; Marx et al. 2005; Crowther et al. 2008) and the serine cycle (Chistoserdova et al. 2003) (Figure S2.1, Appendix 2). Of late, genes encoding a dissimilatory version of the H_4F-dependent C_1 transfer pathway (Vannelli et al. 1999) (characterized by the presence of *folD* and *purU* instead of *mtdA*, *fch*, and *ftfL*) have been found in the vicinity of the NMG pathway gene cluster (Latypova et al. 2010) (Figure 3.1). Additionally, *N*-methylglutamate dehydrogenase (*mgdC*) contains a tetrahydrofolate (H_4F) binding domain and produces CH_2=H_4F in the presence of H_4F *in vitro* (Latypova et al. 2010). In light of these recent findings, CH_2=H_4F, instead of formaldehyde, has been proposed as the end product of the NMG pathway. Like in the case of chloromethane metabolism by *M. extroquens* CM4 (Vannelli et al. 1999; Studer et al. 2002), CH_2=H_4F as the end-product of primary oxidation would seem to circumvent the need for a H_4MPT-dependent formaldehyde oxidation pathway. A portion of the CH_2=H_4F would get directly assimilated via the serine cycle, while the rest would be oxidized by the dissimilatory branch of the H_4F-dependent C_1 transfer pathway (Figure S2.2, Appendix 2). However, with burgeoning sequence data, we now know that methylotrophs, including *Methyloversatilis universalis* FAM5 (the source of the NMGDH assayed *in vitro*) that encode the NMG pathway often do not contain either *folD* or *purU* (data not shown). How do these methylotrophs oxidize CH_2=H_4F to formate, then? Or does MA oxidation via the NMG pathway lead to the production of some free formaldehyde, instead?

In order to better understand how the NMG pathway operates *in vivo*, we genetically dissected its physiology in *M. extorquens* PA1 (hereafter PA1). Although PA1 utilizes methanol in the same way as the better characterized AM1 strain (Nayak and Marx 2014), here we find that it lacks methylamine dehydrogenase and only possesses the NMG pathway for MA use. By creating mutant strains with lesions in one or more genes of the NMG pathway and assaying the growth patterns of each of these strains on

MA, we uncovered that the NMG pathway has a linear topology in PA1 akin to that very recently suggested for DM4 and *M. silvestris* BL2. MA growth of null mutants in genes encoding enzymes of modules involved in C_1 transfer pathways revealed a novel pattern; the H_4MPT-dependent formaldehyde oxidation pathway was required for C_1 dissimilation whereas an intact H_4F-mediated C_1 transfer pathway was not required for either formate assimilation or dissimilation of CH_2=H_4F. Further, we unveiled that homologs of FAE (Formaldehyde Activating Enzyme) (Vorholt et al. 2000), often found in genomes of methylotrophs (FAE2, FAE3), (Kalyuzhnaya et al. 2005; Chistoserdova et al. 2009) play a functional role during methylamine growth using the NMG pathway. The presence of either FAE or FAE2 significantly increased growth rate but not yield on methylamine whereas the presence of FAE3 increased yield on methylamine.

Materials and Methods

Bacterial Strains and Growth Conditions

Strains relevant to this study included the following: the Δ*cel* strain of the pink-pigmented 'wildtype' stock of *M. extorquens* AM1 (CM2720), the Δ*cel* strain of the pink-pigmented 'wildtype' stock of *M. extorquens* PA1 (CM2730) as described elsewhere (Delaney et al. 2013a). Unless specified, all growth conditions utilized a modified version of Hypho minimal medium consisting of: 100 mL phosphate salts solution (25.3 g of KH_2PO_4 plus 22.5 g Na_2HPO_4 in 1L deionized water), 100 mL sulfate salts solution (5 g of $(NH_4)_2SO_4$ and 2 g of $MgSO_4 \cdot 7\ H_2O$ in 1L deionized water), 799 mL of deionized water, and 1 mL of trace metal solution (Agashe et al. 2013)). A nitrogen-free version of the modified Hypho minimal media used the same recipe as above but with a nitrogen-free sulfate salts solution: (7 g of $MgSO_4 \cdot 7\ H_2O$ in 1L deionized water).All components were autoclaved separately before mixing under sterile conditions. Filter-sterilized carbon sources were added just prior to inoculation in liquid minimal media with a final concentration of: 3.5 mM sodium succinate, 15 mM methylamine hydrochloride, 15 mM methanol, and 3.5 mM sodium succinate with 7.66 mM methylamine as a nitrogen source.

Growth Rate Measurements

Apart from growth on methylamine as a carbon source, all other growth measurements were conducted using an automated growth platform (Delaney et al. 2013b). All growth regimes consisted of three cycles consisting of inoculation, acclimation, and growth measurement. All strains were stored in vials at -80 °C in 10% DMSO; growth was initiated by transferring 10 μL freezer stock into 10mL of Hypho medium with 3.5 mM succinate in 50 mL flasks (covered with a 50 mL plastic beaker) in a shaking incubator at 225 r.p.m. and maintained at 30ºC. Upon reaching stationary phase (~2 days), cultures were transferred 1:64 into fresh medium (in 48-well microtiter plates- CoStar 3548) with the carbon source to be tested to a final volume of 640 μL, allowed to reach saturation in this acclimation phase, and diluted 1:64 again into fresh medium for the measured (experimental) growth. The 48-well microtiter plates were incubated in a room maintained at 30ºC and 80% humidity in an incubation tower (Liconic USA LTX44 with custom fabricated cassettes) shaking at 650 rpm (Delaney et al. 2013b).The increase in OD_{600} for strains grown in 48-well microtiter plates was measured using an automated, robotic culturing and monitoring system (Delaney et al. 2013b). A series of robotic instruments (including a shovel, a transfer station, and a twister arm), all controlled by Clarity, were used to move the 48-well plates from the incubation tower to a Perkin-Elmer Victor2 plate reader for optical density (OD_{600}) measurements. The dynamics and specific growth rate of cultures were calculated from the log-linear growth phase using an open source, custom-designed growth analysis software called CurveFitter available at http://www.evolvedmicrobe.com/CurveFitter/ .

Growth on methylamine as a carbon source was below the detection threshold of the automated growth platform described above. Growth from freezer stocks at -80 ºC was initiated by transferring 10 μL freezer stock into 10 mL of Hypho medium with 3.5 mM succinate in 50 mL flasks (covered with a 50 mL plastic beaker) in a shaking incubator at 225 r.p.m. and maintained at 30ºC. Upon reaching stationary phase (~2 days), cultures were transferred 1:16 into 9.4 mL fresh medium with 20 mM methylamine hydrochloride and allowed to reach saturation in this acclimation phase (~3 days), and diluted 1:16 again

into 9.4 mL fresh medium with 15 mM methylamine for the measured (experimental) growth (~3 days). A 50 µL aliquot of three replicate cultures, for each strain, was sampled every 8-10 hours during the growth phase. Optical Density of the culture was measured at 600 nm (OD_{600}) using a spectrophotometer (Bio-Rad). The dynamics and specific growth rate of cultures were calculated from the log-linear growth phase. Yield (Max OD_{600}) was measured as the maximum OD_{600} during the growth phase. Growth rate and yield reported for each strain and condition is the mean calculated from three biological replicates, unless otherwise noted.

Methanol and Methylamine Shock Experiments

10 µL of the freezer stock of CM3803 (Δ*mptG* in CM2730) and CM 2730 were grown in 48-well microtiter plates with 3.5 mM succinate as the carbon source. . Upon reaching stationary phase (~2 days) CM3803 and CM2730 were transferred 1:64 into 630 µL of fresh medium with 3.5 mM succinate in two 48-well microtiter plates. After 12 hours of incubation, a pulse of methanol resulting in a final concentration of: a) 1 mM methanol, b) 5 mM methanol , c) 10mM methanol , and d) 50 mM methanol was added to triplicate cultures of CM3803 and CM2730 in one 48-well plate. Similarly, after 12 hours of incubation, a pulse of methylamine resulting in a final concentration of: a) 1 mM methylamine, b) 5 mM methylamine , c) 10mM methylamine , and d) 50 mM methylamine was added to triplicate cultures of CM3803 and CM2730 in the other 48-well plate. Triplicate control wells of CM2730 and CM3803 (to which no methanol and methylamine were added) were maintained in each 48-well plate as well. The increase in OD_{600} was measured as described earlier.

Generation of Mutant Strains

M. extorquens PA1 deletion mutants lacking *mgsABC*, *fae2*, *fae3*, *gmaS* and *mgdABCD* were generated on the genetic background of CM2730 using the allelic exchange vector pCM433 (C. J. Marx 2008). The double deletion mutants lacking *fae* and *fae2* or *fae3* were generated on the genetic background of CM3753 (Δ*fae* in CM2730) using the allelic exchange vector pCM433 (C. J. Marx 2008). The double

deletion mutants lacking *fae2* and *fae3* was generated on the genetic background of CM3757 (Δ*fae2* in CM2730) using the allelic exchange vector pCM433 (C. J. Marx 2008). The double deletion mutants lacking *mgsABC* and *gmaS* was generated on the genetic background of CM3733 (Δ*mgsABC* in CM2730) using the allelic exchange vector pCM433 (C. J. Marx 2008).The triple deletion mutants lacking *fae, fae2,* and *fae3* were generated on the genetic background of CM4208 (Δ*fae*Δ*fae3* in CM2730) using the allelic exchange vector pCM433 (C. J. Marx 2008). A region upstream and downstream of each of these genes or operons of ~0.5 kb was amplified using PCR. The forward primer for the upstream flank was designed to have a 30 bp long sequence at the 5' end homologous to the sequence upstream of the *Not*I cut site in pCM433. The reverse primer for the upstream flank was designed to have a 30 bp sequence at the 5' end homologous to the first 30 bp of the downstream flank. The reverse primer for the downstream flank was designed to have a 30 bp long sequence at the 5' end homologous to the sequence downstream of the *Not*I cut site in pCM433. The PCR products representing the upstream and downstream flank were simultaneously ligated into the pCM433 vector cut with *Not*I using a three-part Gibson assembly protocol described elsewhere (Gibson et al. 2009). Cloning the upstream and downstream flanks for *fae2, fae3, mgsABC, gmaS* and *mgdABCD* in pCM433 resulted in pDN51, pDN52, pDN53, pDN54, pDN55, respectively. Mutant strains of *M. extorquens* PA1 were made by introducing the appropriate donor constructs through conjugation by a tri-parental mating between the NEB 10β competent cells (New England Biolabs, Ipswich, MA) containing the donor construct, an *E. coli* strain containing the conjugative plasmid pRK2073, and PA1 as described elsewhere (C. J. Marx 2008). All mutant strains were confirmed by a diagnostic PCR analysis and validated by Sanger sequencing the mutant locus. All strains and plasmids used and generated for this study are listed in Table 3.1.

Results

M. extorquens PA1 uses a linear version of the *N*-methylglutamate pathway for methylamine utilization

Table 3.1: *M. extorquens* strains and plasmids used in this study

Strain or plasmid	Description	Reference
Strains		
CM2730	Δ*cel M.extorquens* PA1	Delaney et al. 2013
CM3733	[a]Δ*mgsABC*	This study
CM3753	Δ*fae*	Nayak and Marx 2014
CM3757	Δ*fae2*	This study
CM3761	Δ*fae3*	This study
CM3765	Δ*gmaS*	This study
CM3769	Δ*mgdABCD*	This study
CM3773	Δ*ftfL*	Nayak and Marx 2014
CM3799	Δ*glyA*	Nayak and Marx 2014
CM3803	Δ*mptG*	Nayak and Marx 2014
CM3835	Δ*mgsABC*, Δ*gmaS*	This study
CM4208	Δ*fae*, Δ*fae3*	This study
CM4230	Δ*fae*, Δ*fae2*	This study
CM4232	Δ*fae2*, Δ*fae3*	This study
CM4244	Δ*fae*, Δ*fae2*, Δ*fae3*	This study
Plasmids		
pCM433	Allelic exchange vector (tet^R, Suc^S)	C. J. Marx 2008
pDN50	pCM433 with Δ*fae* upstream and downsteam flanks	Nayak and Marx 2014
pDN51	pCM433 with Δ*fae*2 upstream and downsteam flanks	This study
pDN52	pCM433 with Δ*fae*3 upstream and downsteam flanks	This study
pDN53	pCM433 with Δ*mgsABC* upstream and downsteam flanks	This study
pDN54	pCM433 with Δ*gmaS* upstream and downsteam flanks	This study
pDN55	pCM433 with Δ*mgdABCD* upstream and downsteam flanks	This study
pRK2073	Helper plasmid (IncP, *tra*)	Figurski and Helinksi 1979

[a]All manipulations made in the CM2730 background.

Our strain of PA1 lacking the *cel* locus encoding cellulose biosynthesis (to prevent clumping and permit accurate measurement of growth characteristics; simply referred to as WT here) (Delaney et al. 2013a) could grow on 15 mM MA with an average growth rate of 0.042 h^{-1}, and an average final OD_{600} of 0.712 (three biological replicates throughout unless otherwise noted). A 10 kb genomic region encoding enzymes of the NMG pathway was recently characterized in DM4 during the preparation of this manuscript (Gruffaz et al. 2014). In PA1, a completely syntenic cluster of nine genes (of which eight had >95% amino acid identity and one had ~93% amino acid identity to the corresponding genes in DM4) encoding the enzymes of the NMG pathway was observed as well (Figure 2.1). To determine if the NMG pathway is active and involved in MA oxidation, we made and tested the growth of null mutants lacking individual enzymes of the NMG pathway on MA. No growth or measurable change in OD_{600} was observed for the Δ*mgdABCD* mutant, the Δ*mgsABC* mutant, or the Δ*gmaS* mutant on MA as the sole carbon source. Contrary to studies in other methylotrophs (Latypova et al. 2010), we did not detect any growth for the Δ*gmaS* mutant on any concentration of MA ranging from 1 to 25 mM after 7 days, or after a14 day incubation on 15 mM MA. The essential role of all three enzymes (especially GMAS) for methylamine oxidation supported a linear topology for the NMG pathway in PA1.

In order to even more sensitively test whether MA could be converted by mutant strains, we took advantage of the fact that MA can also be used as a nitrogen source given that ammonia (NH_4^+) ions are a by-product of MA oxidation (Figure 3.2a, 3.2b). When MA is used only as a nitrogen source in the presence of another carbon source, the stoichiometric ratio of biomass (A. C. Redfield 1958) and carbon yield of the serine cycle (Van Dien and Lidstrom 2002) indicates that cells need to intake 15-20 fold more carbon than nitrogen. As a result, growth on succinate with MA as a nitrogen source is 5-fold faster than on MA as a carbon source, requires a 3-4 fold lower rate of MA conversion and is still contingent on a functional NMG pathway. We leveraged these fast growth conditions to detect subtle phenotypes for NMG pathway null mutants and further verify the linear topology of the NMG pathway. If the NMG pathway is linear then neither the Δ*mgsABC* mutant nor the Δ*gmaS* mutant should be able to use MA as a

nitrogen source (Figure 3.2a). If the NMG pathway is branched then, both, the Δ*mgsABC* mutant and the Δ*gmaS* mutant should be able to use MA as a nitrogen source (Figure 3.2b). While the Δ*mgsABC* mutant and the Δ*mgsABC*-Δ*gmaS* double mutant could not use MA as a nitrogen source (Figures 3.2c), the Δ*gmaS* mutant grew poorly in succinate with MA as the nitrogen source without the typical log-linear growth characteristics (Figure 3.2c). The marginal ability of the Δ*gmaS* mutant to use MA as a nitrogen source indicated that the conversion of MA to NMG (with a concomitant release of NH_4^+) catalyzed by NMGS is physiologically relevant only when GMAS is absent. Additionally, the inability of the Δ*mgsABC* mutant to use MA as a nitrogen source corroborated the lack of a GMA-dissimilating enzyme in PA1. Altogether, these data are congruent with a linear topology for the NMG pathway in PA1 as indicated in Figure 3.2d.

The H_4MPT-dependent formaldehyde oxidation pathway is required during growth on MA with the NMG pathway

It was recently proposed that, instead of formaldehyde, the oxidized C_1 compound emerging from the NMG pathway might actually be CH_2=H_4F (Latypova et al. 2010). If so, this end-product should obviate the H_4MPT-mediated formaldehyde oxidation pathway during MA growth. We tested the hypothesis that MA growth mediated by the NMG pathway avoids formaldehyde production by examining a mutant lacking *mptG* (encoding β-ribofuranosylaminobenzene 5'-phosphate synthase: the first enzyme of the H_4MPT biosynthesis pathway (Rasche et al. 2004). Previous work with AM1 has shown that methanol oxidation leads to formaldehyde buildup and rapid cell death in the Δ*mptG* mutant, and that MA has the same effect, albeit to a lesser extent (Marx et al. 2003a). We measured the capacity of the Δ*mptG* mutant in PA1 to withstand conditions that might lead to the production of variable amounts of formaldehyde at different rates.

First, we tested the capacity of the Δ*mptG* mutant to tolerate different doses of methanol shock and MA shock during growth on a multi-carbon substrate (succinate). As had been seen with AM1, even a pulse of

1 mM methanol completely inhibited the growth of the Δ*mptG* mutant of PA1 on succinate (Figure 3.3a). In contrast, a pulse of 50 mM MA did not impede the growth of the Δ*mptG* mutant in succinate (Figure 3.3b). Since the Δ*mptG* mutant was resilient to MA shock, we then tested whether it could use MA as the sole nitrogen source. WT, the Δ*mptG* mutant, and the Δ*mgsABC* mutant, were grown to saturation on succinate with NH_4^+ as the nitrogen source, and were then diluted 64-fold in media with succinate as the carbon source and MA as the sole nitrogen source. After ~16 hours, the Δ*mgsABC* mutant could no longer grow whereas WT and the Δ*mptG* mutant continued to grow (Figure 3.3c). These growth data suggested that once the internal nitrogen reservoir ran out, the Δ*mptG* mutant could still use MA as a nitrogen source; growth was moderately compromised (23% slower on succinate with MA as the nitrogen source compared to NH_4^+ as the nitrogen source; $p<0.001$ for the difference in mean growth rate of three biological replicates compared using the Student's t-test). The growth defect incurred by using MA versus NH_4^+ as a nitrogen source for the Δ*mptG* mutant was more severe than for WT, where growth on succinate with MA as the nitrogen source was merely 11% slower than with NH_4^+ as the nitrogen source ($p=0.001$) (Table S2.1, Appendix 2).

Next, we examined the ability of the Δ*mptG* mutant strain to grow on MA as the sole carbon source. No observable growth or significant change in OD_{600} was detected for the Δ*mptG* mutant strain on MA as a carbon source (Figure 3.4). In order to quantify the extent of H_4MPT-dependent formaldehyde oxidation required during MA growth we used a strain lacking *fae* (encoding formaldehyde-activating enzyme that catalyzes the condensation of free formaldehyde with H_4MPT (Vorholt et al. 2000)). A marginal rate of CH_2=H_4MPT production can be sustained by the spontaneous condensation of formaldehyde and H_4MPT in a Δ*fae* mutant (Vorholt et al. 2000). Therefore, the *fae* deletion only partially abolishes the H_4MPT dependent formaldehyde oxidation pathway and leads to an intermediate mutant phenotype in terms of methanol sensitivity (Marx et al. 2003a). Unlike the Δ*mptG* strain, the *fae* deletion showed WT-like MA growth (Figure 3.4).

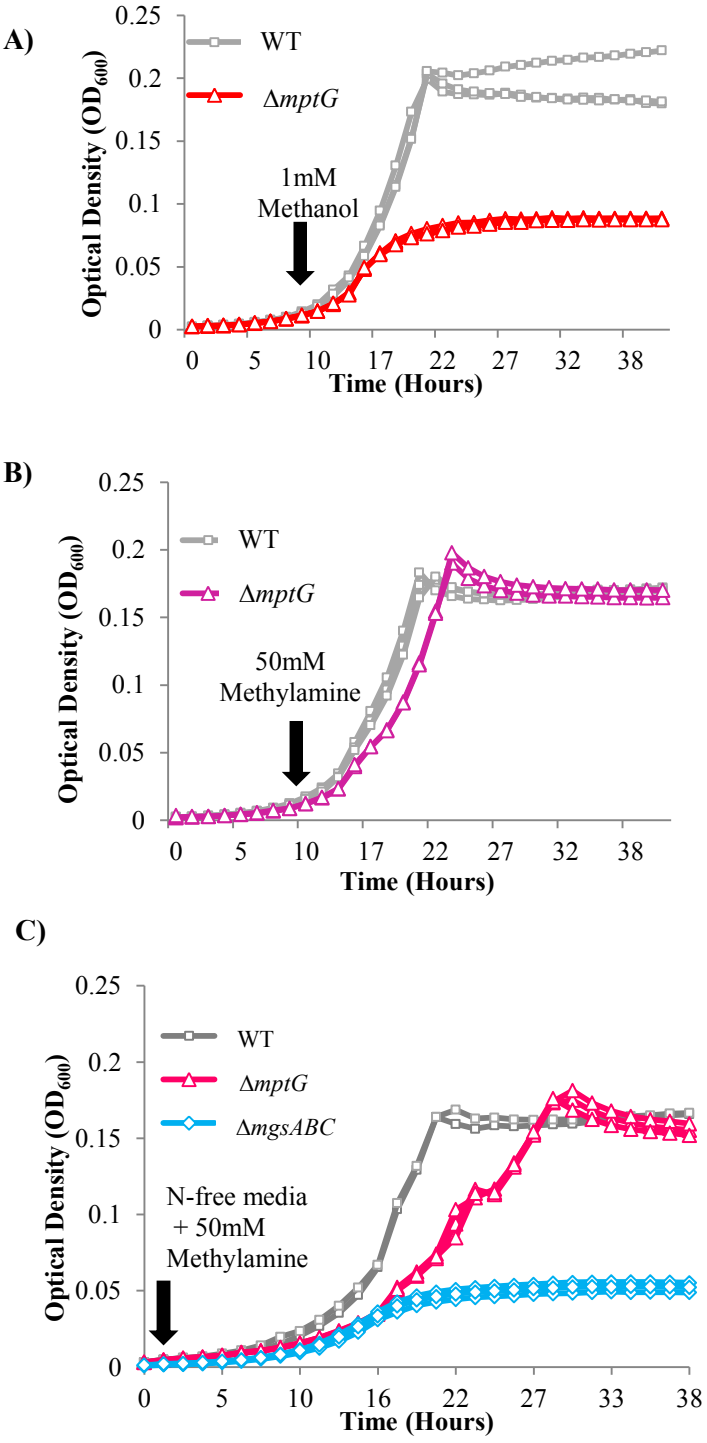

Figure 3.3: A) Optical Density (OD_{600}) versus time plots for three replicate cultures of the Δ*cel* 'wildtype' strain of PA1 (gray) and the Δ*mptG* mutant (red) in media with 3.5mM succinate. A pulse of 1mM methanol was added to the growth media 12 hours after incubation (as indicated by the arrow). **B)** Optical Density (OD_{600}) versus time plots

(**Figure 3.3 Continued)** for three replicate cultures of the Δ*cel* 'wildtype' strain of PA1 (gray) and the Δ*mptG* mutant (purple) in media with 3.5mM succinate. A pulse of 50mM methylamine was added to the growth media 12 hours after incubation (as indicated by the arrow). **C)** Three replicate cultures of the Δ*cel* 'wildtype' strain of PA1 (gray), the Δ*mptG* mutant (pink) and the Δ*mgsABC* mutant (blue), grown to saturation in media with 3.5mM succinate, were transferred ($1/64^{th}$ fold dilution) to nitrogen-free media with 3.5mM succinate and 50mM methylamine (as indicated by the arrow). The Optical Density (OD_{600}) versus time plots follow growth of each of these three genotypes in nitrogen-free media with 3.5mM succinate and 50mM methylamine.

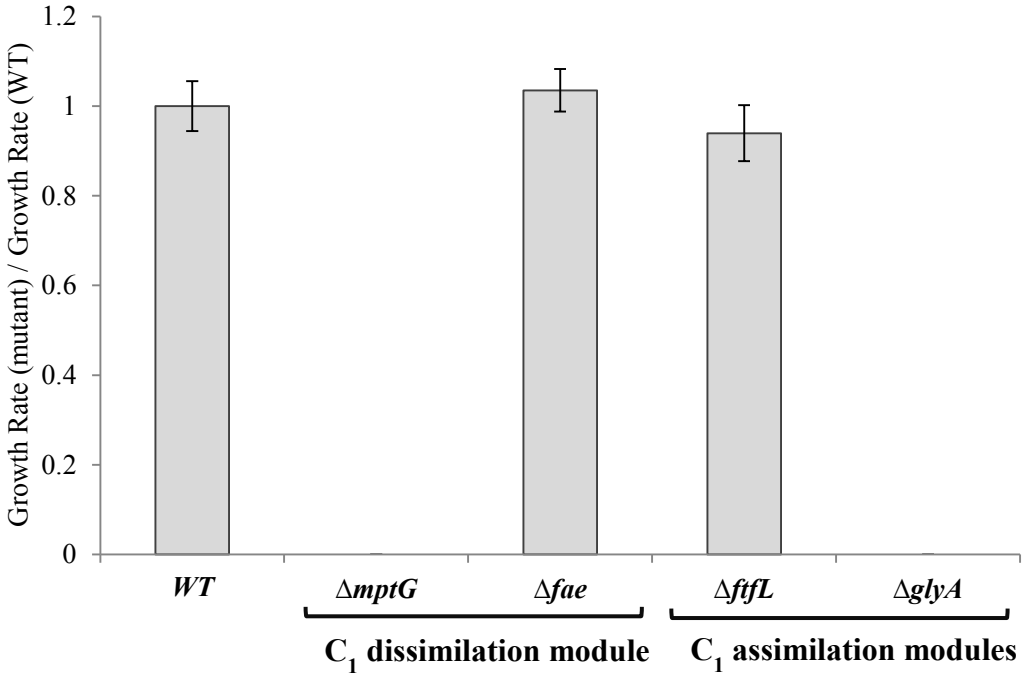

Figure 3.4: Growth rate of mutants with lesions in various methylotrophy specific modules relative to the Δ*cel* 'wildtype' strain of PA1on 15 mM methylamine. The Δ*fae* and Δ*mptG* mutants represent partial/complete lesions in the H_4MPT dependent pathway for formaldehyde oxidation (or C_1 dissimilation) respectively. The Δ*ftfL* mutant represents a lesion in the H_4F dependent pathway for formate assimilation and the Δ*glyA* mutant represents a lesion in the serine cycle for C_1 assimilation. Error bars represent the 95% C.I of the mean ratio of triplicate cultures for each condition.

During MA growth, the absolute requirement for the H_4MPT-mediated formaldehyde oxidation pathway indicates that at least some of the carbon from MA is ending up as formaldehyde, but the slow rate of formaldehyde oxidation needed can be sustained in the absence of FAE.

An intact H_4F pathway is not required for assimilation or dissimilation during methylamine growth of *M. extorquens* PA1

Growth of *M. extorquens* on any methylotrophic compound yet tested requires an intact H_4F pathway for either assimilation (i.e., methanol growth) (Marx et al. 2003) or dissimilation (i.e., chloromethane growth by CM4) (Studer et al. 2002). Given that at least some of the carbon from MA appears to require the H_4MPT pathway for dissimilation, we tested whether a complete H_4F-dependent C_1 transfer pathway was also required for MA growth. A strain lacking *ftfL* (encoding formyl-tetrahydrofolate ligase that catalyzes the reduction of formate and free H_4F to formyl-H_4F in an ATP-dependent manner (Marx et al. 2003b)) cannot grow on C_1 compounds like methanol and formate (Nayak and Marx 2014) because of an early block in assimilation (Marx et al, 2003b). Contrary to other C_1 compounds, the Δ*ftfL* mutant could not only grow on MA, but at a rate indistinguishable from WT ($p = 0.8887$). In contrast, a mutant lacking *glyA* (encoding serine hydroxymethyltransferase (Chistoserdova and Lidstrom 1994)) was incapable of MA growth, confirming that C_1 units are still assimilated via the serine cycle. These data, especially the non-essentiality of *ftfL*, indicate that use of the NMG pathway for MA growth involves a novel flow of carbon through the C_1-specific metabolic pathways such that the H_4MPT-dependent pathway handles oxidation, and CH_2=H_4F enters directly into the serine cycle. This observation is consistent with a shift in the branch-point of metabolism from formate to either formaldehyde or CH_2=H_4F (or both) during MA growth, as depicted in Figure 3.5c and 3.5d.

FAE-homologs play a functional role during MA growth in PA1

Do any unique gene products play a role in rerouting carbon through the C_1-specific metabolic pathways when the NMG pathway operates?

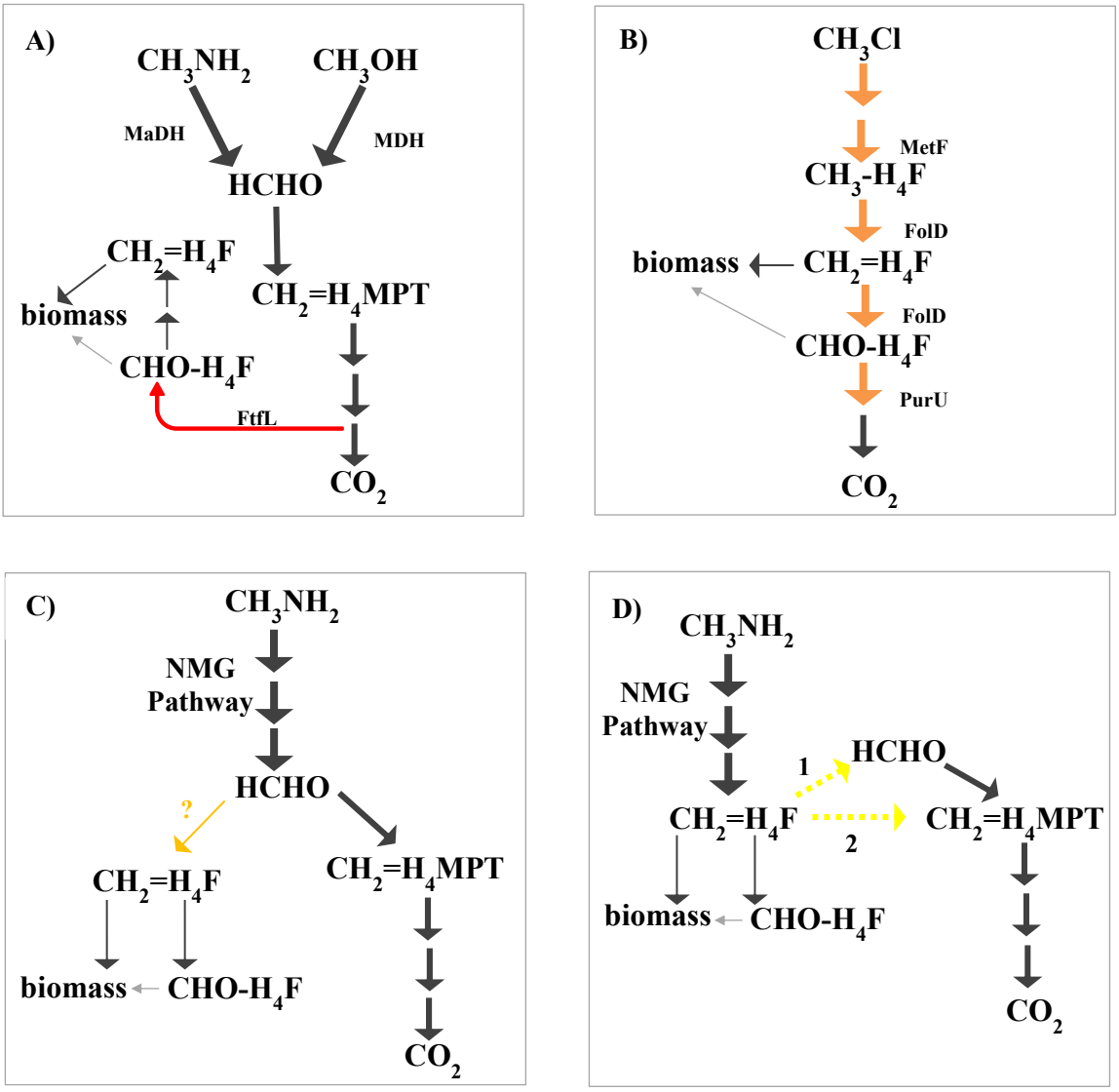

Figure 3.5: A) A schematic representation of methanol, and MaDH mediated methylamine metabolism in *M. extroquens* species. The thickness of arrows represents the flux through each reaction. Primary oxidation generates free formaldehyde which is oxidized to formate by the H_4MPT dependent C_1 dissimilation pathway. Formate is reduced by the H_4F dependent C_1 assimilation pathway and assimilated using the serine cycle. The reaction highlighted in red, mediated by FtfL (formyl tetrahydrofolate ligase), is unique to this topology. **B)** A schematic representation of chloromethane metabolism in *M. extroquens* CM4. The thickness of arrows represents the flux through each reaction. Primary oxidation produces H_4F derivatives, using a H_4F dependent C_1 dissimilation pathway, and completely bypasses formaldehyde production. Methylene tetrahydrofolate (CH_2=H_4F) is assimilated

Figure 3.5(Continued) using the serine cycle. The reactions highlighted in orange - catalyzed by enzymes of the H_4F dependent C_1 dissimilatory pathway (MetF, FolD and PurU) - are unique to this topology. **C)** A schematic representation of the metabolic network involved in methylamine growth if the end-product of the *N*-methylglutamate pathway is formaldehyde. The thickness of arrows represents the flux through each reaction. The condensation of formaldehyde and H_4F to form $CH_2=H_4F$, highlighted in orange, is unique to this topology. **D)** A schematic representation of the metabolic network involved in methylamine growth if the end-product of the *N*-methylglutamate pathway is $CH_2=H_4F$. The thickness of arrows represents the flux through each reaction. $CH_2=H_4F$ enters the H_4MPT mediated C_1 assimilation pathway either by dissociation to formaldehyde (Reaction 1) or by a direct cofactor switch (Reaction 2). These two alternate reactions, indicated in yellow dashed arrows, are unique to this topology. In PA1, the topology of methylamine metabolism *in vivo*, could also be a linear combination of the topology shown in C) and D) if the NMG pathway formaldehyde as well as $CH_2=H_4F$ during primary oxidation of methylamine.

Many methylotrophs, including PA1, have two distant FAE homologs – *fae*2 (Mext_3143) and *fae3* (Mext_1450) – in the genome, yet their role in methylotrophy, if any, remains unknown (Kalyuzhnaya et al. 2005; Chistoserdova et al. 2004). We hypothesized that these gene products may play a role during MA growth, perhaps catalyzing some of the novel reactions in Figure 3.5c and Figure 3.5d. To test our hypothesis, we deleted *fae*, *fae2*, and *fae3* individually and in all possible combinations (Figure 3.6a, 3.6b), and tested the growth of each of these mutants on 15 mM MA. Neither *fae2* nor *fae3* were essential for MA growth since all the single-, double- and triple-knockout mutants could grow on MA. Growth rates of strains encoding either one of *fae* or *fae2* were indistinguishable from or significantly higher than PA1 in the case of the Δ*fae2* mutant (12%; $p = 0.0108$). However, mutant strains lacking both *fae* and *fae2* showed a significant growth defect on MA (Figure 3.6a). In addition, all mutant strains lacking *fae3* showed a significant yield (maximum OD_{600}) defect relative to WT on MA (Figure 3.6b).To determine whether the role of *fae2*, and *fae3* in methylotrophy was limited to growth on MA via the NMG pathway, we tested the growth of each of these mutants on another C_1 compound (methanol), a multi-C compound (succinate), and succinate with MA as the nitrogen source (Figure S2.3, Appendix 2). As expected (Marx

et al. 2003a), strains with a *fae* deletion did not grow on methanol. Deleting either *fae2* or *fae3* led to a 5-10% growth rate defect on methanol (with no significant change in yield) but, the Δ*fae2*-Δ*fae3* mutant recovered to be indistinguishable from WT terms of growth rate (p=0.644) (Figure S2.3, Appendix 2). All mutants grew significantly slower than WT on succinate whereas only the double- and triple-knockout mutants grew significantly slower than WT on succinate while using MA as a nitrogen source (Figure S2.3, Appendix 2). No significant change in yield was observed for any mutant (relative to WT) during growth on succinate (either with NH_4^+ or MA as the nitrogen source). Therefore, FAE and FAE homologs influence a combination of growth and yield on many different compounds but the phenotypic effect of each mutant varies based on the growth conditions tested.

Figure 3.6

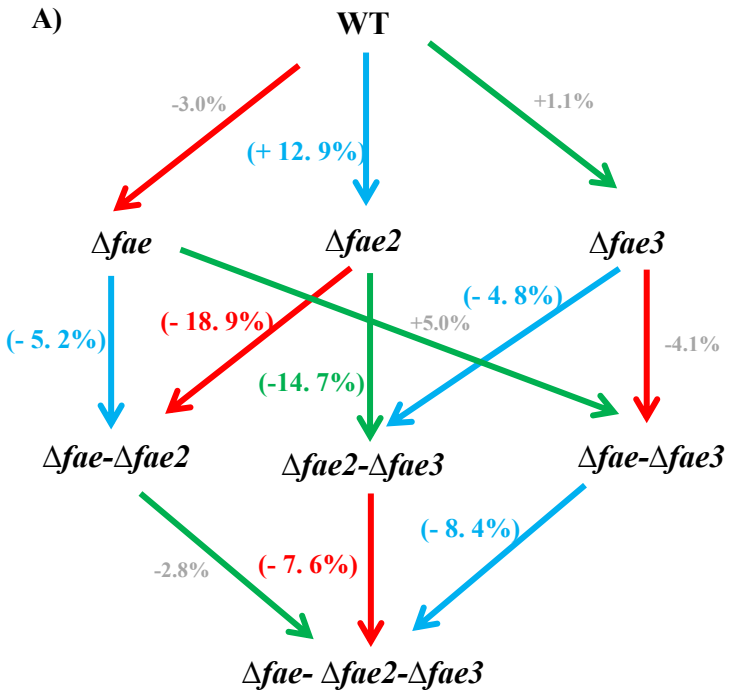

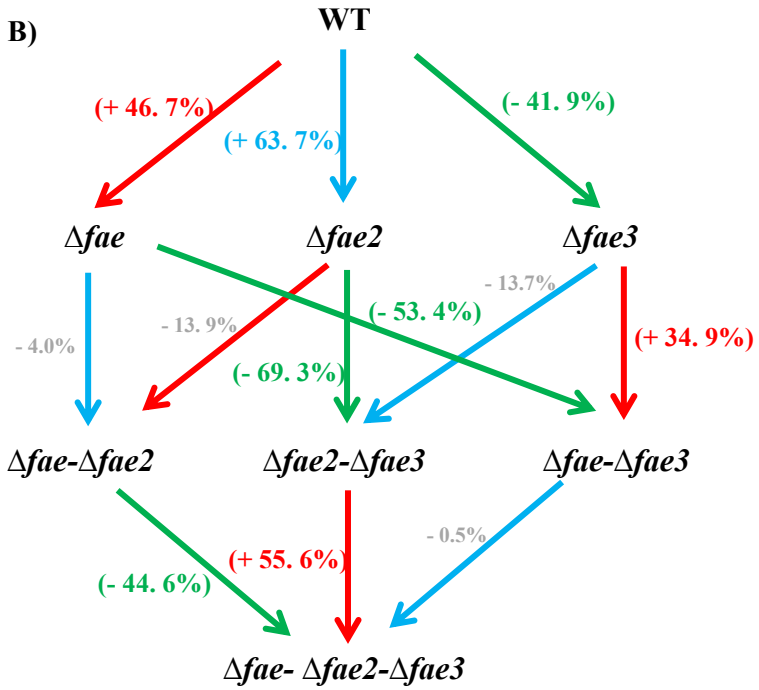

Figure 3.6(Continued): **A)** Arrows labelled in red, blue, green represent a Δ*fae,* Δ*fae2*, and Δ*fae3* deletion in the genomic background from which the arrow originates. Numbers and signs on the arrows represent the percentage increase/decrease in growth rate as a result of the gene deletion. Percentage values shown in bold, brackets indicate a p-value < 0.05 (difference in growth rate of three replicate cultures of the two strains being compared using the Student's t-test). Percentage values shown in gray indicate that the difference in growth rate between the two strains is not significant or p > 0.05. **B)** Arrows labelled in red, blue, green represent a Δ*fae,* Δ*fae2*, and Δ*fae3* deletion in the genomic background from which the arrow originates, respectively. Numbers and signs on the arrows represent the percentage increase/decrease in yield as a result of the gene deletion. Percentage values shown in bold, brackets indicate a p-value < 0.05 (difference in maximum OD_{600} of three replicate cultures of the two strains being compared using the Student's t-test). Percentage values shown in gray indicate that the difference in yield between the two strains is not significant or p > 0.05.

Discussion

In this study we dissected the genetics of the NMG pathway mediating slow MA growth in PA1. All three enzymes of the NMG pathway – NMGS, NMGDH, and GMAS – were essential for using MA as a carbon source, but only NMGDH and NMGS were absolutely essential for using MA as a nitrogen source. These results corroborate the findings of a recent study of the NMG pathway in DM4 (Gruffaz et al. 2014). In DM4 though, it was suggested that a distant *gmaS* homolog (found in all sequenced *M. extroquens* species) partially compensates for a *gmaS* deletion and enables the Δ*gmaS* mutant to use MA as a nitrogen source at much slower rates compared to WT. We observed that the slow, steadily decelerating growth rate of the Δ*gmaS* mutant (Figure 3.2c), in succinate with MA as the nitrogen source, was completely abolished in a Δ*gmaS*-Δ*mgsABC* mutant. Our data supports the notion that NMGS has a physiologically relevant – albeit low – k_{cat} for the conversion of MA to NMG *in vivo* only in the absence of GMAS. In the presence of GMAS, instead of MA, GMA is the true substrate for NMGS. The precision of our automated growth measurement platform (Delaney et al. 2013b) along with a screen that coupled fast growth to a reduced demand upon the NMG pathway (using MA as a nitrogen source in the presence of an alternate carbon source) revealed that the NMG pathway has a linear topology in PA1, akin to that proposed for *M. silvestris* BL2 (Chen et al. 2010a), and very recently DM4 (Gruffaz et al. 2014). This genetic evidence for a linear topology for the NMG pathway (Figure 3.2d) might also explain: a) the extremely low specific activity observed for the conversion of MA and glutamate to NMG by NMGS *in vitro* (Pollock and Hersh 1971) and b) accumulation of GMA in Δ*mgs* mutants (Latypova et al. 2010).

While it has been demonstrated in other systems (Latypova et al. 2010) that the NMG pathway produces CH_2=H_4F, neither FolD nor PurU – enzymes known to work in the dissimilatory direction of the H_4F dependent C_1 transfer pathway to generate formate – are encoded in the PA1 genome. We also observed that the H_4MPT-dependent C_1 dissimilatory module was essential but that deletion of a complete H_4F-

dependent C_1 assimilation pathway had no effect upon growth on MA (Figure 3.4). This result led us reevaluate if $CH_2=H_4F$ really was the end product of the NMG pathway in PA1. The extreme formaldehyde sensitivity of a mutant incapable of synthesizing H_4MPT (Δ*mptG* mutant) – a cofactor involved in formaldehyde oxidation (Marx et al. 2003a, Rasche et al. 2004) – was leveraged to identify whether formaldehyde is generated by the NMG pathway. The Δ*mptG* mutant could not grow on MA as a carbon source but could use MA as a nitrogen source (Figure 3.3c, 3.4). Additionally, a strain with a partial lesion in the H_4MPT mediated formaldehyde oxidation pathway (Δ*fae)* could still grow on MA. These data suggest that at least some formaldehyde is generated during MA growth, but unlike methanol growth (where the Δ*fae* mutant cannot grow) it is likely that either a) less than 100% of MA is oxidized to formaldehyde and/or b) the rate of formaldehyde production is low enough to be sustained by a spontaneous reaction with H_4MPT and H_4F. The rate of formaldehyde production is likely to be even lower when MA is used as a nitrogen source; perhaps low enough that the flux can be handled by non-specific aldehyde dehydrogenases. However, given the reactive nature of formaldehyde, it is almost impossible to resolve whether formaldehyde is generated as the direct end-product (Figure 3.5c) or by the dissociation of $CH_2=H_4F$ (Figure 3.5d). Alternately, we cannot rule out a third scenario where $CH_2=H_4F$ is the end product of the NMG pathway and a methylene transfer occurs to generate $CH_2=H_4$MPT. In this case, *mptG* would be essential for MA growth but not *fae*, which is consistent with our data as well.

Typically, based on whether formaldehyde or $CH_2=H_4F$ is produced as the end-product of primary oxidation, one of two distinct topologies is used for methylotrophic metabolism in *M. extorquens* species (Figure 3.5a, 3.5b). The key difference between the two topologies is whether C_1 flux is channeled through an assimilatory or dissimilatory branch of the H_4F dependent C_1 transfer pathway. In this study we have uncovered a novel topology of C_1 use in PA1 that completely avoids the H_4F-dependent C_1 pathway for net dissimilation or assimilation (Figure 3.5c, 3.5d).

Finally, this paper is the first to report functional roles for FAE homologs (FAE2, FAE3) that are often found in the genomes of methylotrophs. FAE2 and FAE appear to play somewhat redundant roles during

MA growth – positively reinforcing growth rates but not yield (Figure 3.6a). Three of the four key residues that make and stabilize contact with the methyl groups of H_4MPT in FAE (Acharya et al. 2005) are conserved or similar in FAE2 (Figure S2.4, Appendix 2). Therefore, FAE2 could either be an enzyme like FAE but with different kinetic parameters or perhaps a regulator that changes the expression of the H_4MPT-dependent formaldehyde oxidation pathway by sensing one or both of H_4MPT and CH_2=H_4MPT. FAE3 appears to play a distinct role from FAE and FAE2 by only impacting yield during MA growth (Figure 3.6b), and thus likely has a different biochemical function. Specific residues that allow FAE to distinguish H_4MPT and H_4F (Acharya et al. 2005) are not conserved in FAE3. It is thus unlikely to be involved in the H_4MPT dependent formaldehyde oxidation pathway, and may work as either an enzyme or regulator of the H_4F pathway. Further investigation will be required to uncover the precise physiological roles and underlying biochemistry of FAE2 and FAE3.

Extremely slow MA growth (t_D ~1 day) when MA oxidation is mediated by the NMG pathway had occluded the genetic and physiological analysis of methylamine growth mediated by this pathway. Of late though, the NMG pathway is going through a phase of rediscovery in light of its importance in several environmental regimes (Y. Chen 2012; Vorobev et al. 2013; L. Chistoserdova 2011). While various studies with different model systems (Latypova et al, 2010; Martinez-Gomez et al. 2013; Gruffaz et al. 2014) have dissected the genomics, genetics, and physiology of the NMG pathway in isolation, we extended this genetic approach to understand how NMG-dependent MA metabolism links to central C_1-specific metabolic pathways in PA1. Unlike all previously documented instances of methylotrophy, we found that cells simultaneously require the H_4MPT-dependent formaldehyde oxidation pathway and the serine cycle, but do not need to move C_1 units through an intact H_4F dependent C_1 transfer pathway for either assimilation or dissimilation. Our work highlights that a single set of metabolic modules can be used in distinct configurations to route C_1 flux in different ways depending upon the growth substrate in question.

References

1. **Ge X., A. S. Wexler, and S.L. Clegg.** 2011. Atmospheric amines- Part I. A review. Atmospheric Environment **45:**524-546.

2. **Oremland R. S., L. M. Marsh, and S. Polcin.** 1982. Methane production and simultaneous sulphate reduction in anoxic, salt marsh sediments. Nature **296:**143-145.

3. **Chen Y., J. Scanlan , L. Song, A. Crombie, M.T. Rahman, H. Schafer, and J.C. Murrell.** 2010. Γ-glutamylmethylamide is an essential intermediate in the metabolism of methylamine by *Methylocella silvestris.* Appl. Environ. Microbiol. **76:**4350-4357.

4. **Neff J. C., E. A. Holland, F. J. Dentener, W. H. McDowell, and K. M. Russell.** 2002. The origin, composition and rates of organic nitrogen deposition: A missing piece of the nitrogen cycle? Biogeochemistry. **57-58:**99-136.

5. **Anthony C.** 1982. The biochemistry of methylotrophs. Academic Press Ltd., London.

6. **Chen Y., K.L. McAleer, and J. C. Murrell.** 2010. Monomethylamine as a nitrogen source for the nonmethylotrophic bacterium, *Agrobacterium tumefaciens.* Appl. Environ. Microbiol. **76:**4102-4104.

7. **Y. Chen.** 2012. Comparative genomics of methylated amine utilization by marine *Roseobacter* clade bacteria and development of functional gene markers (*tmm, gmaS)*. Environ. Microbiol. **14:** 2308-2322.

8. **Eady R. R., and P. J. Large.** Purification and properties of an amine dehydrogeanse from *Pseudomonas* AM1 and its role in growth on methylamine. 1968. Biochem J. **106:**245-255.

9. **Chistoserdov A. Y., Y.D. Tsygankov, and M. L. Lidstrom.** 1991. Genetic organization of methylamine utilization genes from *Methylobacterium extorquens* AM1. J. Bacteriol. **173:**5901-5908.

10. **Van Iersel J., R. A. van der Meek, and J A. Duine.** 1986. Methylamine oxidase from *Arthrobacter* P1. A bacterial copper-quinoprotein amine oxidase. Eur. J. Biochem. **161:**415-419.

11. **Cai D., and J. P. Klinman.** 1994. Copper amine oxidase: heterologous expression, purification, and characterization of an active enzyme in *Saccharomyces cerevisiae*. Biochemistry. **33:**7647-7653.

12. **Dooley D. M., W.S. McIntire, M. A. McGuirl, C. E Cote, and J. L. Bates.** 1990. Characterization of the active site of *Arthrobacter* P1 methylamine oxidase: evidence for copper-quinone interactions. J. Am. Chem. Soc. **112:**2782-2789.

13. **Shaw W.V., L. Tsai, and R. R. Stadtman.** 1966. The enzymatic synthesis of *N*-methylglutamic acid. J. Biol. Chem. **241:**935-945.

14. **Bamforth C. W., and M. L. O'Connor.** 1979. The isolation of pleiotropic mutants of *Pseudomonas aminovorans* deficient in the ability to grow on methylamine and an examination of their enzymic constitution. Microbiology **110:**143-149.

15. **Latypova E., S. Yang, Y. S. Wang, T. Wang, T. A. Chavkin, M. Hackett, H. Schafer, and M. G. Kalyuzhnaya.** 2010. Genetics of the glutamate-mediated methylamine utilization pathway in the

facultative methylotrophic beta-proteobacteria *Methyloversatilis universalis* FAM5. Mol. Microbiol. **75:**426-439.

16. **Martinez-Gomez N. C., S. Nguyen, and M. E Lidstrom.** 2013. Elucidation of the role of methylene-tetrahydromethanopterin dehydrogenase MtdA in the tetrahydromethanopterin-dependent oxidation pathway in *Methylobacterium extorquens* AM1. J. Bacteriol.**195:**2359-2367.

17. **Gruffaz C., E.E. L. Muller, Y. Louhichi-Jelail, Y. R. Nelli, G. Guichard, and F. Bringel.** 2014. Genes of the *N*-methylglutamate pathway are essential for growth of *Methylobacterium extorquens* DM4 on monomethylamine. Appl. Environ. Microbiol. **80:**3541-3550.

18. **Hersh L.B., J. A. Peterson, and A. A. Thompson.** 1971. An *N*-methylglutamate dehydrogenase from *Pseudomonas* M.A. Archives of Biochemistry and Biophysics. **145:**115-120.

19. **Pollock R J., and L. B. Hersh.** 1973. *N*-methylglutamate synthetase. The use of flavin mononucleotide oxidative catalysis. J. Biol. Chem. **248:**6724-6733.

20. **Bamforth C. W., and P. J. Large.** 1977. Solubilization, partial purification, and properties of *N*-methylglutamate dehydrogeanse from *Pseudomonas aminovorans*. Biochem. J. **161:**357-370.

21. **Bamforth C. W., and P. J. Large.** 1977. The molecular size of *N*-methylglutamate dehydrogenase of *Pseudomonas aminovorans*. Biochem. J. **167:**509-512.

22. **Kung H-F., and C. Wagner.** 1969. Γ-glutamylmethylamide. A new intermediate in the metabolism of methylamine. J. Biol. Chem. **244:**4136-4140.

23. **Boulton C. A., G. W. Haywood, and P. J. Large.** 1979. *N*-methylglutamate dehydrogeanse, a flavoprotein purified from a new pink trimethylamine-utilizing bacterium. Microbiology. **117:**293-304.

24. **Pollock R. J., and L. B. Hersh.** 1971. *N*-methylglutamate synthetase. Purification and properties of the enzyme. J. Biol. Chem. **246:**4737-4743.

25. **Nayak D. D., and C. J. Marx.** 2014. Genotypic and phenotypic comparison of methylotrophy between *Methylobacterium extorquens* strains AM1 and PA1. **In revision for PloS ONE**

26. **Marx C. J., L. Chistoserdova, and M. E. Lidstrom.** 2003. Formaldehyde-detoxifying role of the tetrahydromethanopterin-linked pathway in *Methylobacterium extorquens* AM1. J. Bacteriol. **185:**7160-7168.

27. **Marx C. J., M. Laukel, J. A. Vorholt, and M. E. Lidstrom.** 2003. Purification of the formate-tetrahydrofolate ligase from *Methylobacterium extorquens* AM1 and demonstration of its requirement for methylotrophic growth. J. Bacteriol. **185:**7169-7175.

28. **Marx C. J., S. J. Van Dien, and M. E. Lidstrom.** 2005. Flux analysis uncovers key role of functional redundancy in formaldehyde metabolism, PloS Biol. **3:**e16.

29. **Crowther G. J., G. Kosaly, and M. E. Lidstrom.** 2008. Formate as the main branch point for methylotrophic metabolism in *Methylobacterium extorquens* AM1. J. Bacteriol. **190:**5057-5062.

30. **Chistoserdova L.**, **S. W. Chen, A. Lapidus, and M. E. Lidstrom.** 2003. Methylotrophy in *Methylobacterium extorquens* AM1 from a genomic point of view. J. Bacteriol. **185:**2980-2987.

31. **Vannelli T., M. Messmer, A. Studer, S. Vuilleumier, and T. Leisinger.** 1999. A corrinoid-dependent catabolic pathway for growth of a *Methylobacterium* strain with chloromethane. PNAS **96:**4615-4620.

32. **Studer A., C. McAnulla, R. Buchele, T. Leisinger, and S. Vuilleumier.** 2002. Chloromethane-induced genes define a third C1 utilization pathway in *Methylobacterium chloromethaanicum* CM4. J. Bacteriol. **184:**3476-3484.

33. **Kalyuzhnaya M. G., N. Korotkova, G. Crowther, C.J. Marx, M. E. Lidstrom, and L. Chistoserdova.** 2005. Analysis of gene islands involved in methanopterin-linked C_1 transfer reactions reveals new functions and provides evolutionary insights. J. Bacteriol. **187:**4607-4614.

34. **Chistoserdova L.**, **M. G. Kalyuzhnaya, and M. E. Lidstrom.** 2009. The expanding world of methylotrophic metabolism. Annu. Rev. Microbiol. **63:**477-499.

35. **Delaney N. F., M. E. Kaczmarek, L. M. Ward, P. K. Swanson, M-C. Lee, and C. J. Marx.** 2013. Development of an optimized medium, strain, and high-throughput culturing methods for *Methylobacterium extorquens*. PLoS One. **8:**e62957.

36. **Redfield A.C.** 1958. The biological control of chemical factors in the environment. American Scientist. **46:**205-221.

37. **Van Dien S. J., and M. E. Lidstrom.** 2002. Stoichiometric model for evaluating the metabolic capacities of the facultative methylotroph *Methylobacterium extorquens* AM1, with applications to reconstruction of C3 and C4 metabolism. Biotechnology and Bioengineering **78:**296-312.

38. **Rasche M. E., S. A. Havemann, and M. Rosenzvaig.** 2004. Characterization of two methanopterin biosynthesis mutants of *Methylobacterium extorquens* AM1 by use of a tetrahydromethanopterin bioassay. J. Bacteriol. **186:**1565-1570.

39. **Vorholt J. A., C. J. Marx, M. E. Lidstrom, and R. K. Thauer.** 2000. Novel formaldehyde-activating enzyme in *Methylobacterium extorquens* AM1. **182:**6645-6650.

40. **Chistoserdova L., and M. E. Lidstrom.** 1994. Genetics of the serine cycle in *Methylobacterium extorquens* AM1: cloning, sequence, mutation and physiological effect of *glyA*, the gene for serine hydroxymethyltransferase. **176:** 6759-6762.

41. **Chistoserdova L., C. Jenkins, M. G. Kalyuzhnaya, C. J. Marx, A. Lapidus, J A. Vorholt, J. A. Staley, and M. E. Lidstrom.** 2004. The enigmatic *Planctomycetes* may hold a key to the origins of methanogenesis and methylotrophy. Mol. Biol. Evol. **21:**1234-1241.

42. **Delaney N. F., J. I. Rojas Echenique, and C. J. Marx.** 2013. Clarity: an open-source manager for laboratory automation. J. Lab Autom. **18:**171-177.

43. **Acharya P, M. Goenrich, C. H. Hagemeier, U. Demmer, J. A. Vorholt, R. K. Thauer, and U. Ermler.** 2005. How an enzyme binds the C1 carrier tetrahydromethanopterin. Structure of the tetrahydromethanopterin-dependent formaldehyde-activating enzyme (fae) from *Methylobacterium extorquens* AM1. J. Biol. Chem. **280:**13712-13719.

44. **Vorobev A., D. A. C. Beck, M. G. Kalyuzhnaya, M. E. Lidstrom, and L. Chistoserdova.** 2013. Comparative transcriptomics in three *Methylophilaceae* species uncover different strategies for environmental adaptation. Peer J. **1:**e115.

45. **L. Chistoserdova.** 2011. Methylotrophy in a lake: from metagenomics to single-organism physiology. Appl. Environ. Microbiol. **77:**4705-4711.

46. **Agashe D., N. C. Martinez-Gomez, D. A. Drummond, and C. J. Marx.** 2013. Good codons, bad transcript: large reductions in gene expression and fitness arising from synonymous mutations in a key enzyme. Mol. Biol. Evol. **30:**549-560.

47. **Marx C. J.** 2008. Development of a broad-host-range *sacB*-based vector for unmarked allelic exchange. BMC Res. Notes. **1:**1.

48. **Gibson D. G., L. Young, R. Y. Chuang, J. C. Venter, C. A. Hutchison 3rd, and H. O. Smith.** 2009. Enzymatic assembly of DNA molecules up to several hundred kilobases. Nat. Methods. **6:**343-345.

49. **Figurski D. H., and D.R. Helinski**.1979. Replication of an origin-containing derivative of plasmid RK2 dependent on a plasmid function provided *in trans*. PNAS.**76:** 1648-1652.

Chapter 4

Horizontal Gene transfer overcomes the adaptive constraints posed by a sub-optimal pathway for methylamine utilization in *Methylobacterium extorquens* PA1

Horizontal Gene Transfer overcomes the adaptive constraints posed by a sub-optimal pathway for methylamine utilization in *Methylobacterium extorquens* PA1

Running title: Adaptive constraints prevent fitness increase in novel environments

Dipti D. Nayak[1] and Christopher J. Marx[1, 2, 3, 4, *]

[1]Organismic and Evolutionary Biology, Harvard University, Cambridge, MA, USA, [2]Faculty of Arts and Sciences Center for Systems Biology, Harvard University, Cambridge, MA, USA, [3]Biological Sciences, University of Idaho, Moscow, ID, USA, [4]Institute for Bioinformatics and Evolutionary Studies, University of Idaho, Moscow, ID, USA.

* Corresponding author: Biological Sciences, University of Idaho, Moscow, ID 83843, USA. Tel.: + 1 208 885 8594; Fax: + 1 208 885 7905; E-mail: cmarx@uidaho.edu

Abstract

It is commonly assumed that genotypes which are phenotypically farther away from fitness optima can adapt rapidly. This intuition, formalized in Fisher's geometric model, has been validated by numerous laboratory evolution studies across many organisms and environments. On the contrary, a multi-peaked adaptive landscape invoked by Wright suggests evolutionary recalcitrance; that some genotypes simply exist in regions where they are stuck on a lower fitness peak. Therefore, when the fitness of two closely related organisms in a given environment differs greatly, it is generally unclear whether the low fitness genotype is capable of rapidly improving to match the phenotype of the fitter genotype, or whether there are fundamental constraints that would prevent this. The competitive fitness of strains of the *Methylobacterium extroquens* species during growth on methylamine is correlated with the presence of a *mau* (methylamine utilization) gene cluster in the genome; likely to have been introduced via horizontal gene transfer (HGT). Strains like *M. extorquens* AM1, which possess the *mau* gene cluster, had at least five fold higher competitive fitness than strains like *M. extorquens* PA1. We evolved three replicate populations of *M. extorquens* PA1 on 20 mM methylamine as the sole carbon and energy source for 150 generations. Despite low initial fitness, scant indication of fitness improvement was detected. In contrast, by mimicking a HGT event, we introduced the *mau* gene cluster in the PA1genome. Instantaneously, an eleven-fold fitness increase, which even surpassed the fitness of AM1, was observed. These results suggest that, despite the low fitness, certain environments can pose evolutionary constraints that are difficult to overcome via adaptive mutations, but can be readily overcome by HGT.

Introduction

An *a priori* intuition of the adaptive landscape is a big challenge in evolutionary biology. Whether a low fitness strain has easy access to routes that lead to higher fitness or if constraints exist that would frustrate improvement is hard to determine by just examining the genotype. However, in almost all instances of experimental evolution reported thus far, microorganisms have been shown to rapidly evolve

to grow faster on substrates and conditions that they were originally poorly adapted to. Some of these studies have focused on rapid recovery in genetically modified strains with low initial fitness due perturbations that removed or added new metabolic pathways. *Escherichia coli* strains with deletions in key metabolic genes have been shown to recover and even surpass WT growth within 10 days (Fong and Palsson 2004); an engineered strain of *Methylobacterium,* forced to utilize a foreign central metabolic pathway, can show a 40% improvement in growth in just 72 generations (Lee and Marx 2013). Other studies where multiple starting points with differing fitness have been tested, a quantitative trend toward compensation has often emerged; the least fit strains evolves the fastest, independent of the genotype (Travisano et al. 1995; Moore et al. 2000; MacLean et al. 2010; Kryazhimskiy et al. 2014).

These experimental results have given rise to an evolutionary heuristic: the rate of evolutionary adaptation is primarily dependent on the initial fitness of an organism relative to what it can achieve in a given environment. The underlying basis for this widely accepted notion is that the adaptive potential of a microorganism can surpasses most, if not all, physiological constraints posed by a novel or sub-optimal environmental condition or substrate (Hottes et al. 2013); and diminishing returns epistasis reduces the fitness gain resulting from an adaptive mutation as the organismal fitness increases (Khan et al. 2011; Chou et al. 2011; Kvitek and Sherlock, 2011; Rokyta et al. 2011). This rule-of-thumb finds its theoretical origin in Fisher's geometric model (FGM) (R. A. Fisher, 1930; H. A. Orr, 2005; Gordo and Campos, 2012): in an adaptive landscape which contains a single, static fitness peak, the frequency and magnitude of beneficial mutations decrease as an organism moves closer to the fitness optima. Here we present an example that counters the wide-spread generalization that low fitness genotypes can adapt quickly, and further show that introduction of new genes can immediately overcome adaptive constraints in such cases.

Closely-related strains within the *Methylobacterium extroquens* species can all grow on reduced single carbon compounds like methanol or methylamine as their sole source of carbon and energy (C. Anthony, 1982). Even though these strains are more than 99% identical at the 16s rRNA locus (Marx et

al. 2012) and share a core metabolic repertoire (Nayak and Marx, 2014a), some stark phenotypic differences have been observed (Nayak and Marx, 2014a; Nayak and Marx, 2014b). For instance, *M. extorquens* AM1 (referred to as AM1 henceforth) can grow five-fold faster than *M. extorquens* PA1 (referred to as PA1 henceforth) on methylamine. The genomic basis for this marked distinction in methylamine growth rates is well established (Vuillimier et al. 2009; Nayak and Marx, 2014a): all *M. extorquens* strains possess the sub-optimal, energetically expensive *N*-methylglutamate (NMG) pathway (Shaw et al. 1966; Latypova et al. 2010; Gruffaz et al. 2014; Nayak and Marx, 2014b), whereas only AM1 and CM4 also contain the methylamine dehydrogeanse (referred to as MaDH henceforth))Eady and Large, 1968; Chistoserdov et al. 1991), (Figure 4.1). In AM1, the *mau* gene cluster (Chistoserdov et al. 1991 and 1994) encoding MaDH is present in a 10 kb genomic region that is flanked by two IS (Insertion Sequence) elements of the ISMex15 family, indicative of recent acquisition by HGT (Vuillimier et al. 2009). The MaDH functions by producing formaldehyde and ammonia in the periplasm, and electrons are passed to the electron transport chain (Eady and Large, 1968). In contrast, the NMG pathway is cytoplasmic, requires an ATP, and generates an NADH (Latypova et al. 2010). Thus, beyond possible kinetic differences, distinct localization and cofactor coupling could pose constraints upon the efficiency of each pathway.

Given the large difference in methylamine growth rate for a strain with MaDH versus another that only possesses the NMG pathway, will selection for growth on methylamine rapidly improve use of the NMG pathway in the low fitness strain? Or, will one or more of the physiological differences between the pathways pose constraints that are difficult to overcome, short of introduction of MaDH via HGT? We experimentally evolved replicate populations of PA1 on methylamine as the sole carbon and energy source for 150 generations. To our surprise, the competitive fitness and growth rate of populations or isolates after 150 generations of evolution were no different or even slightly lower than the founding ancestor.

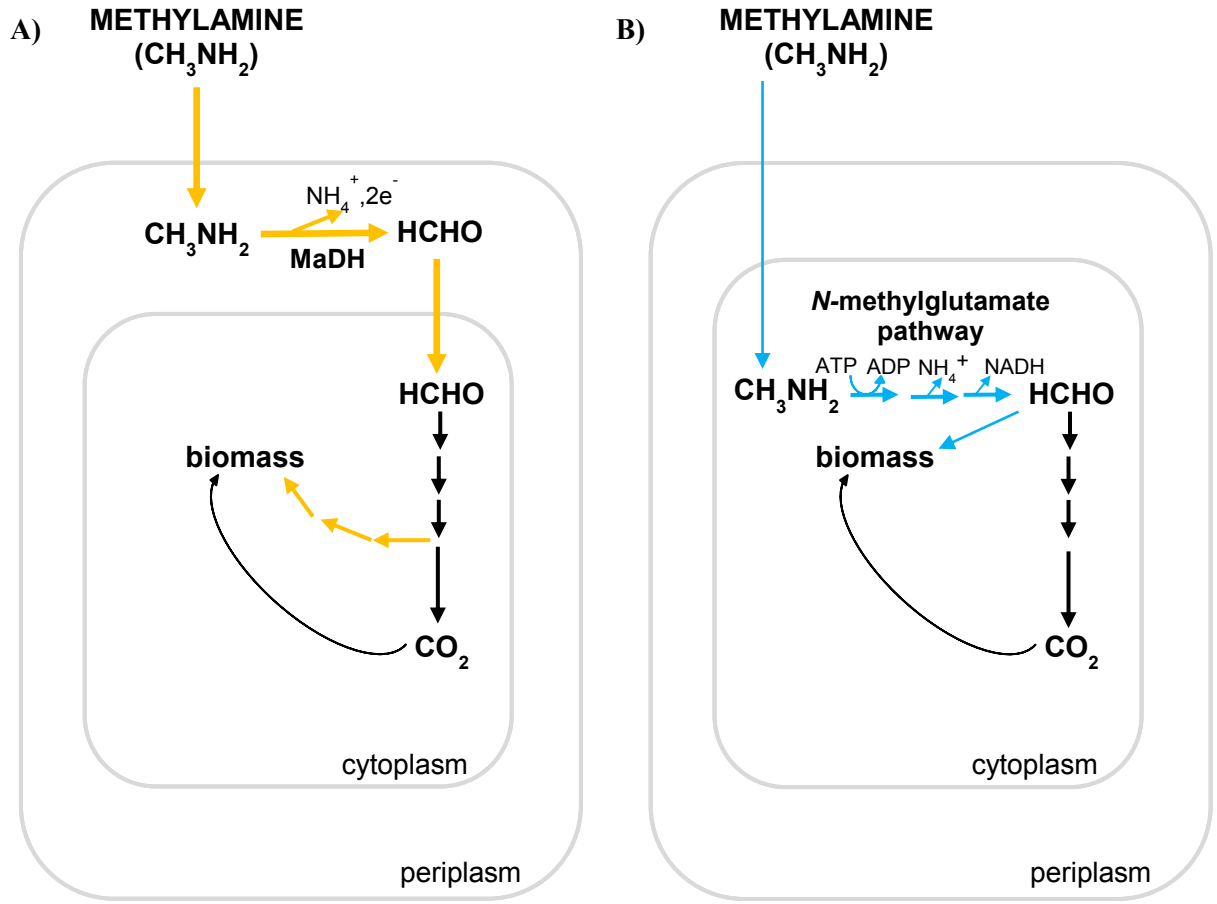

Figure 4.1: A) A schematic of methylamine metabolism using the methylamine dehydrogeanse (encoded by the *mau* gene cluster) for methylamine oxidation (orange)**. B)** A schematic of methylamine metabolism using the *N*-methylglutamate pathway for methylamine oxidation (blue). MaDH: Methylamine dehydrogeanse

Based on mutations identified by sequencing the genome of evolved isolates across replicate populations, it was clear some degree of adaptation occurred, but not in a manner that led to rapid growth or a fitness increase in competition assays. In contrast, by simply introducing MaDH on a plasmid to simulate the HGT events inferred to have occurred naturally, the methylamine fitness of the PA1 transconjugant was even higher than AM1. These results provide a counter example to the common pattern in microbial evolution of rapid adaptation for low fitness strains. Furthermore, we directly demonstrate the speed with

which an HGT event can overcome previous physiological constraints and dramatically change the performance and fitness of an organism.

Materials and Methods

Chemicals and media

All chemicals were purchased from Sigma-Aldrich (St. Louis, MO) unless otherwise noted. *Escherichia coli* were grown in LB at 37 °C with the standard antibiotic concentrations. Standard growth conditions for *M. extroquens* PA1 and *M. extorquens* AM1 utilized a modified version of Hypho minimal medium consisting of: 100 mL phosphate salts solution (25.3 g of K_2HPO_4 plus 22.5 g Na_2HPO_4 in 1L deionized water), 100 mL sulfate salts solution (5 g of $(NH_4)_2SO_4$ and 2 g of $MgSO_4 \cdot 7\ H_2O$ in 1L deionized water), 799 mL of deionized water, and 1 mL of trace metal solution (Agashe et al. 2013). Filter-sterilized carbon sources were added just prior to inoculation in liquid minimal media with a final concentration of 3.5 mM for sodium succinate and 20 mM for methylamine hydrochloride,

Experimental Evolution

Three independent colonies of the Δ*cel* strain of *M. extorquens* PA1 (CM2730; Delaney et al. 2013) were isolated from Hypho, succinate, agar (2% w/v) plates and were inoculated in 50 mL flasks with 10 mL of Hypho minimal media and 20 mM methylamine hydrochloride to initiated three replicate populations for experimental evolution. Flasks were incubated in a 30 ºC shaking incubator at 225 rpm for 3.5 days after which a 32-fold dilution (for the first 11 transfers) and a 128-fold dilution (for the next 14 transfers) was transferred in fresh Hypho minimal media with 20 mM methylamine hydrochloride. At regular intervals, populations were frozen at -80ºC with 10% DMSO. *M. extorquens* AM1 contamination was tested after every transfer by using *mau* specific primers for PCR amplification from the population lysate. Evolved clones were obtained as independent colonies from Hypho, 7.5 mM sodium succinate, 20 mM methylamine, agar (2% w/v) plates.

Fitness Assays

Competitive fitness was measured by competing strains against a fluorescently labelled ancestor (*M. extorquens* PA1 Δ*cel*-Δ*hpt*::P_{tac}-*mCherry* (CM3839)) described elsewhere (Michener et al. 2014) using modified version of a protocol described elsewhere (Lee et al. 2009; Chou and Marx, 2012). Growth was initiated by transferring 10 µL freezer stock into 10 mL of Hypho medium with 3.5 mM succinate. Upon reaching stationary phase, cultures were transferred 1:128 into fresh medium with the carbon source to be tested in 50 mL flasks with a total culture volume of 10 mL. At the end of the acclimation phase, CM3839 and the test strain or the mixed population were mixed in equal proportions by volume and this initial mix (T_0) was transferred 1:128 into fresh media with the same conditions as the acclimation phase. To test fitness at a 32-fold dilution, 1:32 transfers were performed for both the acclimation and testing growth cycles. 450 µL of the T_0 mix was also mixed with 10% DMSO and frozen at -80 ºC. A 500 µL sample at the end of the growth phase (T_1) was collected and the ratio of CM3839 and the test strain or the mixed population before and after the growth phase was ascertained using flow cytometry. Cells were diluted appropriately such that at a flow rate of 0.5 µl/sec on the LSRFortesssa (BD, Franklin Lakes, NJ) ~1000 events/sec would be recorded. Fluorescent mCherry was excited at 561 nm and measured at 620/10 nm. The competitive fitness was calculated as $W = \frac{\log(\frac{R1*N}{R0})}{\log(\frac{(1-R1)*N}{(1-R0)})}$ where R1 and R0 represent the population fraction of the test strain before and after mixed growth, and N represents the fold increase in the population density. Competitive fitness assays were conducted in triplicate unless specified. Data are reported as the mean fitness ± 95% confidence interval of the mean fitness value.

Genome Sequencing

Each strain grown to saturation in hypho media with 7 mM succinate, was centrifuged, re-suspended in Tris-EDTA buffer with 1% Triton-X 100, and then lysed using a combination of lysozyme and heat shock at 70 ºC-90 ºC for 10 minutes. Lysed cells were treated with proteinase K and RNase A at 37 ºC for 2 hours and genomic DNA was extracted using the phenol-chloroform extraction protocol. DNA concentration was quantified using the Nanodrop spectrophotometer (ND-1000, Thermo Fischer

Scientific, Wilmington, DE). Single-end 50 bp reads for Illumina sequencing were prepared using the TruSeq DNA sample prep Kit (Illumina, San Diego, CA) as per the manufacturer's instructions and sequenced using an Illumina Hi-Seq machine at the Genomics and Microarray Core Facility, Huntsman Cancer Institute, Salt lake City, Utah. Reads were assembled and aligned on the *M. extroquens* PA1 reference genome using Breseq version 0.21 (Deatherage et al. 2014). Mutations were verified by PCR amplification and subsequent Sanger sequencing. Allele frequencies were measured by amplifying the Mext_2327 locus or the promoter region for Mext_2010 in eight isolates from each replicate population as well as the entire mixed population.

Plasmids and Strains

Chromosomal allele replacement from the evolved isolates in the ancestral background was conducted using the allelic exchange vector pCM433 (Marx, 2008). A genomic region containing a 200 bp region upstream of Mext_2010 as well as the entire coding sequence of Mext_2010 was amplified using PCR. The forward primer was designed to have a 30 bp long sequence at the 5' end homologous to the sequence upstream of the *Not*I cut site in pCM433(*ATGGATGCATATGCTGCAGCTCGAGCGGCCGC*CGG TCGCGTAGATCAGGTTG). The reverse primer was designed to have a 30 bp long sequence at the 5' end homologous to the sequence downstream of the *Not*I cut site in pCM433 (*GGTTAACACGCGTACGTAGGG CCCGCGGCCGC*CGGTTT CAGAGCGATGCTCC).The PCR product was ligated on the pCM433 vector cut with *Not*I using the Gibson assembly protocol described elsewhere (Gibson et al. 2009). Cloning the promoter mutation upstream of Mext_2010 in pCM433 resulted in pDN93. A region upstream and downstream of Mext_2010 was also amplified using PCR. The forward primer for the upstream flank was designed to have a 30 bp long sequence at the 5' end homologous to the sequence upstream of the *Not*I cut site in pCM433 (*ATGGATGCATATGCTGCAGCTCGAGCGGCCGC*GTCTTGGTCTGGAGCTGGAAGC and reverse primer TAC GCGCTGAACCTCACGAAGG) . The forward primer for the downstream flank was designed to have a 30 bp sequence at the 5' end homologous to the last 30 bp of the upstream flank (*TACGCGCTGAACCTCACGAAGG*CGTGAACGCCGAGGATGACG). The reverse primer for the downstream

flank was designed to have a 30 bp long sequence at the 5' end homologous to the sequence downstream of the *Not*I cut site in pCM433 (*GGTTAACACGCGTACGTAGGGCCCGCGGCCGC*CGCCCT GAAGTTCGACAAACC). The PCR products representing the upstream and downstream flank were ligated on the pCM433 vector cut with *Not*I using the Gibson assembly protocol described elsewhere (Gibson et al. 2009). Cloning the upstream and downstream flanks for Mext_2010 in pCM433 resulted in pDN94. Mutant strains of *M. extorquens* PA1 were made by introducing the appropriate donor constructs through conjugation by a tri-parental mating between 10β competent cells (New England Biolabs, Ipswich, MA) containing the donor construct, an *E. coli* strain containing the conjugative plasmid pRK2073, and *M. extorquens* PA1 as described elsewhere (Marx, 2008). All mutant strains were confirmed by a diagnostic PCR analysis and validated by Sanger sequencing the mutant locus. All strains and plasmids used for this study are listed in Table 4.1.

Growth Rate Measurement

Growth from freezer stocks at -80 ºC was initiated by transferring 10 µL freezer stock into 10 mL of Hypho medium with 3.5 mM succinate in 50 mL flasks in a shaking incubator at 225 rpm and maintained at 30 ºC. Upon reaching stationary phase (2 days), cultures were transferred 1:16 into 9.4 mL fresh medium with 20 mM methylamine hydrochloride and allowed to reach saturation in this acclimation phase (3.5 days), and diluted 1:32 again into 9.4 mL fresh medium with 20 mM methylamine for the measured (experimental) growth (3.5 days). A 50 µL aliquot of three replicate cultures, for each strain, was sampled every 8-10 hours during the growth phase. Optical density of the culture was measured at 600 nm (OD_{600}) using a spectrophotometer (Bio-Rad, Hercules, CA). The dynamics and specific growth rate of cultures were calculated from the log-linear growth phase using CurveFitter (Delaney et al. 2013). Yield was measured as the maximum OD_{600} during the growth phase. Growth rate and yield reported for each strain and condition is the mean calculated from three biological replicates, unless otherwise noted.

Table 4.1: *M. extorquens* strains and plasmids generated in this study

Strains or plasmid	Description	Reference
Strains		
CM4	*M. extorquens* CM4	Marx et al. 2012
DM4	*M. extorquens* DM4	Marx et al. 2012
populi	*M. extorquens* populi	Marx et al. 2012
CM2720	Δ*cel M.extorquens* AM1	Delaney et al. 2013
CM2730	Δ*cel M.extorquens* PA1	Delaney et al. 2013
CM3120	Δ*katA*::P_{tac}-*mCherry* in CM2720[a]	Michener et al. 2014
CM3839	Δ*hpt*::P_{tac}-*mCherry* in CM2730[b]	Michener et al. 2014
CM3881	ΔMext_2010 in CM2730	This study
CM4385	*oprB* allele form E2 in CM2730	This study
CM4408	E1	This study
CM4409	E2	This study
CM4410	E3	This study
Plasmids		
pCM433	Allelic exchange vector (Tet^R, Suc^S)	Marx 2008
pDN93	pCM433 with Mext_2010 promoter region from CM3500	This study
pDN94	pCM433 with ΔMext_2010 upstream and downsteam flanks	This study
pRK2073	Helper plasmid (IncP, *tra*, Str^R)	Figurski and Helinski, 1979
pAYC139	Plasmid (IncP, *tra,* Tet^R) with *mau* gene cluster from *M. extorquens* AM1	Chistosrdov et al. 1991

[a]*katA* ,catalase [b]*hpt*: hypoxanthine phosphoribosyltransferase

Results

The methylamine fitness of *M. extorquens* species is dependent on the metabolic module used for methylamine oxidation

Strains of the *M. extorquens* species differ in whether or not they possess MaDH. We measured the methylamine fitness of five different strains under identical conditions to determine whether it correlated with the presence of MaDH.

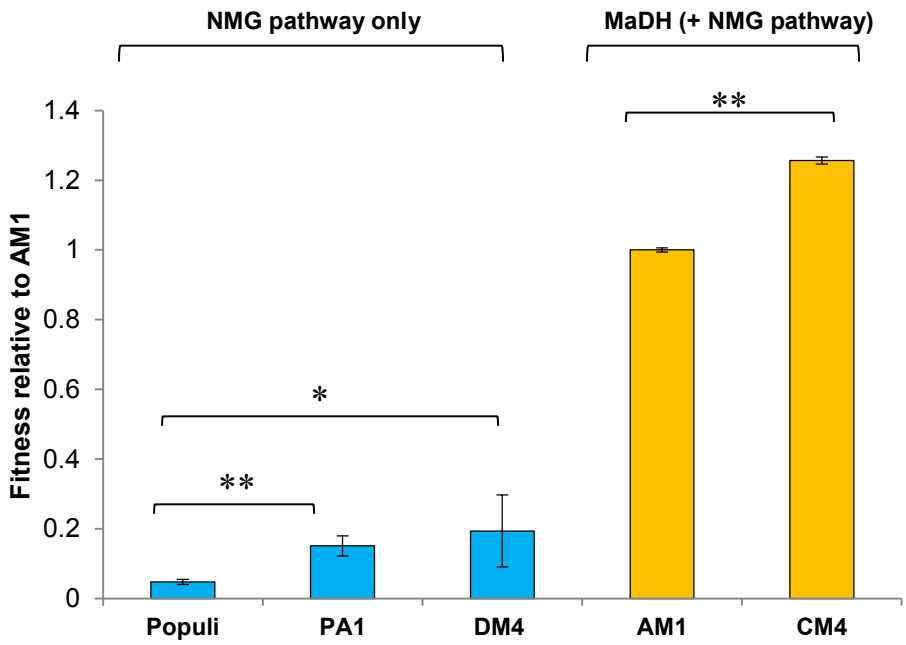

Figure 4.2: Methylamine fitness of *M. extorquens* species relative to AM1. Strains that use the *N*-methylglutamate pathway are depicted in blue and strains that use the methylamine dehydrogenase enzyme (but also contain the *N*-methylglutamate pathway) are depicted in orange. Error bars depict the 95% confidence interval (C.I.) of the mean relative fitness determined by three replicate competition assays. ** $p < 0.01$ and *$p < 0.05$ for a significant difference in fitness on methylamine for strains that use the same pathway for methylamine oxidation.

The resulting fitness values were quite variable but had a simple pattern: the two strains encoding MaDH, AM1 and CM4, were 5 to 20-fold more fit than PA1, DM4, and BJ001 which only possess the NMG pathway (Figure 4.2). Thus, although there were small, but significant differences between strains with the same pathway for methylamine utilization, the dominant factor influencing fitness on methylamine is the presence of MaDH.

Adaptive evolution did not lead to a rapid increase in methylamine fitness for *M. extorquens* PA1

In order to test whether a strain with the NMG pathway could evolve rapidly toward the growth rate observed for a strain containing MaDH, we evolved replicate populations of PA1 on methylamine for

over 150 generations. Three replicate populations were grown in minimal media with 20 mM methylamine as the sole source of carbon and energy. Cells were transferred into fresh media every 3.5 days, at a 32-fold dilution for the first 55 generations, and then 128-fold for the final 98 generations. Single isolates from each evolved population were obtained, denoted as E1, E2, and E3, and fitness on methylamine was measured relative to the ancestor expressing the fluorescent protein mCherry (Figure 4.3a). None of the isolates were more fit than the ancestor and, to our surprise, E1 and E3 actually had significantly lower fitness on methylamine ($p = 0.01$ and $p < 0.01$, respectively). To check whether the strains isolated were anomalous in their performance, we also performed the same competition using the mixed populations against the labeled ancestor. Two of the three populations were significantly less fit than the ancestor (P1 and P3; $p < 0.01$ in each case) and the fitness of one population was not significantly different from the ancestor (P2; $p = 0.17$ (Figure 4.3b). We also examined the growth rates and yield (assayed via max OD_{600}) of two of the evolved isolates (Figure 4.3c) and neither of these traits changed significantly, either ($p > 0.2$ for all tests). Altogether, these data indicate that the fitness or growth rate on methylamine did not increase despite 150 generations of selection for fast growth.

Genome sequencing reveals parallel mutations across replicates that suggest adaptation over 150 generations of selection on methylamine

Even though there was no net increase in growth or fitness relative to the ancestor, we sequenced the genomes of E1, E2, and E3 to determine whether any mutational changes had occurred over the course of evolution. E1 and E3 had a single base (+C) insertion and a 35 bp deletion in the coding sequence of a hypothetical exported protein (gene ID: Mext_2327) respectively, whereas E2 had a C->T mutation 32 bases upstream of a carbohydrate-specific porin of the OprB family (Gene ID: Mext_2010) (Wylie and Worobec, 1995) (Table 4.2).

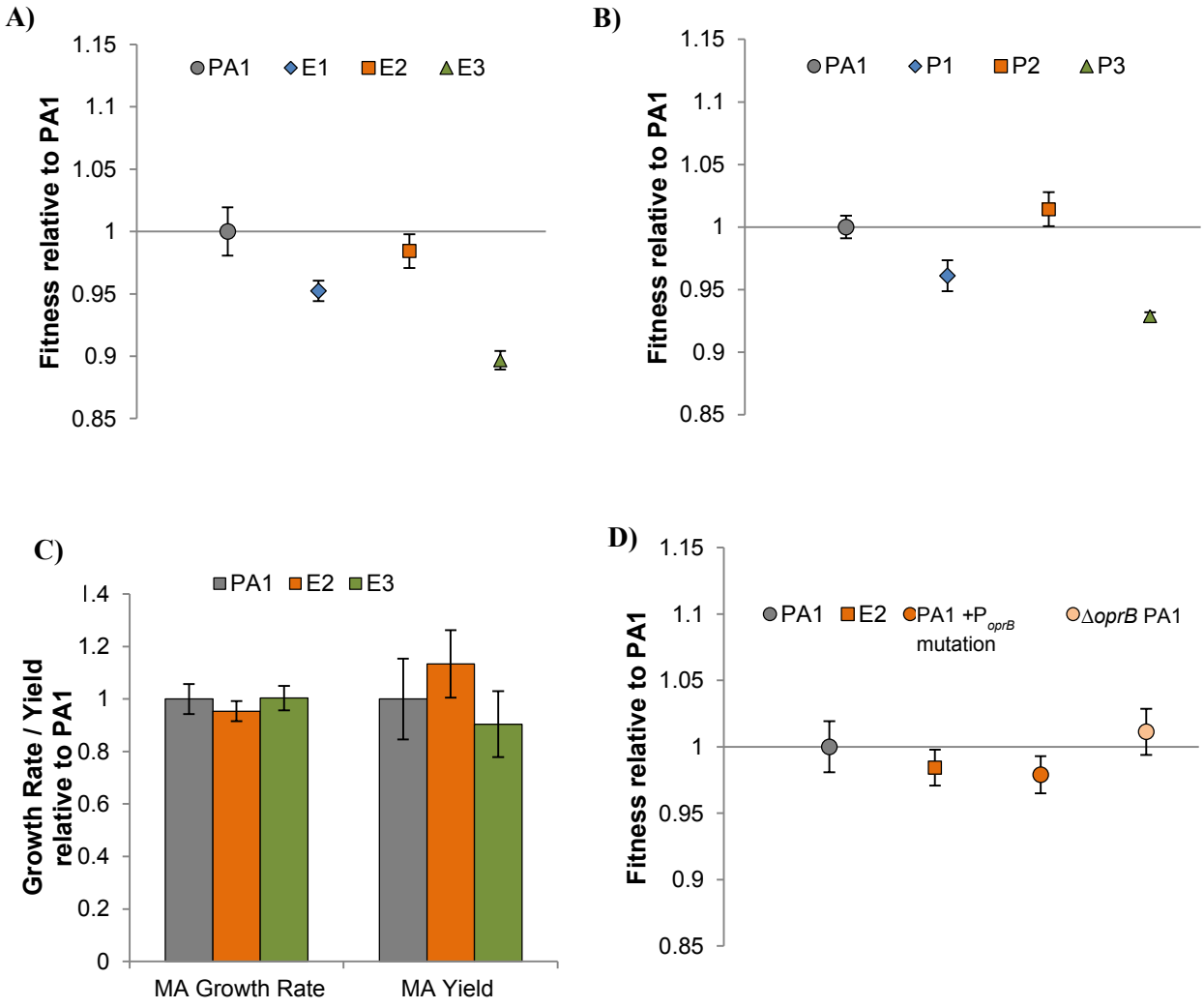

Figure 4.3: A) Methylamine fitness of Δ*cel M. extorquens* PA1 (gray) and an evolved isolate from each population (E1: Blue, E2: Orange and E3: Green) relative to mCherry PA1. **B)** Methylamine fitness of Δ*cel* PA1 (gray) and the mixed population at generation 150 (P1: Blue, P2: Orange and P3: Green) relative to mCherry PA1. **C)** Methylamine growth rate and yield (maximum OD_{600}) of PA1 (gray), E2 (orange) and E3 (green). **D)** Methylamine fitness of PA1 (gray circle), E2 (orange square), PA1 with the $oprB^{E2}$ (orange circle), and Δ*oprB* PA1 (light orange circle) relative to mCherry PA1. Error bars depict the 95% C.I. of the mean relative fitness determined by three replicate competition assays or the 95% confidence interval of the mean growth rate/ mean yield of three biological replicates.

Table 4.2: Mutations in evolved isolates and replicate populations of Δ*cel M. extorquens* PA1 after 150 generations of evolution on 20 mM methylamine.

Evolved allele	Population (Final frequency), Isolate
Mext_2327 (+C) 121 aa after start codon	**P1(1.0), E1**
Mext_2327 2x5 bp 24 aa after start codon	**P2 (0.75)**
C->T 32 bp upstream of Mext_2010	**P2 (0.25), E2**
Mext_2327 (– A) 71 aa after start codon	**P3 (0.5)**
Mext_2327 Δ35 bp 80 aa after start codon	**P3(0.5), E3**

We amplified these two loci in each population and used Sanger sequencing to generate a rough estimate of allele frequencies at 150 generations. The Mext_2327^{E1} allele appeared to have fixed in that population. The *oprB*^{E2} allele was at 25% in the second population, which was consistent with finding a new Mext_2327 allele (Mext_2327^{P2}, 5 bp duplication 24 amino acids after the start codon) at 75% in the same population. In the third population, the Mext_2327^{E3} allele was at 50%, while a second Mext_2327 allele (Mext_2327^{P3}, (-A) 71 amino acids after the start codon) was also at 50%. A rapid increase in allele frequency, and rampant parallelism of apparent loss-of-function alleles in Mext_2327 are consistent with adaptation. We introduced the *oprB*^{E2} allele in the ancestral genomic background, generated a Δ*oprB* strain and tested the fitness of these strains on methylamine. Consistent with the results from evolved isolates, neither of these mutations changed fitness significantly ($p = 0.16$, $p = 0.44$, respectively) (Figure 4.3d). Additional competitions for isolates were run at the initial 32-fold dilution, but unlike previous experiments (Marx, 2012), density-dependent fitness effects were not observed (data not shown).

HGT of the *mau* gene cluster in *M. extorquens* PA1 leads to an instantaneous increase in fitness and growth rate on methylamine

M. extorquens strains with MaDH have an order of magnitude higher fitness on methylamine compared to either ancestral or evolved PA1. Would the introduction of genes encoding MaDH in the PA1 genome be sufficient to speed up methylamine growth in the absence of subsequent evolutionary refinement? We simulated the HGT events that are likely to have occurred naturally for AM1 and CM4 by transforming a low-copy plasmid (pAYC139) (Chistoserdov et al. 1991) containing the *mau* genes, which encode MaDH, into PA1. The methylamine growth rate of the pAYC139^{+} PA1 transconjugant was 4.3-fold greater than PA1 ($p < 0.01$) and only 15% lower than AM1 ($p< 0.01$) (Figure 4.4). Despite slightly slower growth than AM1, the pAYC139^{+} PA1 transconjugant was 75% more fit than AM1 ($p< 0.001$) (Figure 4.4).

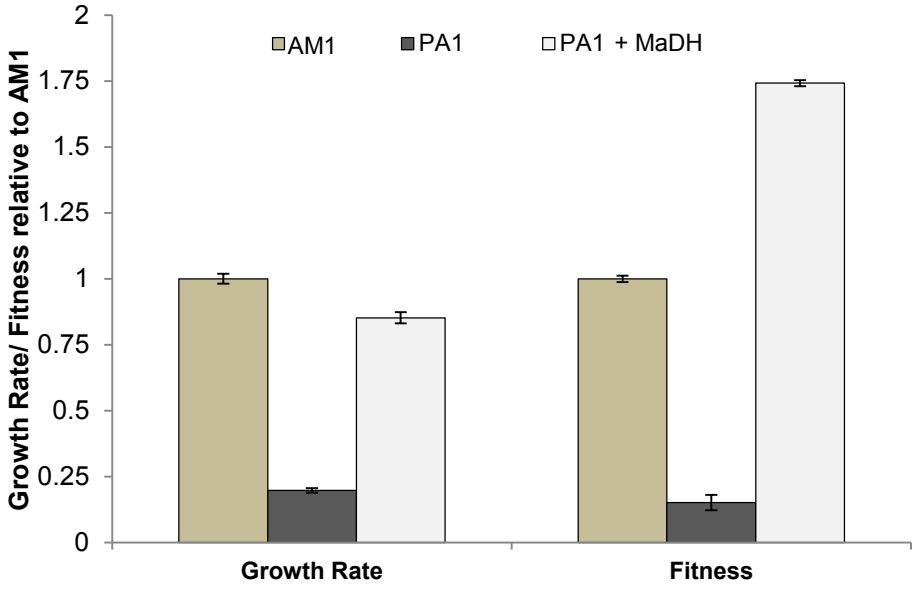

Figure 4.4: Methylamine growth rate and fitness of AM1 (light brown), PA1 (dark gray), and PA1 + pAYC139 expressing MaDH (light gray) relative to AM1 (for growth rate) or mCherry AM1 (for fitness). Error bars depict the 95% C.I. of the mean relative growth rate of three biological replicates and the 95% C.I. of the mean relative fitness determined by three replicate competition assays.

Discussion

In this study we show that, for closely related, natural isolates with distinct fitness values in a given environment, the heuristic that the rate of evolutionary adaptation is negatively correlated with the initial fitness and independent of the starting genotype does not necessarily hold (Perfetio et al. 2014; Kryazhimskiy et al. 2014). The methylamine fitness of strains of the *M. extorquens* species was extremely variable (Figure 4.2), but mostly dependent upon the metabolic module used for methylamine oxidation. The two strains that possessed MaDH had five fold or greater fitness than the three strains which only encode the NMG pathway. We evolved replicate populations of PA1, a strain with low initial fitness, on methylamine for over 150 generations to observe that, despite clear signs of adaptation (Table 4.2), the competitive fitness or growth rates of the evolved isolates or populations was no different or even slightly lower than that of the founding ancestor. However, genome sequencing revealed parallel mutations – apparent loss-of-function alleles of Mext_2327 (a conserved exported protein of unknown function) – and a rapid rise in the frequency of these alleles within 150 generations. Genetic parallelism suggests some degree of non-transitivity, as was previously observed for AM1 on methanol (Lee et al. 2009), which will require further study beyond the scope of this work. Though, it is clear that this experiment is in sharp contrast to previous laboratory evolution experiments with engineered *M. extorquens* strains in which adaptation was rapid and growth rate and fitness increased by 40% within 72 generations (Lee and Marx, 2013).

The observation that adaptive mutations did not lead to an increase in growth or competitive fitness suggests that various *Methylobacterium* strains inhabit a multi-peaked, rugged adaptive landscape (S. A Wright, 1932; Kvitek and Sherlock, 2011) that can constrain further improvement. This is in contrast to the common assumption of a single, static fitness peak in the adaptive landscape (R. A. Fisher, 1930) that is observed in most examples of laboratory evolution (Bennett et al. 1992; Travisano et al. 1995; Estes and Lynch, 2007; Joseph and Kirkpatrick, 2008; Lee and Marx, 2013). In a rugged, multi-peaked adaptive landscape, the adaptive mutations that overcome constraints might be dependent on

complex epistatic interactions (Quandt et al. 2014) as was observed in the citrate^{+} *E.coli* that evolved after 31,000 generations of laboratory evolution (Blount et al. 2012). As a result of these complex interactions, the rate of adaption slows down and becomes difficult, if not impossible, to generalize across different microorganisms and in different environments.

In this we work we also showed that introducing the *mau* gene cluster (Chistoserdov et al. 1991) encoding methylamine dehydrogeanse on a plasmid increased the methylamine fitness and growth rate of PA1 instantaneously and the resulting strain had higher fitness than AM1 (Figure 4.4). This outcome suggests that the NMG pathway poses one or more physiological constraints – perhaps linked to the cofactors or cellular locations that distinguish the NMG pathway from MaDH – which is difficult to overcome by adaptive mutations but can be overcome with a new pathway in its place. Based on the observed frequency of gene transfer across natural lineages (Koonin et al. 2001) and the rapid fitness gains without any evolutionary refinement observed in this study, we suggest that HGT can plays a major role in the evolutionary dynamics of microorganisms in nature and permits microbial populations to instantly jump across the fitness landscape to overcome adaptive constraints.

References

1. Agashe D, Martinez-Gomez NC, Drummond DA, and Marx CJ: **Good codons, bad transcript: large reductions in gene expression and fitness arising from synonymous mutations in a key enzyme**. *Mol Biol Evol* 2013, 3**0:**549-560.

2. Anthony C: **The biochemistry of methylotrophs**. Academic Press Ltd., London, 1982.

3. Bennett AF, Lenski RE, Miller JE: **Evolutionary adaptation to temperature. I. Fitness response of *Escherichia coli* to changes in its thermal environment.** *Evolution* 1992, **46:**16-30.

4. Blount ZD, Barrick JE, Davidson CJ, Lenski RE: **Genomic analysis of a key innovation in an experimental *Escherichia coli* population.** *Nature* 2012, **489:**513-518.

5. Chistoserdov AY, Tsygankov YD, Lidstrom ME: **Genetic organization of methylamine utilization genes from *Methylobacterium extorquens* AM1**. *J Bacteriol* 1991, **173:**5901-5908.

6. Chou HH, Chiu HC, Delaney NF, Segre D, Marx CJ: **Diminishing returns epistasis among beneficial mutations decelerates adaptation.** *Science* 2011, **332:**1190-1192.

7. Chou HH, Marx CJ: **Optimization of gene expression through divergent mutational paths.** *Cell Reports* 2012, **1:**133-140.

8. Deatherage DE, Barrick JE: **Identification of mutations in laboratory-evolved microbes from next-generation sequencing data using *Breseq*** .Methods Mol Biol 2014, **1151:**165-188.
9. Delaney NF, Rojas Echenique JI, Marx CJ: **Clarity: an open-source manager for laboratory automation.** *J Lab Autom* 2013, **18:**171-177.

10. Delaney NF, Kaczmarek ME, Ward LM, Swanson PK, Lee MC, Marx CJ: **Development of an optimized medium, strain, and high-throughput culturing methods for *Methylobacterium extorquens*.** *PLoS One* 2012, **8:**e62957.

11. Eady RR, Large PJ: **Purification and properties of an amine dehydrogeanse from *Pseudomonas* AM1 and its role in growth on methylamine.** *Biochem J* 1968, **106:**245-255.

12. Elena SF., Cooper VS, Lenski RE: **Punctuated evolution caused by selection of rare beneficial mutations.** *Science* 1996, **272:**1802-1804.

13. Estes S, Lynch M: **Rapid fitness recovery in mutationally degraded lines of *Caenorhabditis elegans.*** *Evolution* 2007, **57:**1022-1030.

14. Figurski DH, Helinski DR: **Replication of an origin-containing derivative of plasmid RK2 dependent on a plasmid function provided *in trans*.** *PNAS* 1979, **76:**1648-1652.

15. Fisher RA: **The genetical theory of natural selection.** Oxford Univ. Press, Oxford, 1930.

16. Fong SS, BØ Palsson BØ: **Metabolic gene-deletion strains of *Escherichia coli* evolve to computationally predicted growth phenotypes.** *Nat Genet* 2004, **36:**1056-1058.

17. Gordo I, Campos PRA: **Evolution of clonal populations approaching a fitness peak.** *Biol Lett* 2013, **9:** 20120239.

18. Gruffaz C, Muller EEL, Louhichi-Jelail Y, Nelli YR, Guichard G, Bringel F: **Genes of the *N*-methylglutamate pathway are essential for growth of *Methylobacterium extorquens* DM4 on monomethylamine.** *Appl Environ Microbiol* 2014, **80:**3541-3550.

19. Hottes SK, Freddolino PL , Khare A, Donnell ZN, Liu JC, Tavazoie S: **Bacterial adaptation through Loss of Function.** *PloS Genet* 2013, **9:**e1003617.

20. Joseph SB, Kirkpatrick M: **Effects of the [PSI+] prion on the rates of adaptation in yeast**. *J Evol Biol* 2008, **21:**773-780.

21. Khan AI, Dinh DM, Schneider D, Lenski RE, Cooper TF: **Negative epistasis between beneficial mutations in an evolving bacterial population.** *Science* 2011, **332:**1193-1196.

22. Koonin EV, Marakova KS, Aravind L: **Horizontal gene transfer in prokaryotes: Quantification and classification.** *Ann Rev Microbiol* 2001, **55:**709-742.

23. Kryazhimskiy S, Rice DP, Jerison E, Desai MM: **Global epistasis makes adaptation predictable despite sequence-level stochasticity.** *Science* 2014, **344:**1519-1522.

24. Kvitek DJ, Sherlock G: **Reciprocal sign epistasis between frequently experimentally evolved mutations causes a rugged fitness landscape.** *PLoS Genet* 2011, **7:**e1002056.

25. Latypova E, Yang S, Wang YS, Wang T, Chavkin TA, Hackett M, Schafer H, Kalyuzhnaya MG: **Genetics of the glutamate-mediated methylamine utilization pathway in the facultative methylotrophic beta-proteobacteria *Methyloversatilis universalis* FAM5.** *Mol Microbiol* 2010, **75:**426-439.

26. Lee MC, Chou HH, Marx CJ: **Asymmetric, bimodal trade-offs during adaptation of *Methylobacterium* to different growth substrates.** *Evolution* 2009, **63:**2816-2830.

27. Lee MC, Marx CJ: **Synchronous waves of failed soft sweeps in the laboratory: remarkably rampant clonal interference of alleles at a single locus.** *Genetics* 2013, **193:**943-952.

28. MacLean RAC, Perron GG, Gardner A: **Diminishing returns from beneficial mutations and pervasive epistasis shape the fitness landscape for rifamycin resistance in *Pseudomonas aeruginosa.*** *Genetics* 2010, **186:**1345-1354.

29. Marx CJ: **Development of a broad-host-range *sacB*-based vector for unmarked allelic exchange.** *BMC Res Notes* 2008, **1:**1.

30. Marx CJ, Bringer F, Chistoserdova L, Moulin L, Ul Haque MF, Fleischman DE, Gruffaz C, Jourand P, Knief C, Lee MC, Muller EEL, Nadalig T, Peyraud R, Roselli S, Russ L, Goodwin LA, Ivanova N, Kyrpides N, Lajus A, Land ML, Medigue C, Mikhailova Nolan NM, Woyke T, Stolyar S, Vorholt JA, Vuilleumier S: **Complete genome sequences of six strains of the genus *Methylobacterium***. *J. Bacteriol* 2012, **194:**4746-4748.

31. Marx CJ: **Recovering from a bad start: rapid adaptation and tradeoffs to growth below a threshold density**. *BMC Evol Biol* 2012, **12:**109.

32. Michener JK, Vuilleumier S, Bringer F, Marx CJ: **Phylogeny poorly predicts the utility of a challenging horizontally transferred gene in *Methylobacterium* strains.** *J Bacteriol* 2014, **196:**2101-2107.

33. Moore FBG, Rozen DE, Lenski RE: **Pervasive compensatory adaptations in *Escherichia coli.*** *Proc R Soc Lond B* 2000, **267:**515-522.

34. Nayak DD, Marx CJ: **Genetic and phenotypic comparison of methylotrophy between *Methylobacterium extorquens* strains PA1 and AM1.** *PLoS One* 2014, in revision.

35. Nayak DD, Marx CJ: **Methylamine utilization via a linear *N*-methylglutamate pathway does not require the tetrahydrofolate-dependent C1 transfer pathway.** *J Bacteriol* 2014, in review.

36. Orr HA: **The genetic theory of adaptation: a brief history.** *Nat Rev Genet* 2005, **6:**119-127.

37. Perfeito L, Sousa A, Bataillon T, Gordo I: **Rates of fitness decline and rebound suggest pervasive epistasis.** *Evolution* 2014, **68:**150-162.

38. Quandt EM, Deatherage DE, Ellington AD, Georgiou G, Barrick JE**: Recursive genomewide recombination and sequencing reveals a key refinement step in the evolution of a metabolic innovation in *Escherichia coli.*** *PNAS* 2014, **111:**2217-2222.

39. Rokyta DR, Joyce P, Caudle SB, Miller C, Beisel CJ, Wichman HA: **Epistasis between beneficial mutations and the phenotype-to-fitness map for a ssDNA virus.** *PLoS Genet* 2011, **7:**e1002075.

40. Shaw WV, Tsai L, Stadtman RR: **The enzymatic synthesis of *N*-methylglutamic acid**. *J Biol Chem* 1966, **241:**935-945.

41. Travisano M, Mongold JA, Bennett AF, Lenski RE: **Experimental tests of the role of adaptation, chance, and history in evolution.** *Science* 1995, **267:**87-90.

42. Vuilleumier S, Chistoserdova L, Lee MC, Bringer F, Lajus A, Zhou Y, Gourion B, Barbe V, Chang J, Cruveiller S, Dossat C, Gillett W, Gruffaz C, Haugen E, Hourcade E, Levy R, Mangenot S, Muller E, Nadalig T, Pagni M, Penny C, Peyraud R, Robinson DG, Roche D, Rouy Z, Saenampechek C, Salvignol G, Vallenet D, Wu Z, Marx CJ, Vorholt JA, Olson MV, Kaul R, Weissenbach J, Medigue C, Lidstrom ME: ***Methylobacterium* genome sequences: a reference blueprint to investigate microbial metabolism of C_1 compounds from natural and industrial sources.** *PLoS One* 2009, **4:**e5584.

43. Wright S: **The role of mutation, inbreeding, crossbreeding and selection in evolution.** *Sixth International Congress on Genetics* 1932, **1:**356-366.

44. Wylie JL, Worobec EA: **The OprB porin plays a central role in carbohydrate uptake in *Pseudomonas aeruginosa***. *J Bacteriol* 1995, **177:**3021-3026.

Chapter 5

Experimental evolution reveals ecologically distinct roles
for two functionally degenerate routes for methylamine oxidation
in *Methylobacterium extorquens* AM1

Experimental evolution reveals ecologically distinct roles for two functionally degenerate routes for methylamine oxidation in *Methylobacterium extorquens* AM1

Dipti D. Nayak[1], Deepa Agashe[2], Ming-Chun Lee[3], and Christopher J. Marx[1, 4, 5, 6, #,*]

[1]Organismic and Evolutionary Biology, Harvard University, Cambridge, MA, USA, [2]National Centre for Biological Sciences, Bangalore, India. [3]Department of Biochemistry, University of Hong Kong, Pokfulam, Hong Kong. [4]Faculty of Arts and Sciences Center for Systems Biology, Harvard University, Cambridge, MA, USA.[5]Department of Biological Sciences, University of Idaho, Moscow, ID, USA. [6]Institute for Bioinformatics and Evolutionary Studies, University of Idaho, Moscow, ID, USA.

Present address: Biological Sciences, University of Idaho, Moscow, ID, USA

* Corresponding author: Biological Sciences, University of Idaho, Moscow, ID 83843, USA. Tel.: + 1 208 885 8594; Fax: + 1 208 885 7905; E-mail: cmarx@uidaho.edu

Abstract

Bacterial genomes often encode multiple, biochemically distinct, but functionally degenerate pathways for a particular metabolic reaction. In some cases degeneracy adds robustness to the metabolic network, but in others it reveals a discrepancy between the genomic potential and physiological relevance. We sought to uncover physiological constraints that prevent a cell from tapping into functional degenerate pathways in the well-studied aerobic methylotroph – *Methylobacterium extorquens* AM1. *M. extorquens* AM1 encodes two non-orthologous routes for methylamine oxidation; methylamine dehydrogenase (MaDH) and the *N*-methylglutamate (NMG) pathway. Despite an intact NMG pathway, strains lacking a functional MaDH are completely incapable of methylamine growth. Two distinct genotypes of *M.extorquens* AM1, in which the MaDH was either deleted or suppressed, were experimentally evolved on methylamine as the sole carbon and energy source. Genomic and genetic analyses of the evolved strains revealed three key physiological constraints that prevented WT from channeling methylamine flux through the NMG pathway. Deleting the *mau* gene cluster (encoding MaDH) was the first step towards using the NMG pathway for methylamine growth. Mutations that increased the expression level of the NMG pathway and buffered a rise in cytoplasmic pH due to ammonia buildup further enhanced growth on methylamine. Two distinct mechanisms to buffer pH during ammonia buildup were discovered: constitutive expression of the *kefB* potassium/proton anti-porter and up-regulation of an ABC- transporter associated with the *ykkC/yxkD* RNA element to serve as a urea efflux pump. We also tested and validated the hypothesis that these two pathways for methylamine oxidation in AM1 are ecologically specialized to enable the cell to optimally utilize methylamine as a carbon source as well as a nitrogen source.

Introduction

Degeneracy in biological functions, especially metabolism, is prevalent across the bacterial domain. Distinct enzymes and pathways, with unique biochemistry and cofactors, are known to catalyze the same (set of) metabolic reaction/s (Romano and Connway1996; Edelman and Gally 2001; Boucher et al. 2003;

Marx et al. 2005; L. Chistoserdova et al. 2011; I. Berg 2011; Flamholz et al. 2013). The distribution of these functionally degenerate enzymes and pathways in bacteria is dependent on a set of complex criteria including phylogenetic relatedness (Flamholz et al. 2013), the ecological niche which may comprise of one or more of temperature (I. Berg 2011), oxygen (I. Berg 2011), cofactor availability (I. Berg 2011; Martiny et al. 2006), and thermodynamic constraints or the energy yield versus cost trade-offs (Flamholz et al. 2013). Metabolic degeneracy also manifests within a single bacterium; many bacteria encode more than one pathway for a particular (set of) reaction/s in their genome (Chain et al. 2007; Flamholz et al. 2013). Despite the cost, functional degeneracy is beneficial in highly variable, unpredictable natural environments. By buffering environmental fluctuations, multiple pathways can ensure a constant flux through key metabolic reactions (Stelling et al. 2004; Deutscher et al. 2006). For instance, the genome of *Burkholderia xenovorans* LB400 (Chain et al. 2007) contains three functionally degenerate pathways for formaldehyde oxidation and null mutants in one/two pathways do not lead to a significant decrease in the formaldehyde detoxification potential (Marx et al. 2004). Sometimes though, an interesting paradox manifests; despite metabolic degeneracy at the genomic level, the metabolic flux is primarily channeled through one route. For instance, the genome of *Methylobacillus flagellatus* KT contains two functionally degenerate pathways for formaldehyde oxidation (Chistoserdova et al. 2000; Chistoserdova et al. 2007) but only one is essential during growth on single-carbon compounds. A discrepancy between metabolic degeneracy at the genomic level and functional level is often uncovered (Marx et al. 2004; Flamholz et al. 2013) but the underlying physiological basis is rarely investigated.

Methylotrophs are a group of microorganisms that grow on reduced single carbon (C_1) compounds, like methane and methylamine, as the sole carbon and energy source (C. Anthony 1982). Physiological analysis of methylamine utilization in a facultative methylotrophic Alphaproteobacteria-*Methylobacterium extroquens* AM1 (referred to as AM1 from here on) - led to the discovery of a periplasmic methylamine dehydrogenase (MaDH) (Eady and Large 1968; McIntire et al. 1991) and ancillary proteins that are encoded by the *mau* gene cluster (Chistoserdov et al. 1991). MaDH, a

quinoprotein (Chen et al. 1994), catalyzes the primary oxidation of methylamine to formaldehyde and transfers the electrons released to cytochrome c via an amicyanin electron acceptor (Tobari and Harada 1981; Chen et al. 1992). Recent genomic (Nayak and Marx 2014 a) and genetic analyses have revealed that a completely non-orthologous pathway for the primary oxidation of methylamine – the *N*-methylglutamate (NMG) pathway (Shaw et al. 1966; Latypova et al. 2010; Chen et al. 2010) – is not just present but also active (Martinez-Gomez et al. 2013) in AM1 and other *M. extorquens* species (Gruffaz et al. 2014; Nayak and Marx 2014b). Unlike MaDH, the NMG pathway mediates the primary oxidation of methylamine in three enzymatic steps (Figure 5.1a). *γ*-glutamylmethylamide synthase (GMAS) catalyzes the condensation of methylamine and glutamate to form *γ*-glutamylmethylamide which is converted to *N*-methylglutamate by *N*-methylglutamate synthase (NMGS) and then oxidized to formaldehyde by *N*-methylglutamate dehydrogenase (NMGDH). Apart from biochemistry, the NMG pathway and MaDH also differ in their cellular localization. MaDH and its ancillary proteins are found in the periplasmic space (Eady and Large 1968; McIntire et al. 1991) whereas enzymes of the NMG pathway are cytoplasmic (Latypova et al. 2010). These two pathways have different energy yields and cofactor requirements as well; the NMG pathway oxidizes methylamine in an ATP-dependent set of reactions (1mol ATP/mol methylamine) and produces NADH (Kung and Wagner 1969; Latypova et al. 2010) whereas MaDH oxidizes methylamine in an ATP-independent manner. Mutants of AM1 lacking a functional MaDH are known to be completely incapable of methylamine growth (Chistoserdov et al. 1991).Thus, despite an 'apparent' functional degeneracy, the NMG pathway cannot, even partially, rescue the growth defect of the Δ*mau* mutant in methylamine. To uncover the physiological constraints that prevent the NMG pathway from taking over in the absence of MaDH, we experimentally evolved two distinct genotypes of AM1 (Figure 5.1b, Figure 5.1c), to switch to the NMG pathway for primary oxidation during growth on methylamine. The adaptive mutations were used to infer the physiological constraints that prevented methylamine growth using the NMG pathway.

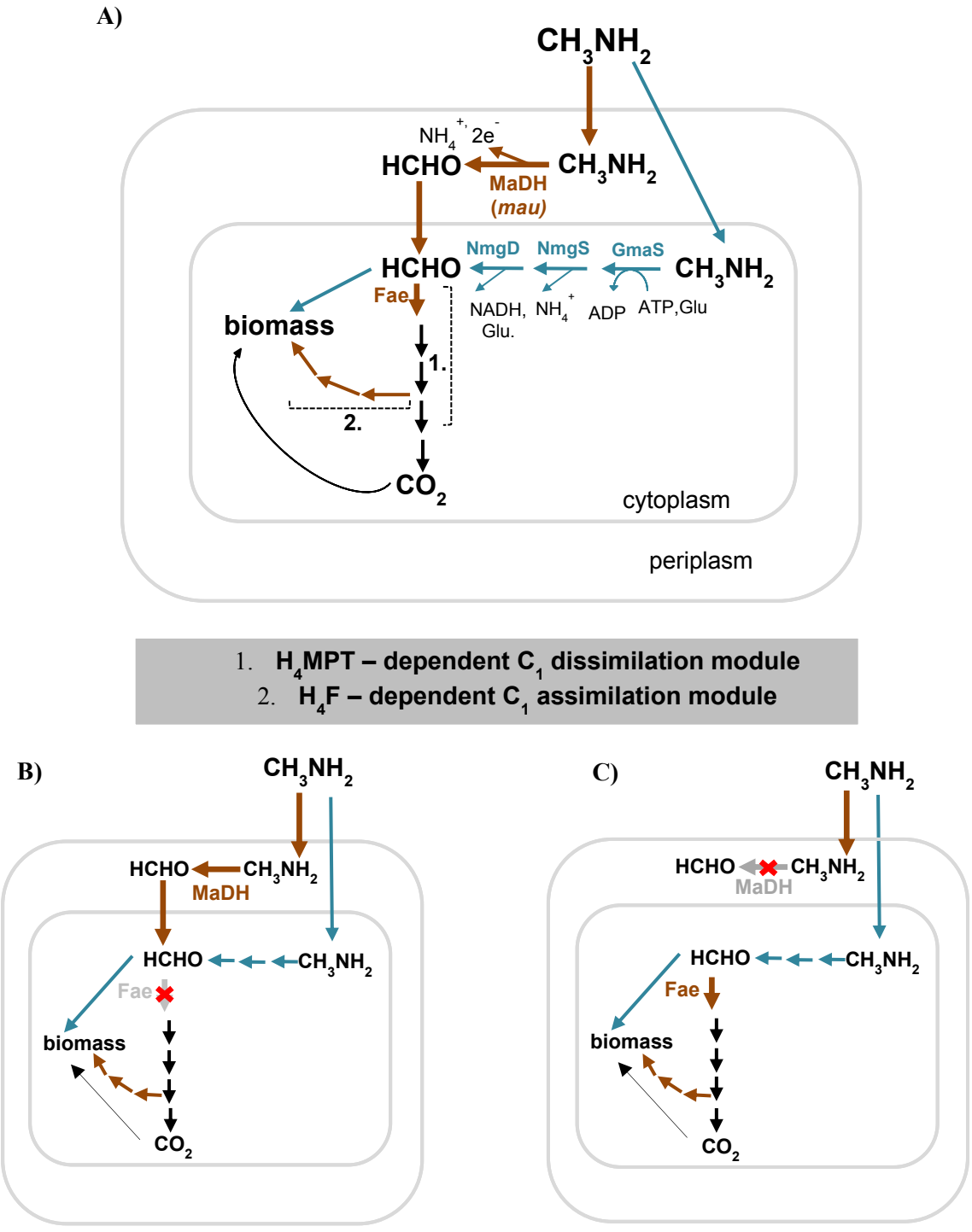

Figure 5.1: **A)** A schematic representation of the two functionally degenerate methylamine utilization pathways in *M. extorquens* AM1.AM1 is known to only use the methylamine dehydrogenase route (brown) during methylamine growth. **B, C)** A schematic representation of the genotype of A1 and A2 respectively; A1 lacks *fae* (an essential

(Figure 5.1 continued) enzyme immediately downstream of methylamine oxidation) and A2 lacks the entire *mau* gene cluster encoding methylamine dehydrogeanse.

MaDH: Methylamine dehydrogenase; NmgD: *N*-methylglutamate dehydrogeanse; NmgS: *N*-methylglutamate synthase; GmaS: γ-glutamylmethylamide synthetase; Glu: Glutamate; Fae: Formaldehyde activating Enzyme; H_4MPT: Tetrahydromethanopterin; H_4F: Tetrahydrofolate

The NMG pathway has extremely low expression in WT and when overexpressed leads to a rise in the cytoplasmic pH due to ammonia buildup. Based on the physiological constraints we were able to infer and test ecologically distinct roles for these two functionally, degenerate pathways. MaDH is a highly expressed, poorly regulated, energetically favorable enzyme that enables AM1 to grow on high concentrations of methylamine with relatively fast growth rates. In contrast, NMG pathway has low basal expression, is tightly regulated, has lower energetic yield but is likely to have a greater affinity (lower $K_{m)}$ for methylamine than MaDH since it is especially beneficial in environments with ≤ 1 mM methylamine as the sole nitrogen source.

Materials and Methods

Chemicals and media

All chemicals were purchased from Sigma-Aldrich (St. Louis, MO) unless otherwise noted. *Escherichia coli* were grown in LB at 37 °C with the standard antibiotic concentrations. Standard growth conditions for *Methylobacterium extroquens* AM1utilized a modified version of Hypho minimal medium consisting of: 100 mL phosphate salts solution (25.3 g of K_2HPO_4 plus 22.5 g Na_2HPO_4 in 1L deionized water), 100 mL sulfate salts solution (5 g of $(NH_4)_2SO_4$ and 2 g of $MgSO_4 \cdot 7\ H_2O$ in 1L deionized water), 799 mL of deionized water, and 1 mL of trace metal solution (Agashe et al. 2013). Growth conditions that utilized a nitrogen-free version of the modified Hypho minimal media consisted of: 100 mL phosphate salts solution (25.3 g of KH_2PO_4 plus 22.5 g Na_2HPO_4 in 1L deionized water), and 100 mL nitrogen- free sulfate salts solution (7 g of $MgSO_4 \cdot 7\ H_2O$ in 1L deionized water), 799 mL of deionized water, and 1

mL of trace metal solution All components were autoclaved separately before mixing under sterile conditions. Filter-sterilized carbon sources were added just prior to inoculation in liquid minimal media with a final concentration of 3.5 mM for sodium succinate, 20 mM for methylamine hydrochloride, 15mM for methanol, and 15mM for sodium formate.

Experimental Evolution

Experimental Evolution I: A Δ*fae* Δ*cel* strain of AM1 (CM2770) was experimentally evolved in 48-well microtiter plates (CoStar-3548) - in an incubation tower (Liconic USA LTX44 with custom fabricated cassettes) shaking at 650 rpm, in a room that was constantly maintained at 30 ºC and 80% humidity, (Delaney et al. 2013) - containing hypho medium with 20mM methylamine hydrochloride to a volume of 640 μL. A 32-fold dilution was serially passaged in fresh hypho medium with 20 mM methylamine hydrochloride at regular intervals for 150 generations.

Experimental Evolution II: Eight replicate populations of WT AM1 (CM501 and CM502) were evolved in hypho media with 1.75 mM disodium succinate and 7.5 mM methanol for 1500 generations as described earlier (Lee and Marx 2012). CM1054, an evolved isolate could no longer grow on 20 mM methylamine hydrochloride in liquid media, therefore was evolved on 20 mM methylamine hydrochloride in a 50 mL flask with 10 mL of culture in a shaking incubator maintained at a constant speed (225 r.pm.) and temperature (30ºC). The culture was allowed to grow for ~ 14 days till the media turned cloudy and then plated on hypho, methylamine, agar (2% w/v) plates. E2 (or CM3014) was isolated and used for the analyses described in the text.

Growth Rate Measurements

Cells were acclimated and grown in 48-well microtiter plates (CoStar-3548) in an incubation tower (Liconic USA LTX44 with custom fabricated cassettes) shaking at 650 rpm, in a room that was constantly maintained at 30 ºC and 80% humidity, (Delaney et al. 2013), containing Hypho medium with the appropriate carbon source to a volume of 640 μL. All growth rate measurements were conducted as

described in Nayak and Marx 2014a. The dynamics and specific growth rate of cultures were calculated from the log-linear growth phase using an open source, custom-designed growth analysis software called CurveFitter available at http://www.evolvedmicrobe.com/CurveFitter/ . Growth rates reported for each strain and condition are the mean plus 95% CI calculated from triplicate biological replicates, unless otherwise noted.

Plasmids and Strains

Chromosomal allele replacement was conducted using the allelic exchange vector pCM433 (Marx 2008). For Mext_1544- the entire gene- and for *kefB* -a1000bp of the intergenic region containing the mutant or ancestral allele- was amplified using PCR. The forward primer was designed to have a 30 bp long sequence at the 5' end homologous to the sequence upstream of the *Not*I cut site in pCM433. The reverse primer was designed to have a 30 bp long sequence at the 5' end homologous to the sequence downstream of the *Not*I cut site in pCM433. The PCR product was ligated on the pCM433 vector cut with *Not*I using the Gibson assembly protocol described elsewhere (Gibson et al. 2009). Cloning the WT and evolved allele of Mext_1544 in pCM433 resulted in pDN150 and pDN151. Cloning the evolved and WT allele of *kefB* in pCM433 resulted in pDN136 and pDN137. Deletion mutants lacking *mptG, mgdABCD*, *kefB* were generated in the evolved, ancestral and WT genomic background using the allelic exchange vector pCM433 (Marx 2008). A region upstream and downstream of each of these genes or operons of ~0.5 kb was amplified using PCR. The forward primer for the upstream flank was designed to have a 30 bp long sequence at the 5' end homologous to the sequence upstream of the *Not*I cut site in pCM433. The reverse primer for the upstream flank was designed to have a 30 bp sequence at the 5' end homologous to the first 30 bp of the downstream flank. The reverse primer for the downstream flank was designed to have a 30 bp long sequence at the 5' end homologous to the sequence downstream of the *Not*I cut site in pCM433. The PCR products representing the upstream and downstream flank were ligated on the pCM433 vector cut with *Not*I using the Gibson assembly protocol described elsewhere (Gibson et al. 2009). Cloning the upstream and downstream flanks for *mptG, mgdABCD*, and *kefB* in pCM433 resulted in pDN69 and

pDN112 and pDN142. Mutant strains of *M. extorquens* AM1 were made by introducing the appropriate donor constructs through conjugation by a tri-parental mating between 10β competent cells (New England Biolabs, Ipswich, MA) containing the donor construct, an *E. coli* strain containing the conjugative plasmid pRK2073, and AM1 as described elsewhere (Marx 2008). All mutant strains were confirmed by a diagnostic PCR analysis and validated by Sanger sequencing the mutant locus. All strains and plasmids used and generated for this study are listed in Table 5.1.

Competitive Fitness Assays

Competitive fitness was measured by competing each strain against a *M. extorquens* AM1 Δ*cel*-Δ*katA*::P_{tac}-mCherry (CM3120) described elsewhere (Michener et al. 2014) using a modified version of a protocol described elsewhere (Lee et al. 2009; Chou and Marx 2012). Growth was initiated by transferring 10 µL freezer stock into 10mL of Hypho medium with 3.5 mM succinate. Upon reaching stationary phase, cultures were transferred 1:64 into fresh medium with the carbon source to be tested in 48-well microtiter plates (CoStar-3548) and allowed to reach saturation in this acclimation phase. The acclimation phase for strains that could barely grow in methylamine consisted of growth in media with equimolar succinate and methylamine. At the end of the acclimation phase, CM3120 and the test strain was mixed in equal proportions by volume and this initial mix (T_0) was transferred 1:64 into fresh media with the same conditions as the acclimation phase. 450 µL of the T_0 mix was also mixed with 10% DMSO and frozen at -80ºC. A 500 µL sample at the end of the growth phase (T_1) was collected and the ratio of CM3120 and the test strain before and after the growth phase was ascertained using flow cytometry. Cells were diluted appropriately such that at a flow rate of 0.5 µl/ sec on the LSRFortesssa (BD, Franklin Lakes, NJ) ~1000events/second would be recorded. Fluorescent mCherry was excited at 561 nm and measured at 620/10 nm. The competitive fitness was calculated as $W = \frac{\log(\frac{R1*N}{R0})}{\log(\frac{(1-R1)*N}{(1-R0)})}$ where R1 and R0 represent the population fraction of the test strain before and after mixed growth, and N represents the fold increase in the population density. Since the test strains were unlabeled, the population

fraction was the ratio of mCherry-negative cells to mCherry-positive cells. Competitive fitness assays were conducted in triplicate unless specified. Data are reported as the mean fitness ± 95% confidence interval of the mean fitness value.

_N_-methylglutamate Dehydrogenase Assay

Three biological replicates per strain were grown to half maximum OD_{600} in hypho and 7.0 mM succinate and induced with 20 mM methylamine hydrochloride overnight. Cells were centrifuged, resuspended in Tris-HCl (pH 7.5), and lysed using a FastPrep-24 (MP Bio, Santa Ana, CA) and lysing matrix B (MP Bio). Lysates were centrifuged at 13000 rpm for 5 minutes and total protein in the supernatant was quantified using the Quick Start Bradford Assay (BioRad, Hercules, CA) using bovine serum albumin (BSA) as a standard. Approximately, 0.1mg of protein was incubated in 50 mM sodium phosphate buffer (pH= 7.6) with 5mM *N*-methylglutamate and 0.5mM NAD at room temperature for 40 minutes. An equal volume of the Nash reagent was added to each reaction tube at T_0 as well as T_{40} and incubated at 58ºC for 30 minutes. Formaldehyde production was estimated by measuring the absorbance at 412 nm (Nash 1958) and comparison to a standard curve generated for formaldehyde concentrations ranging from 50 μM to 1 mM. NMGDH activity was measured as the nmol formaldehyde produced / (mg protein. minute) and reported as the mean ± 95% confidence interval of three biological replicates.

Genome Sequencing

Cells grown to saturation in hypho media with 7mM succinate were centrifuged, re-suspended in Tris-EDTA buffer with 1% Triton-X 100, and lysed using a combination of lysozyme and heat shock at 70ºC-90ºC for 10 minutes. Lysed cells were treated with proteinase K and RNase A at 37ºC for two hours and genomic DNA was extracted using the phenol-chloroform extraction protocol. DNA concentration was quantified using the Nanodrop spectrophotometer ND-1000 (Thermo Fischer Scientific, Wilmington, DE). Single-end 50 bp reads for Illumina sequencing were prepared using the TruSeq DNA sample prep Kit (Illumina, San Diego, CA) and sequenced using an Illumina Hi-Seq machine at the Microarray and

Genomics Core Facility, Huntsman Cancer Institute, Utah. Reads were assembled and aligned on the *M. extroquens* AM1 genome using Breseq version 0.21 (Deatherage and Barrick 2014). Mutations were verified by PCR and Sanger sequencing.

q-RT PCR

Three biological replicates per strain were grown to half maximum OD_{600} in hypho and 7.0 mM succinate and induced with 20 mM methylamine hydrochloride overnight. Cultures were centrifuged at 4ºC for 10 mins at 4500g and RNA was extracted using an RNeasy Kit (Qiagen, Germantown, MD) and RNAse-free DNAse (Qiagen). Total RNA concentration was quantified using a Nanodrop spectrophotometer ND-1000 (Thermo Fischer Scientific, Wilmington, DE). For the synthesis of cDNA, 1 µg RNA was reverse transcribed using SuperScript III (Life Technologies, Carlsbad, CA). qPCR was performed using a CFX-96 qPCR machine (Bio-Rad, Hercules, CA) and EvaGreen qPCR mix (Biotium, Hayward, CA). The transcript level of the ribosomal protein RpsB was used as an internal standard and the relative expression of Meta1_4101 and Meta1_4102 was quantified using the protocol described elsewhere (Chou et al. 2009; Agashe et al. 2013). A no template control, a no RT control, and a standard curve with DNA concentrations from 1 ng to 10^{-6} ng was run for every primer pair.

Urea Quantification Assay

The urea concentration in the spent media was tested in two conditions: a) half maximum OD_{600} in hypho with 3.5 mM succinate and induction with 20 mM methylamine hydrochloride overnight and b) half maximum OD_{600} in hypho with 3.5 mM succinate. Spent media was collected by centrifuging the cells at 4500g for 10 mins and running the supernatant through a 1 micron sterile membrane filter (Millipore). Urea concentration was measured using the Urea Assay Kit (Sigma-Aldrich, St. Louis, MO) as per the manufacturer's instructions. Two technical replicates were performed per biological replicate. The urea concentration reported is the mean ± 95% confidence interval of three biological replicates.

Table 5.1: *M.extorquens* strains and plasmids used in this study

Strain or plasmid	Description	Reference
Strains		
CM501	*M.extorquens* AM1	Lee et al., 2009
CM1054	A2	Lee and Marx 2012
CM2351	Δ*mau* in *M. extorquens* AM1	This study
CM2720	Δ*cel* in *M. extorquens* AM1	Delaney et al., 2013
CM2770	Δ*fae* in CM2720 (A1)	This study
CM2986	E1	This study
CM3014	E2	This study
CM3488	CM2986 + pAYC139	This study
CM3807	Δ*mptG* in CM2720	This study
CM3811	Δ*mptG* in CM2986	This study
CM3813	Δ*mptG* in CM3014	This study
CM4135	$kefB^{E1}$ in CM2770	This study
CM4140	Δ*kefB* in CM2986	This study
CM4142	$kefB^{WT}$ in CM2986	This study
CM4149	Δ*mgdABCD* in CM2986	This study
CM4152	Δ*mgdABCD* in CM3014	This study
CM4153	$Meta1\_1544^{WT}$ in CM3014	This study
CM4169	$kefB^{E1}$ in CM2720	This study
CM4187	Δ*mgdABCD* in CM2720	This study
CM4189	Δ*mgdABCD'*in CM4149	This study
CM4194	$Meta1\_1544^{E2}$ in CM2720	This study
CM4311	Δ*mau* Δ*fae* in *M. extorquens* AM1	This study
Plasmids		
pCM433	Allelic exchange vector (Tet^R, Suc^S)	C. J. Marx 2008
pDN50	pCM433 with Δ*fae* upstream and downsteam flanks	Nayak and Marx 2014a
pDN69	pCM433 with Δ*mptG* upstream and downsteam flanks	This study
pDN112	pCM433 with Δ*mgdABCD* upstream and downsteam flanks	This study
pDN136	pCM433 with *kefB* allele from E1	This study
pDN137	pCM433 with *kefB* allele from WT	This study
pDN142	pCM433 with Δ*kefB* upstream and downsteam flanks	This study
pDN150	pCM433 with Meta1_1544 from E2	This study
pDN151	pCM433 with Meta1_1544 from WT	This study
pAYC139	Plasmid with *mau* gene cluster from AM1 (IncP, *tra,* Tet^R)	Chistoserdov et al. 1991
pRK2073	Conjugative helper plasmid (IncP, *tra,* Str^R)	Figurski and Helinski 1979

Results

Experimental evolution of *Methylobacterium extorquens* AM1 mutants to grow on methylamine via the *N*-methylglutamate pathway

AM1 encodes two alternate routes for the primary oxidation of methylamine in its genome: MaDH and the NMG pathway. While MaDH is essential for methylamine growth in AM1 (Chistoserdov et al. 1991), the NMG pathway is not (M. E. Lidstrom 2006). To unravel a physiological basis for this discrepancy between degeneracy in the metabolic context and the organismal context, we experimentally evolved two distinct strains of AM1that were incapable of methylamine growth but still had an intact NMG pathway for the primary oxidation of methylamine.

The first strain (Figure 5.1b) (referred to as A1 from here on) had a lesion in *fae* (Vorholt et al. 2000). FAE (Formaldehyde Activating Enzyme) catalyzes the condensation of formaldehyde and tetrahydromethanopterin (H_4MPT) (Vorholt et al. 2000); a reaction immediately downstream of primary oxidation of C_1 compounds (Figure 5.1a). While *fae* is essential when MaDH mediates the primary oxidation of methylamine (Agashe et al. 2013), it is not requires when the NMG pathway is (Nayak and Marx 2014b) used instead. The second strain (Figure 5.1c) (referred to as A2 from here on) was isolated from a population of AM1 that was evolved for 1500 generations in media containing a C_1 substrate (methanol) as well as a multi-C substrate (succinate) (CJ Marx, unpublished; Lee and Marx 2012). Phenotypic assays post-isolation revealed that A2 could not grow on methylamine in liquid media and genome sequencing of A2 elucidated the underlying genotype: an IS-mediated recombination event that led to the deletion of the *mau* gene cluster (Figure 5.1c) (TableS3.1, Appendix 3). The methylamine fitness of A1 and A2 relative to AM1 expressing the fluorescent protein mCherry (Michener et al. 2014) was extremely low; the mean fitness values (calculated from three replicate competitions) were 0.4% and 1.0% respectively (Figure 5.2c).

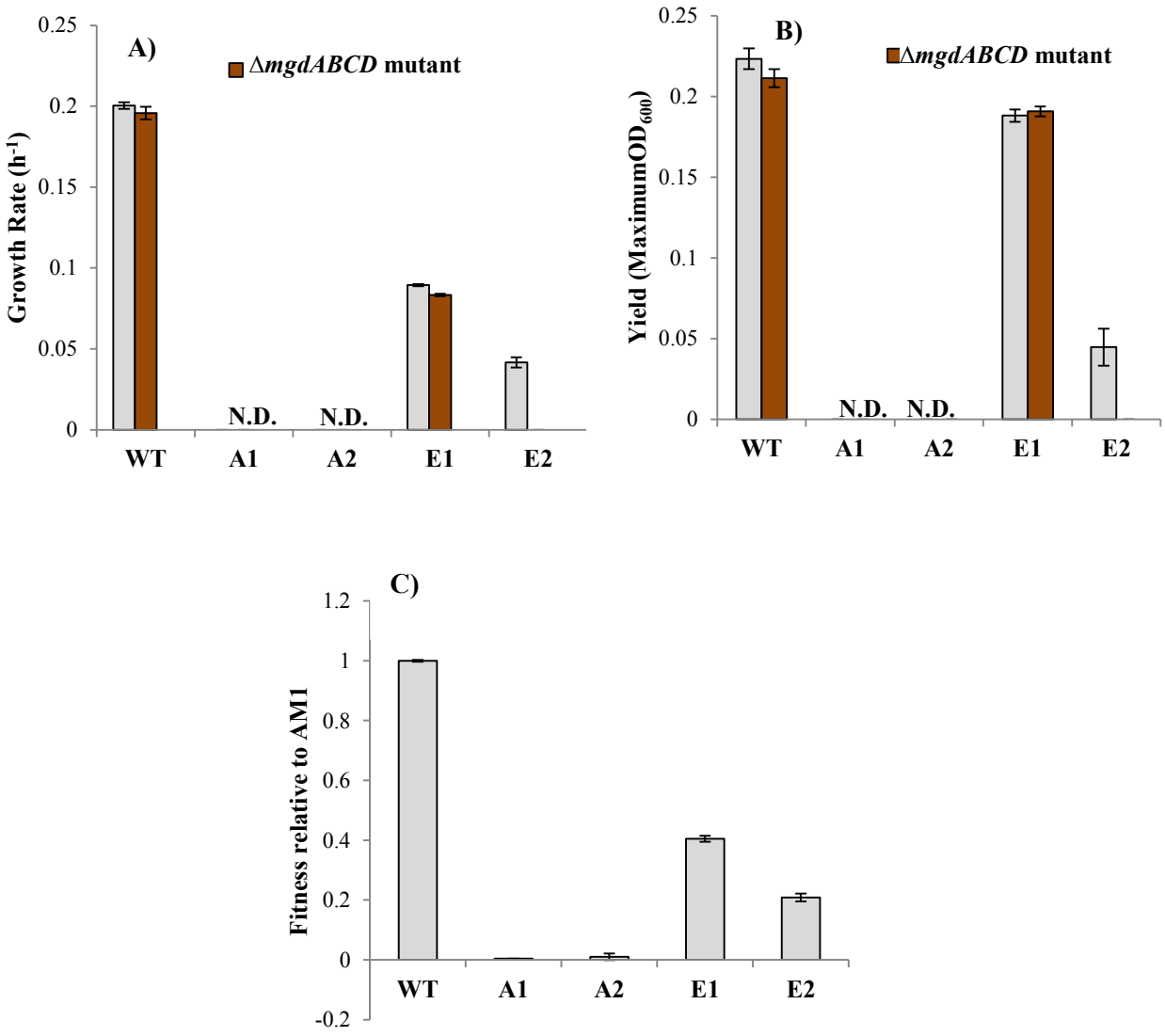

Figure 5.2: A) Growth rate and **B)** Yield or maximum OD_{600} on 20 mM methylamine of WT, the two ancestral strains, and the two evolved isolates with (gray) and without the *N*-methylglutamate pathway (brown). **C)** Competitive fitness of WT, the two ancestral strains, and the two evolved isolates on 20 mM methylamine hydrochloride relative to a strain of *M. extorquens* AM1 expressing the fluorescent protein *mCherry*. The error bars represent the 95% confidence interval of the mean of three biological replicates.

N. D. Not Detected

The methylamine fitness of A1 and A2 was also significantly lower than other *M. extorquens* strains like PA1 (Nayak and Marx 2014c) which only possess the NMG pathway for methylamine oxidation (Nayak and Marx 2014b). These low fitness values further corroborate that the NMG pathway has a miniscule contribution towards methylamine growth in AM1.

A single population of A1 as well as A2 was experimentally evolved to grow on 20 mM methylamine as the sole carbon and energy source. The methylamine fitness of A1 increased by 110.5-fold after 150 generations whereas the methylamine fitness of A2 in methylamine increased by 21.7-fold after ~20-50 generations (Figure 5.2c). A single isolate, representative of each population in terms of the mean fitness on methylamine (referred to as E1 and E2 from here on), was used to conduct further analyses. Despite being significantly faster than their respective ancestors, E1 and E2 grew 53.8% ($p< 0.01$) and 79.2% ($p<0.01$) slower with 15.7% ($p<0.01$) and 80% ($p<0.01$) lower yield (measured as maximum OD_{600}) than WT on methylamine (Figure 5.2a, Figure 5.2b).

To ascertain if the NMG pathway mediates in E1 and E2, we deleted *mgdABCD* - encoding *N*-methylglutamate dehydrogeanse (NMGDH) (Martinez-Gomez et al. 2013; Gruffaz et al. 2014) (Figure 5.2a, Figure 5.2b) – in each of these strains. The Δ*mgdABCD* mutant of E2 could no longer grow on methylamine whereas the Δ*mgdABCD* mutant of E1 was only 7% slower ($p<0.01$). Residual NMGDH activity in the Δ*mgdABCD* mutant of E1 (Table S3.2, Appendix 3) indicated a second copy of *mgdABCD* in theE1 genome which was subsequently deleted and the resulting double knockout could no longer grow on methylamine.

While MaDH produces free formaldehyde as the end product (McIntire et al. 1991; Chistoserdova et al. 2003), the end product of the NMG pathway is still being debated (Latypova et al. 2010; Martinez-Gomez et al. 2013; Nayak and Marx 2014b). Prior work with *M. extorquens* PA1, a strain that grows on methylamine only using the NMG pathway, has shown that the H_4MPT-dependent formaldehyde oxidation pathway (Nayak and Marx, 2014b) is essential during methylamine growth but it was unclear

formaldehyde was the sole end-product of methylamine oxidation. We deleted *mptG* (encoding β ribofuranosylaminobenzene 5'phosphate synthase, an enzyme that catalyzes the first step of the H_4MPT biosynthesis pathway (Rasche et al. 2004) in WT, E1, and E2. None of the resulting mutants grew on methylamine. Contrary to the Δ*mptG* mutant of PA1 (Nayak and Marx 2014 a), the Δ*mptG* mutants of E1 as well as E2 could no longer use methylamine as a nitrogen source. Surprisingly though, the Δ*mptG* WT strain could still use (albeit poorly) methylamine as a nitrogen source (data not shown). Therefore, the extreme sensitivity of the Δ*mptG* mutants of E1 and E2 to methylamine suggested that methylamine oxidation via the NMG pathway might actually produce free formaldehyde as the end-product.

Genetic basis of adaptation to grow on methylamine using the *N*-methylglutamate pathway

To unravel the physiological constraints that needed to be overcome to grow on methylamine using the NMG pathway, we sequenced the genome of E1, A2, and E2 and mapped the mutations relative to the AM1 reference genome (Table S3.1, Appendix 3; Figure 5.3a, Figure 5.3b). E1 had three unique mutations relative to A1 (Figure 5.3a): a) an IS mediated recombination event that led to the deletion of the *mau* gene cluster, b) a Q446* mutation in *kefB* and c) a duplication of a 10kb genomic region comprising the genes that encode enzymes of the NMG pathway. E2 had two unique mutations relative to A2: a) a W173* mutation in Meta1_1544 (a gene upstream of the 10 kb gene cluster encoding the three enzymes of the NMG pathway) and b) an IS insertion in the *ykkC/yxkD* RNA element (Barrick et al. 2004) immediately upstream of an ABC transporter (TableS3.1, Appendix 4; Figure5.3b).

We investigated the role of each of these mutations on methylamine growth by introducing the mutant alleles from the evolved strain in the ancestor (or vice versa) in isolation and also in combination with each other. Of the three mutations in E1, only the mutation that led to the deletion of the *mau* operon significantly was beneficial in the A1genomic background (Figure 5.3c). A combination of the mutations that lead to the deletion of the *mau* gene cluster and the duplication of the NMG pathway genes was extremely beneficial; this strain was 93-fold more fit than A1 on methylamine ($p < 0.01$).

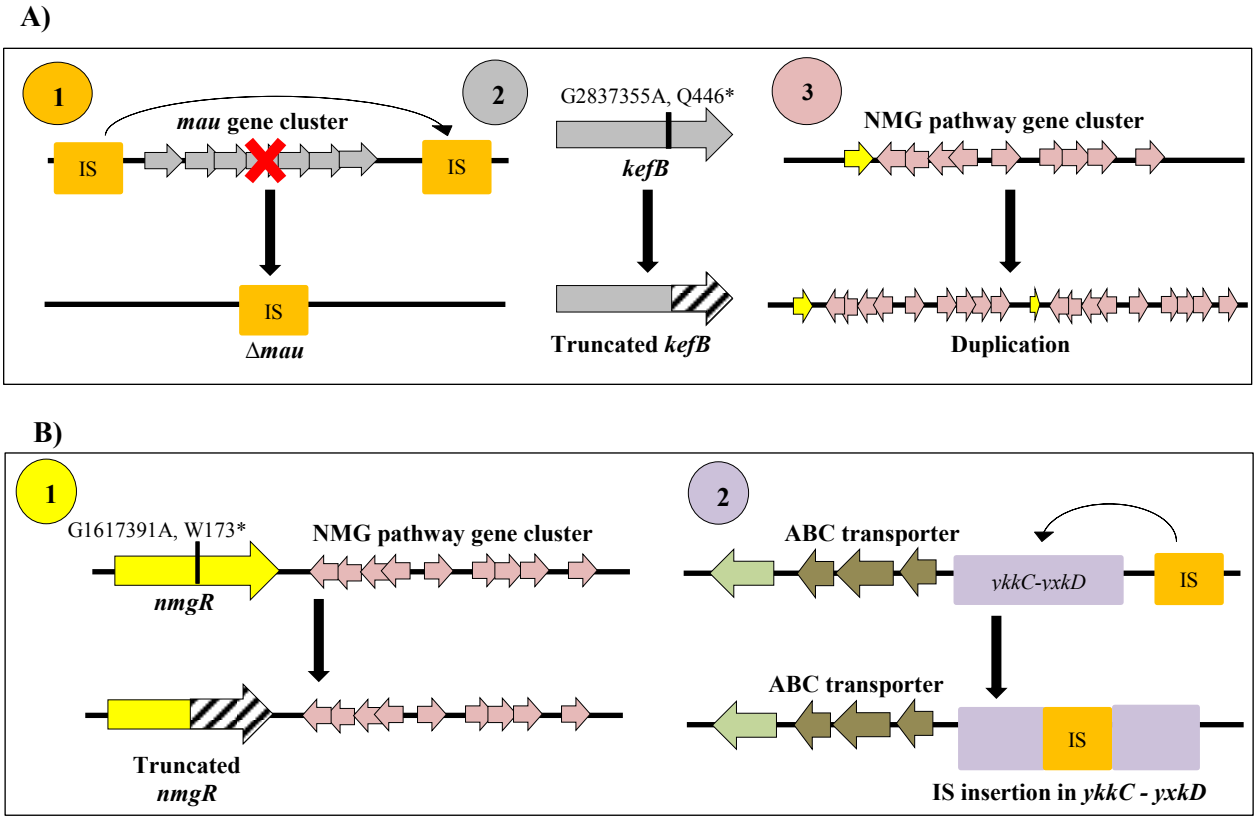

Figure 5.3: A) Mutations in the evolved isolate (E1) derived from the Δ*fae* ancestor: 1) an ISMex15 (orange) mediated recombination event that led to the deletion of a30kb genomic region containing the *mau* gene cluster. 2)

(**Figure 5.3 Continued**) A non-synonymous point mutation leading to a premature stop codon in *kefB*. 3) A tandem duplication of a 10 kb genomic region containing the NMG pathway genes (in pink) **B)** Mutations in the evolved isolate (E2) derived from the Δ*mau* ancestor. 1) A non-synonymous point mutation leading to a premature stop codon in a gene (yellow) directly upstream of the NMG pathway gene cluster (pink). 2) An ISMex15 family mediated transposition event in the *ykkC/yxkD* RNA element (purple) 488 bp upstream of ABC transporter. **C)** Competitive fitness of strains with different combinations of mutations from E1 on 20mM methylamine. **D)** Competitive fitness of strains with different combinations of mutations from E2 on 20mM methylamine. The error bars represent the 95% confidence interval of the mean of three biological replicates.

The Q446* mutation in *kefB* further increased the fitness on methylamine by 14.1% (Figure 5.3c). To determine whether this truncated *kefB* allele behaves like a null mutant, we deleted *kefB* in the E1 genomic background. The methylamine fitness of the E1+ Δ*kefB* mutant was significantly lower than E1 (8%; $p < 0.01$) (Figure S3.1, Appendix 3) suggesting that the truncated version of *kefB* is not a null mutation, and encodes functional protein. The fitness data of different combination of mutations that arose in E1 suggested that the deletion of the *mau* gene cluster was the first mutation to have fixed in the A1 population. In fact, when the *mau* gene cluster was re-introduced on a plasmid (pAYC139) (Chistoserdov et al. 1991) in the E1 genomic background, the fitness of the resulting transconjugant on methylamine was -12.4% ($p < 0.01$) (Figure 5.3c).

Contrary to E1, no evidence of sign epistasis was detected in E2 (Figure 3d). Both mutations were beneficial; the IS insertion in the *ykkC/yxkD* RNA element increased the fitness on methylamine by 15-fold ($p < 0.01$) and the W173* mutation in Meta1_1544 increased the fitness further by 37% ($p < 0.01$) (Figure 5.3d).

Low expression levels prevent methylamine growth using the *N*-methylglutamate pathway in *M. extroquens* AM1

The duplication of the 10 kb genomic region with the genes of the NMG pathway in E1 as well the W173* mutation in Meta1_1544 (immediately upstream of the NMG pathway genes) in E2 suggested

that the expression level of the NMG pathway may have changed over the course of evolution. As a proxy for the expression level of the NMG pathway, we measured the enzyme activity of NMGDH in WT, E1, and E2 grown in succinate and induced with methylamine overnight. The activity of NMGDH in E1 and E2 was 9.3-fold and 5.2-fold greater than the activity observed in WT (Figure 5.4a). Genomic proximity, along with phenotypic evidence that a missense mutation in Meta1_1544 increased the expression level of the NMG pathway genes, suggests that this gene acts as a repressor of the NMG pathway and we have renamed it *nmgR* (for NMG pathway repressor). The heightened expression of the NMG pathway also increased the growth rate and yield when methylamine was used as a nitrogen source in the presence of an alternate carbon source (succinate) (Figure 5.4b). The ratio of growth rate on succinate with methylamine as a nitrogen source versus ammonia as a nitrogen source ($\mathbf{k}_{\text{succinate, methylamine}}/\mathbf{k}_{\text{succinate, ammonia}}$) for E1 was 2.1-fold higher than A1 and for E2 was 18% greater than A2. Unlike WT though, the growth rate or yield for E1 and E2 on a combination of methylamine and succinate was not greater than that on succinate alone (Table S3.3, Appendix 3).

Cytoplasmic pH increases drastically during methylamine growth using the *N*- methylglutamate pathway

Ammonium ions (NH_4^+) are a by-product of methylamine oxidation (Figure 5.1). 1 mol of NH_4^+ is released per mol of methylamine oxidized (Latypova et al. 2010; Chen et al. 2010), so is likely to rapidly buildup in either the periplasm or the cytoplasm depending on whether primary oxidation is mediated by MaDH or the NMG pathway. NH_4^+ buildup can lead to a drastic increase in pH among other toxic effects previously noted (K. S. Warren 1962). Even a small change in the cytoplasmic pH is extremely detrimental to the cell (Maurer et al. 2005). Thus, when AM1 switches to and overexpresses the NMG pathway for the primary oxidation of methylamine, a concomitant rise in cytoplasmic pH might emerge as a novel physiological constraint.

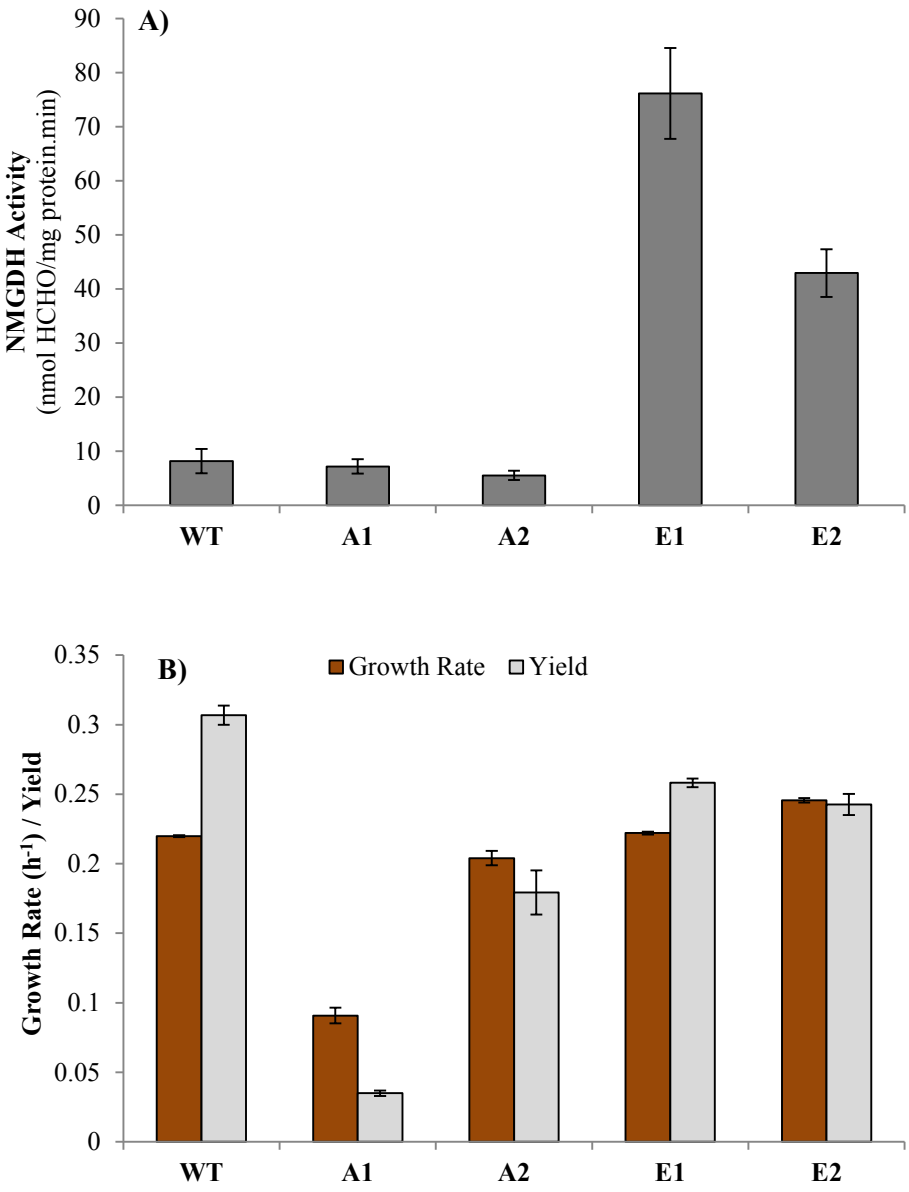

Figure 5.4: A) The mean activity of the *N*-methylglutamate dehydrogenase enzyme in crude extracts from methylamine induced cells of WT, the two ancestral strains, and the two evolved isolates. The error bars represent the 95% confidence interval of the mean activity for three biological replicates. **B)** The growth rate (in brown) and yield or maximum OD_{600} (gray) of WT, the two ancestral strains, and the two evolved isolates in nitrogen-free media with succinate as the carbon source and methylamine as the sole nitrogen source. The error bars represent the 95% confidence interval of the mean growth rate/ yield of three biological replicates.

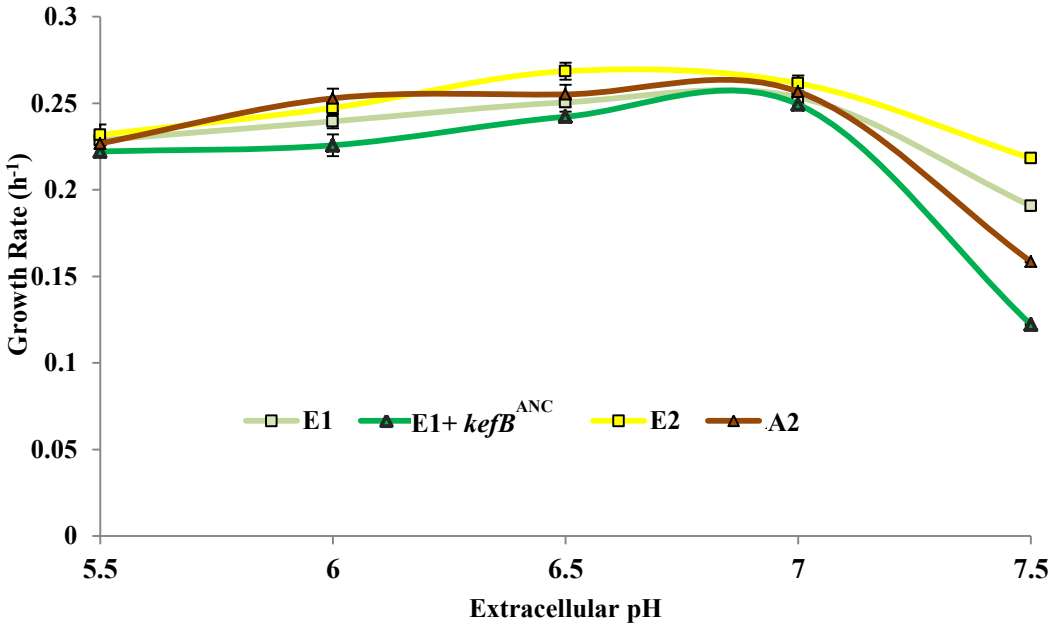

Figure 5.5: Succinate growth rates of E1 (light green squares), E1 containing the ancestral allele of *kefB* (dark green triangle), E2 (yellow squares), and A2 in media buffered to a pH range of 5.5-7.5. The error bars represent the 95% confidence interval of the mean growth rate of three biological replicates.

We hypothesized that the Q446* mutation in *kefB* in E1 as well as the IS insertion in the *ykkC/yxkD* RNA element (Barrick et al. 2004; W. C. Winkler 2005; Meyer et al. 2011) in E2 are unique adaptations to counteract the increase in cytoplasmic pH/NH_4^+ buildup during methylamine growth. First, we tested this hypothesis by measuring the ability of E1, a mutant strain of E1 with the ancestral allele of *kefB* (E1 + $kefB^{Ancestral}$), E2, and A2 to grow on succinate in minimal media buffered to different pH values ranging from 5.5 to 7.5 (Figure 5.5). We predicted that the ability to counteract an increase in internal pH might also make E1 and E2 more resistant to media with high pH. In accord with our predictions, the growth rate of E1 was 2.3 fold greater than E1+$kefB^{Ancestral}$ ($p < 0.01$) and of E2 was 37.2% ($p < 0.01$) greater than A2 (Figure 5.5) only in media at pH = 7.5. This outcome suggested that the Q446* mutation in *kefB* might lead to the constitutive expression of the *kefB* potassium/proton anti-porter (Ferguson et al. 1997; I. R. Booth 2007) for buffering cytoplasmic pH during methylamine growth.

The IS insertion in the *ykkC-yxkD* RNA element is likely to change the expression pattern of the flanking nitrate/sulfonate/bicarbonate ABC transporter that is often associated with this RNA element (Barrick et al. 2004). Since this particular ABC transporter is downstream of urea biosynthesis/degradation genes, we hypothesized that it might act as an efflux pump for urea or a related compound and buffer ammonia buildup during methylamine metabolism. As a first step to test our hypothesis, we measured the urea concentration in the spent media of E2 as well as A2. 6.08±1.90 ng/µl urea (mean±95% confidence interval of the mean urea concentration for three biological replicates) was detected in the spent media when E2 was grown on succinate and 5.57±1.04 ng/µl urea was detected when succinate cultures of E2 were induced with methylamine overnight. No significant amount of urea was detected in the spent media of A2 during succinate growth or after methylamine induction .To further verify if urea was being excreted by the nitrate/sulfonate/bicarbonate ABC transporter upstream of the *ykkC-yxkD* RNA element, we quantified mRNA levels of this ABC transporter in E2 and A2 after an overnight induction of succinate grown cells with methylamine. The relative expression of this ABC transporter in E2 was 58.1% ($p < 0.05$; Welch's t-test with two degrees of freedom) higher than in A2.

Mutations that alleviate ammonia buildup are beneficial during methylamine growth in WT

Does the cost of simultaneously expressing two functionally degenerate pathways for methylamine outweigh the benefit of increased flux through primary oxidation or vice versa? Two key physiological constraints, low basal expression level as well as a sharp increase in cytoplasmic pH, prevent the NMG pathway from being expressed along with MaDH when AM1 grows on methylamine. To increase the expression of the NMG pathway, we introduced the nonsense mutation (W173*) in *nmgR* in WT (WT + $nmgR^{Evo}$). To buffer cytoplasmic ammonia buildup, we introduced the Q446* mutation in *kefB* in WT (WT + $kefB^{Evo}$).

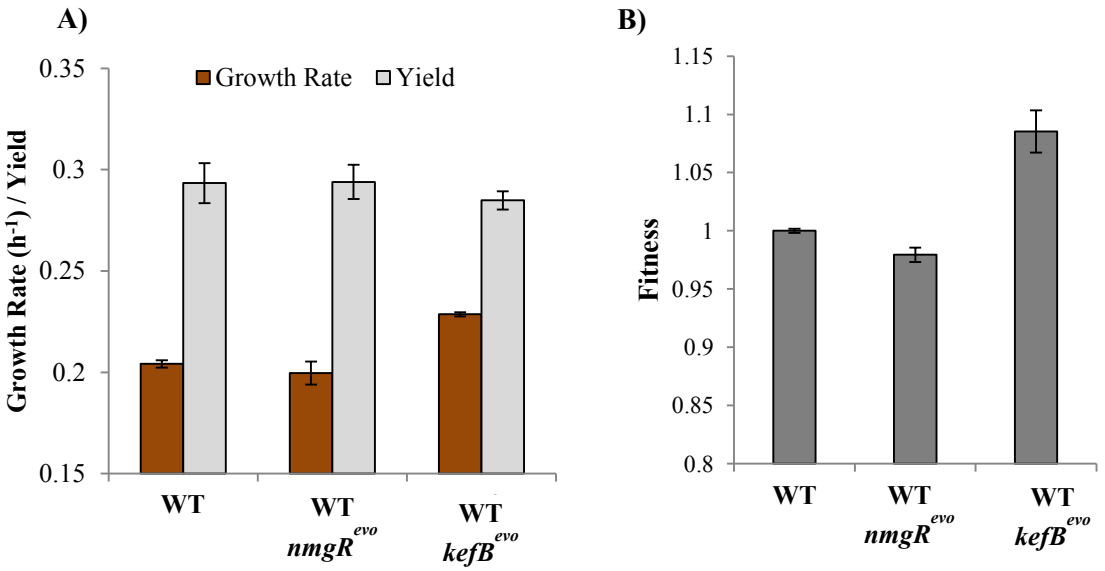

Figure 5.6: A) Growth rate (brown), yield or maximum OD_{600} (gray) and **B)** competitive fitness on 20 mM methylamine for WT, WT with the evolved allele of *kefB* from E1, WT with the evolved allele of *nmgR* from E2. The error bars represent the 95% confidence interval of the mean of three biological replicates.

Relative to WT, no significant difference in growth rate ($p = 0.6555$), yield ($p= 0.7915$) or competitive fitness ($p = 0.0749$) on methylamine was observed for WT + $nmgR^{Evo}$. (Figure 5.6a, Figure 5.6b). In contrast, WT + $kefB^{Evo}$ was 8.5% more fit ($p < 0.01$) and grew 12.0% faster ($p < 0.01$) on methylamine but had a 2.9% decrease in yield ($p < 0.01$) compared to WT (Figure 5.6a, Figure 6b). Additionally, WT + $kefB^{Evo}$ was 14.0 %, 14.3%, and 4.1% more fit than WT on succinate ($p < 0.01$), methanol ($p < 0.01$) and formate ($p < 0.01$) respectively (FigureS3.2, Appendix 3). Altogether, overexpressing the NMG pathway in WT does not change the growth rate or yield in methylamine but physiological solutions that alleviate NH_4^+ buildup are beneficial in WT too.

Discussion

Decades of research had established that MaDH was the sole pathway for the primary oxidation of methylamine in AM1. This notion was recently challenged when a study (Martinez-Gomez et al. 2013)

reported that enzymes of the NMG pathway for methylamine oxidation are also encoded and, under specific conditions, highly expressed in AM1. Then why was this degeneracy not discovered earlier? What physiological constraints occluded the functional realization of metabolic degeneracy in AM1? To answer these questions two mutant strains of AM1, conventionally known to have a methylamine$^-$ phenotype, were experimentally evolved on methylamine as the sole carbon and energy source. The first strain, a Δ*fae* mutant (A1) , had a partial lesion in the H_4MPT dependent formaldehyde oxidation module so as to constrain the rate of formaldehyde oxidation to that mediated by the spontaneous reaction with H_4MPT (Marx et al. 2003). In the presence of methylamine, free formaldehyde rapidly builds up in the Δ*fae* mutant; by switching to the NMG pathway this mutant should be able to sustain methylamine growth, albeit at a slower rate (Nayak and Marx 2014b). The second strain (A2) had an IS mediated recombination that led to the deletion of the entire *mau* gene cluster encoding MaDH and ancillary proteins. Comparative genomic analysis of the evolved mutants revealed three key adaptive mutations that were required to facilitate the functional actualization of genomic degeneracy. The potentiating mutation, a deletion of the *mau* operon, was unique to the Δ*fae* evolved population (E1). Deletion of MaDH counters the buildup of free formaldehyde inside the cell and is likely to increase the survival of the Δ*fae* mutant on methylamine drastically. Also, mutations that increased the flux through the NMG pathway were contingent on a Δ*mau* deletion background. Sign epistasis between rate-enhancing mutations and survival-enhancing mutations are likely to manifest in environments where survival, rather than growth rate, is the first and foremost evolutionary hurdle cells have to overcome.

A striking observation about mutants lacking a functional MaDH is that they can still use methylamine as a nitrogen source (Chistoserdov et al. 1991). Also, as a consequence of increasing flux through the NMG pathway, the growth rate of both the evolved isolates on methylamine as a nitrogen source improved tremendously (Figure 5.4b). These data suggest that, in the natural environment, AM1 probably encounters methylamine in two completely different roles - as a carbon source or as a nitrogen source. In environments where methylamine is abundant and serves as the preferred carbon source,

MaDH catalyzes primary oxidation. In environments with other carbon source/s but with methylamine as the sole/preferred nitrogen source, the NMG pathway might be recruited for primary oxidation instead. Functionally degenerate pathways specialized for unique ecological roles would only co-exist in a genome if there were trade-offs. We theorize that the NMG pathway should have a much lower K_m than MaDH to use low concentrations of methylamine as a nitrogen source and MaDH should have a higher V_{max} than the NMG pathway to use methylamine as a carbon source.

An increase in the expression level of the NMG pathway was observed in both evolved populations. A tandem duplication of the entire 10kb genomic region containing the NMG pathway genes (Figure 5.3a) in E1 and a nonsense mutation in a repressor of the NMG pathway gene cluster (named *nmgR*) (Figure 5.3b) in E2 were extremely beneficial and led to a significant increase in the competitive fitness as well as growth rate on methylamine (Figure 5.3c, Figure 5.3d). These adaptive mutations reveal two salient aspects of regulation that prevent functional degeneracy: 1) if a functional MaDH is present, the NMG pathway is tightly repressed, even in the presence of methylamine (Figure 5.4a and 5. 2) even if MaDH is absent, the expression level of the NMG pathway is much lower than that has been observed for MaDH (Figure 5.4a) (McIntire et al. 1991). Compared to MaDH, the NMG pathway is energetically unfavorable because it oxidizes methylamine in an ATP-dependent manner (Kung and Wagner 1969; Latypova et al. 2010). A regulatory framework that controls the expression of the NMG pathway and restricts it to those environments (with low concentrations of methylamine as a nitrogen source) in which the MaDH is suboptimal would enable higher yield/growth rate on methylamine as a carbon source. The exact mechanism by which the cell determines the methylamine concentration and switches between these two pathways is yet to be determined

Overexpression of the NMG pathway in methylotrophs like AM1, that typically use a periplasmic MaDH for methylamine growth, results in alkalization of the cytoplasmic space. Unique physiological innovations to counter the rise in cytoplasmic pH/ NH_4^+ ions were observed in each of the evolved populations. KefB, a glutathione-gated K^+/H^+ anti-porter protects *E. coli* from electrophiles by acidifying

the cytoplasm (Ferguson et al. 1997; I. R. Booth et al. 2007). KefB is inhibited by glutathione and activated by glutathione adducts (formed in the presence of electrophiles) that bind to a C-terminal domain (Ness and Booth 199). A Q446* mutation in *kefB* abolishes the C-terminal glutathione-binding domain and uncouples the activity of the K^+/H^+ anti-porter from the redox state of the cell. The truncated KefB, by increasing H^+ influx, prevents cytoplasmic alkalization during methylamine growth. Eukaryotes mitigate NH_4^+ buildup by converting it to the less toxic, less basic, nitrogenous compound urea (Mommsen and Walsh 1992; M. A. Singer 2003). In E2, an IS insertion in the *ykkC/yxkD* RNA element increased the expression of a proximal ABC transporter by 58% which, in turn, led to a significant increase in the urea concentration in the spent media. As in other bacteria (Barrick et al. 2004; W. C. Winkler 2005), the *ykkC/yxkD* RNA element in AM1 is proximal to urea utilization genes (Figure 3b). Our data suggests that the *ykkC/yxkD* RNA element represses the neighboring transporter unless bound to an unknown ligand. An IS insertion in this RNA element de-represses the transporter and converts it into a urea efflux pump. Whether this ABC transporter is specific for urea or has a wide substrate-breath for urea-based compounds, including many natural antimicrobial agents (Tegos et al. 2008), remains to be determined. To the best of our knowledge, this is the first study to show that members of the bacterial domain use active transport to remove nitrogenous waste from cells. Furthermore, *Helicobacter pylori,* commonly associated with gastric ulcers, is known to import urea and enzymatically degrade it to release ammonia in the cytoplasm as a unique adaptation to buffer the acidic environment in the human stomach (Weeks et al. 2000). It is remarkable that we observed a distantly related bacterial species innovate the same general physiological mechanism to deal with the inverse problem – a rise in intracellular pH.

Methylamine metabolism is unique because it can provide methylotrophs carbon and/or nitrogen. Two functionally degenerate pathways with different expression levels, regulatory patterns, energetic yields, and potentially kinetic parameters play ecologically specialized roles by allowing AM1 to optimally use methylamine as a carbon source as well as a nitrogen source. The MaDH/ NMG pathway degeneracy (Figure 5.7a, 5.7b) is verisimilar to the well-established mechanism by which *E. coli* cells

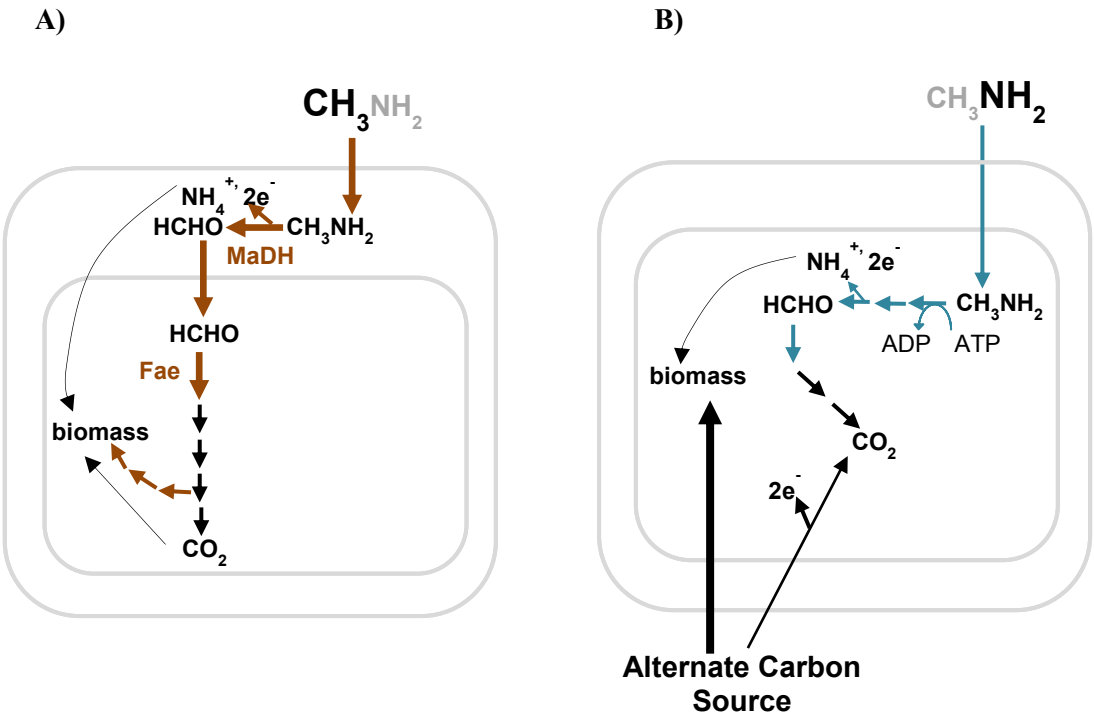

Figure 5.7: **A)** A schematic representing the metabolic route followed by methylamine when *M. extorquens* AM1 grows on abundant methylamine as a carbon source and/or a nitrogen source. Methylamine dehydrogeanse is the sole module involved in primary oxidation. **B)** A schematic representing the metabolic route likely to be followed by methylamine when *M. extorquens* AM1 uses limiting concentrations of methylamine as the sole nitrogen source in the presence of other, more abundant, carbon substrate/s. The *N*-methylglutamate pathway is the sole module involved in primary oxidation.

MaDH: Methylamine dehydrogeanse

exploit one of glutamine synthetase-glutamate synthase (GOGAT) and glutamate dehydrogenase (GDH) for optimal ammonia assimilation based on substrate and ammonia availability (Yuan et al. 2009; L. Reitzer 2003). Thus, metabolic degeneracy that isn't functionally relevant in the laboratory might still be environmentally relevant by allowing the cells to exploit a wider concentration gradient or optimally use different units of a complex compound.

References

1. Romano AH, Conway T (1996) Evolution of carbohydrate metabolic pathways. Res. Microbiol. 147:448-455.

2. Edelman GM, Gally JA (2001) Degeneracy and complexity in biological systems. PNAS 98:13763-13768.

3. Boucher Y, Douady CJ, Papke RT, Walsh DA, Boudreau MER, NesbØ CL, Case RJ, Doolittle WF (2003) Lateral gene transfer and the origins of prokaryotic groups. Ann. Rev. Genet. 37:283-328.

4. Marx CJ, Van Dien SJ, Lidstrom ME (2005) Flux analysis uncovers key role of functional redundancy in formaldehyde metabolism. PLoS Biol. 3: e16.

5. Chistoserdova L (2011) Modularity of methylotrophy, revisited. Environ. Microbiol. 13:2603-2622.

6. Berg IA (2011) Ecological aspects of the distribution of different autotrophic CO2 fixation pathways. Appl. Environ. Microbiol. 77:1925-1936

7. Flamholz A, Noor E, Bar-Even A, Liebermeister W, Milo R (2013) Glycolytic strategy as a tradeoff between energy yield and protein cost. PNAS 110:10039-10044.

8. Martiny JBH, Bohannan BJM, Brown JH, et al., (2006) Microbial biogeography: putting microorganisms on the map. Nat. Rev. Microbiol. 4:102-112.

9. Chain PSG, Denaf VJ, Konstantinidis KT, et al., (2007) *Burkholderia xenovorans* LB400 harbors a multi-replicon 9.73-Mbp genome shaped for versatility. PNAS 103:15280-15287

10. Stelling J, Sauer U, Szallasi Z, Doyle III FJ, Doyle J (2004) Robustness of cellular functions. Cell 118:675-685.

11. Deutscher D, Meilijson I, Kupiec M, Ruppin E (2006) Multiple knockout analysis of genetic robustness in the yeast metabolic network. Nat. Genet. 38:993-998.

12. Marx CJ, Miller JA, Chistoserdova L, Lidstrom ME (2004) Multiple formaldehyde oxidation/detoxification pathways in *Burkholderia fungorum* LB400. J. Bacteriol. 186:2173-2178.

13. Chistoserdova L, Gomelsky L, Vorholt JA, Gomelsky M, Tsygankov YD, Lidstrom ME (2000) Analysis of two formaldehyde oxidation pathways in *Methylobacillus flagellatus* KT, a Ribulose monophosphate cycle methylotroph. Microbiology 146:233-238.

14. Chistoserdova L, Lapidus A, Han C, et al., (2007) Genome of *Methylobacillus flagellatus*, molecular basis for obligate methylotrophy, and polyphyletic origin of methylotrophy. J. Bacteriol. 189:4040-4027.

15. Anthony C (1982) The biochemistry of methylotrophs. Academic Press Ltd., London.

16. Eady RR, Large PJ (1968) Purification and properties of an amine dehydrogenase from *Pseudomonas* AM1 and its role in growth on methylamine. Biochem J., 106:245-255.

17. McIntire WS, Wemmer DE, Chistoserdov A, Lidstrom ME (1991) A new cofactor in a prokaryotic enzyme: tryptophan tryptophylquinone as the redox prosthetic group in methylamine dehydrogeanse. Science 252:817-824.

18. Chistoserdov AY, Tsygankov YD, Lidstrom ME (1991) Genetic organization of methylamine utilization genes from *Methylobacterium extorquens* AM1. J. Bacteriol. 18:5901-5908.

19. Chen L, Durley RC, Mathews FS, Davidson VL (1994) Structure of an electron transfer complex: methylamine dehydrogeanse, amicyanin, and cytochrome c551i. Science 264:86-90.

20. Tobari J, Harada Y (1981) Amicyanin: an electron acceptor of methylamine dehydrogeanse. Biochem. Biophysics Res. Comm. 101:502-508.

21. Chen L, Durley R, Poliks BJ, Hamada K, Chen Z, Mathews FS, Davidson VL, Satow Y, Huizinga E (1992) Crystal structure of an electron-transfer complex between methylamine dehydrogeanse and amicyanin. Biochemistry 31:4959-4964.

22. Nayak DD, Marx CJ (2014) Genetic and phenotypic comparison of methylotrophy between *Methylobacterium extorquens* strains AM1 and PA1. PloS One (in revision)

23. Shaw WV, Tsai L, Stadtman (1966) The enzymatic synthesis of *N*-methylglutamic acid. J. Biol. Chem. 241:935-945.

24. Latypova E, Yang S, Wang YS, Wang T, Chavkin TA, Hackett M, Schafer H, Kalyuzhnaya MG (2010) Genetics of the glutamate-mediated methylamine utilization pathway in the facultative methylotrophic beta-proteobacteria *Methyloversatilis universalis* FAM5. Mol. Microbiol. 75:426-439.

25. Chen Y, Scanlan J , Song L, Crombie A, Rahman MT, Schafer H, Murrell JC (2010) γ-glutamylmethylamide is an essential intermediate in the metabolism of methylamine by *Methylocella silvestris.* Appl. Environ. Microbiol. 76:4350-4357.

26. Martinez-Gomez NC, Nguyen S, Lidstrom ME (2013) Elucidation of the role of methylene-tetrahydromethanopterin dehydrogenase MtdA in the tetrahydromethanopterin-dependent oxidation pathway in *Methylobacterium extorquens* AM1. J. Bacteriol.195:2359-2367.

27. Gruffaz C, Muller EEL, Louhichi-Jelail Y, Nelli YR, Guichard G, Bringel F (2014) Genes of the N-methylglutamate pathway are essential for growth of *Methylobacterium extorquens* DM4 on monomethylamine. Appl. Environ. Microbiol. 80:3541-3550.

28. Nayak DD, Marx CJ (2014) Methylamine utilization via a linear *N*-methylglutamate pathway in *Methylobacterium extorquens* PA1 does not require the tetrahydrofolate-dependent C_1 transfer pathway. J. Bacteriol (in revision)

29. Kung HF, C Wagner (1969) γ-glutamylmethylamide a new intermediate in the metabolism of methylamine. J. Biol. Chem. 244:4136-4140.

30. Agashe D, Martinez-Gomez NC, Drummond DA, Marx CJ (2013) Good codons, bad transcript: large reductions in gene expression and fitness arising from synonymous mutations in a key enzyme. Mol. Biol. Evol. 30: 549-560.

31. Michener JK, Vuilleumier S, Bringer F, Marx CJ (2014) Phylogeny poorly predicts the utility of a challenging horizontally transferred gene in *Methylobacterium* strains. J. Bacteriol. 196:2101-2107.

32. Lee M-C, Marx CJ (2012) Repeated, selection-driven genome reduction of accessory genes in experimental populations. PLoS Genetics. 8: e1002651.

33. Delaney NF, Kaczmarek ME, Ward LM, Swanson PK, Lee M-C, Marx CJ (2013) Development of an optimized medium, strain, and high-throughput culturing methods for *Methylobacterium extorquens*. PLoS One. 8: e62957.

34. Gibson DG, Young L, Chuang RY et al. (2009) Enzymatic assembly of DNA molecules up to several hundred kilobases. Nat. Methods. 6: 343-345.

35. Marx CJ (2008) Development of a broad-host-range *sacB*-based vector for unmarked allelic exchange. BMC Res. Notes. 1: 1.

36. Lee M-C, Chou H-H, Marx CJ (2009) Asymmetric, bimodal trade-offs during adaptation of *Methylobacterium* to different growth substrates. Evolution. 63: 2816-2830.

37. Chou H-H, Marx CJ (2012) Optimization of gene expression through divergent mutational paths. Cell Rep. 1: 133-140.

38. Figurski DH, Helinski DR (1979) Replication of an origin-containing derivative of plasmid RK2 dependent on a plasmid function provided *in trans*. PNAS.76: 1648-1652.

39. Lidstrom ME (2006) Aerobic methylotrophic prokaryotes. Prokaryotes 2:618-634.

40. Vorholt JA, Marx CJ, Lidstrom ME, Thauer RK (2000) Novel formaldehyde-activating enzyme in *Methylobacterium extorquens* AM1. 182: 6645-6650.

41. Nayak DD, Marx CJ (2014). Horizontal gene transfer overcomes the adaptive constraints posed by a sub-optimal pathway for methylamine utilization in *Methylobacterium extorquens* PA1. BMC Evolutionary Biology (in review)

42. Chistoserdova L, Chen SW, Lapidus A, Lidstrom ME (2003) Methylotrophy in *Methylobacterium extorquens* AM1 from a genomic point of view. J. Bacteriol. 185:2980-2987.

43. Rasche ME, Havemann SA, Rosenzvaig M (2004) Characterization of two methanopterin biosynthesis mutants of *Methylobacterium extorquens* AM1 by use of a tetrahydromethanopterin bioassay. J. Bacteriol. 186: 1565-1570.

44. Barrick Je, Corbino KA, Winkler WC, et al., (2004) New RNA motifs suggest an expanding scope for riboswitches in bacterial genetic control. PNAS 101:6421-6426.

45. Warren KS (1962) Ammonia toxicity and pH. Nature 195:47-49.

46. Maurer LM, Yohannes E, Bondurant SS, Radmacher M, Slonczewski JL (2005) pH regulates genes for flagellar motility, catabolism and oxidative stress in *Escherichia coli* K-12. J. Bacteriol. 187:304-319

47. Winkler WC, Breaker RR (2005) Regulation of bacterial gene expression by riboswitches. Ann. Rev. Microbiol. 59:487-517.

48. Meyer MM, Hammond MC, Salinas Y, Roth A, Sudarsan N, Breaker RR (2011) Challenges of ligand identification for riboswitch candidates. RNA Biol. 8:5-10.

49. Ferguson GP, Nikolaev Y, McLaggan D, Maclean M, Booth IR (1997) Survival during exposure to the electrophilic reagent N-ethylmaleimide in *Escherichia coli* : role of KefB and KefC potassium channels. J. Bacteriol. 179:1007-1012.

50. Booth IR (2007) The regulation of intracellular pH in bacteria. Novartis Foundation Symposium 221 – Bacterial responses to pH, John Wiley & Sons, Ltd.

51. Marx CJ, Chistoserdova L, Lidstrom ME (2003) Formaldehyde-detoxifying role of the tetrahydromethanopterin-linked pathway in *Methylobacterium extorquens* AM1. J. Bacteriol. 185: 7160-7168.

52. Different foci for the regulation of the activity of the KefB and KefC glutathione-gated K^+ efflux systems. J. Biol. Chem. 274:9524-9530.

53. Mommsen TJ, Walsh PJ (1992) Biochemical and environmental perspectives on nitrogen metabolism in fishes. Experientia 48:583-593.

54. Singer MA (2003) Do mammals, birds, reptiles, and fish have similar nitrogen conserving systems? Comp. Biochem. Phys. Part B: Biochem. And Mol. Biol. 134:543-558.

55. Tegos GP, Masago K, Aziz F, Higginbottom A, Stermitiz FR, Hamblin MR (2008) Inhibitors of bacterial multidrug efflux pumps potentiate antimicrobial photoinactivation. Antimicrob. Agents Chemother. 52:3202-3209.

56. Weeks DL, Eskandari S, Scott DR, Sachs G (2000) An H^+-gated urea channel: the link between *Helicobacter pylori* urease and gastric colonization. Science 287: 482-485

57. Yuan J, Doucette CD, Fowler WU, Feng XJ, Piazza M, Rabitz HA, Wingreen NS, Rabinowitz JD (2009) Metabolomics-driven quantitative analysis of ammonia assimilation in *E. coli.* Mol. Sys. Biol. 5:302.

58. Reitzer L (20030 Nitrogen assimilation and global regulation in *Escherichia coli*. Ann. Rev. Microbiol. 57:155-176.

Appendix 1

Supplementary Material for Chapter 2

Supplementary Table S1.1: A list of methylotrophy-specific genes shared between *M. extorquens* strains AM1 and PA1. (Green: genes involved in methanol oxidation, pink: genes involved in the H_4MPT dependent formaldehyde oxidation pathway, purple: genes involved in the H_4F-dependent formate reduction pathway, orange: genes encoding each of the four formate dehydrogenases and gray: C_1 assimilation genes)

Gene Name	Locus in AM1	Locus in PA1	% Amino Acid Identity
mxaB	**Meta1_4525**	**Mext_4137**	**100**
mxaH	**Meta1_4526**	**Mext_4138**	**98.46**
mxaE	**Meta1_4527**	**Mext_4139**	**96.82**
mxaD	**Meta1_4528**	**Mext_4140**	**99.43**
mxaL	**Meta1_4529**	**Mext_4141**	**97.59**
mxaK	**Meta1_4530**	**Mext_4142**	**98.56**
mxaC	**Meta1_4531**	**Mext_4143**	**99.15**
mxaA	**Meta1_4532**	**Mext_4144**	**96.42**
mxaS	**Meta1_4533**	**Mext_4145**	**96.89**
mxaR	**Meta1_4534**	**Mext_4146**	**99.42**
mxaI	**Meta1_4535**	**Mext_4147**	**100**
mxaG	**Meta1_4536**	**Mext_4148**	**99.49**
mxaJ	**Meta1_4537**	**Mext_4149**	**97.33**
mxaF	**Meta1_4538**	**Mext_4150**	**100**
mxaW	**Meta1_4539**	**Mext_4151**	**96.97**
mxbM	**Meta1_1752**	**Mext_1821**	**100**
mxbD	**Meta1_1753**	**Mext_1822**	**99.63**
mxcQ	**Meta1_4896**	**Mext_4452**	**99.19**
mxcE	**Meta1_4897**	**Mext_4453**	**100**
pqqE	**Meta1_1748**	**Mext_1817**	**99.47**
pqqCD	**Meta1_1749**	**Mext_1818**	**98.12**
pqqB	**Meta1_1750**	**Mext_1819**	**98.7**
pqqA	**Meta1_1751**	**Mext_1820**	**100**
dmrA	**Meta1_4312**	**Mext_3930**	**100**
mptG	**Meta1_1760**	**Mext_1828**	**99.4**
OrfY	**Meta1_1762**	**Mext_1830**	**95.19**
Orf5	**Meta1_1764**	**Mext_1832**	**99.67**
Orf7	**Meta1_1765**	**Mext_1833**	**99.31**
Orf17	**Meta1_1767**	**Mext_1835**	**98.16**
Orf9	**Meta1_1768**	**Mext_1836**	**97.57**
Orf19	**Meta1_1773**	**Mext_1841**	**97.47**
Orf20	**Meta1_1774**	**Mext_1842**	**99.05**
Orf21	**Meta1_1775**	**Mext_1843**	**95.1**
Orf22	**Meta1_1776**	**Mext_1844**	**97.03**
fae	**Meta1_1766**	**Mext_1834**	**100**
mtdB	**Meta1_1761**	**Mext_1829**	**100**
fhcC	**Meta1_1755**	**Mext_1824**	**98.49**
fhcD	**Meta1_1756**	**Mext_1825**	**100**
fhcA	**Meta1_1757**	**Mext_1826**	**99.64**
fhcB	**Meta1_1758**	**Mext_1827**	**99.72**

mch	**Meta1_1763**	**Mext_1831**	**100**
drfA	**Meta1_2852**	**Mext_2659**	**96.99**
folK	**Meta1_1743**	**Mext_1812**	**98.1**
folB	**Meta1_1744**	**Mext_1813**	**97.69**
folP	**Meta1_1745**	**Mext_1814**	**98.62**
folC	**Meta1_4888**	**Mext_4444**	**99.55**
folE	**Meta1_2264**	**Mext_2685**	**100**
ftfL	**Meta1_0329**	**Mext_0414**	**99.82**
mtdA	**Meta1_1728**	**Mext_1797**	**99.65**
fch	**Meta1_1729**	**Mext_1798**	**98.56**
fdh3A	**Meta1_0303**	**Mext_0389**	**99.9**
fdh3B	**Meta1_0304**	**Mext_0390**	**100**
fdh3C	**Meta1_0305**	**Mext_0391**	**99.42**
fdh4B	**Meta1_2093**	**Mext_2104**	**98**
fdh4A	**Meta1_2094**	**Mext_2105**	**98.96**
fdh2C	**Meta1_4846**	**Mext_4404**	**100**
fdh2B	**Meta1_4847**	**Mext_4405**	**98.84**
fdh2A	**Meta1_4848**	**Mext_4406**	**99.68**
fdh1B	**Meta1_5031**	**Mext_4581**	**99.65**
fdh1A	**Meta1_5032**	**Mext_4582**	**99.9**
sga	**Meta1_1726**	**Mext_1795**	**99.75**
hprA	**Meta1_1727**	**Mext_1796**	**99.68**
ppc	**Meta1_1732**	**Mext_1801**	**99.78**
mtkA	**Meta1_1730**	**Mext_1799**	**100**
mtkB	**Meta1_1731**	**Mext_1800**	**100**
mcl	**Meta1_1733**	**Mext_1802**	**100**
glyA	**Meta1_3384**	**Mext_3171**	**100**
gck	**Meta1_2944**	**Mext_2747**	**98.86**
eno	**Meta1_2984**	**Mext_2784**	**100**
mdh	**Meta1_1537**	**Mext_1643**	**100**
qscR	**Meta1_0756**	**Mext_0978**	**99.7**
phaA	**Meta1_3700**	**Mext_3469**	**100**
phaB	**Meta1_3701**	**Mext_3470**	**99.59**
phaR	**Meta1_3699**	**Mext_3468**	**99.01**
croR	**Meta1_3675**	**Mext_3444**	**100**
pccA	**Meta1_3203**	**Mext_2996**	**99.55**
pccB	**Meta1_0172**	**Mext_0282**	**99.8**
ccr	**Meta1_0178**	**Mext_0288**	**99.77**
meaA	**Meta1_0180**	**Mext_0290**	**99.56**
meaB	**Meta1_0188**	**Mext_0298**	**99.7**
meaC	**Meta1_4153**	**Mext_3781**	**99.14**
meaD	**Meta1_1432**	**Mext_1541**	**99.53**
ibd2	**Meta1_2223**	**Mext_2228**	**99.82**
mcmA	**Meta1_5251**	**Mext_4797**	**99.72**
mcmB	**Meta1_2390**	**Mext_2388**	**97.02**
sdhA	**Meta1_3861**	**Mext_3602**	**99.5**
sdhB	**Meta1_3863**	**Mext_3604**	**100**
sdhC	**Meta1_3859**	**Mext_3600**	**98.5**
sdhD	**Meta1_3860**	**Mext_3601**	**99.28**

fumC	**Meta1_1338**	**Mext_1449**	**99.81**

Supplementary Table S1.2: Mean FSC (Forward Scatter) and and SSC (Side Scatter) of 50,000 cells of *M. extroquens* AM1 and *M extroquens* PA1 (grown in 3.5mM succinate) using a flow cytometer. FSC is an estimate for the relative size of the cell and SSC is an estimate for the granularity or the biomass/OD_{600} ratio of the cell. Values are reported as mean ± 95% confidence interval of the mean for three independent flow cytometer runs with 50,000 cells each.

Strain	Mean FSC	Mean SSC
M. extorquens AM1	797±23	5923±219
M. extorquens PA1	806±34	5422±321

***M. extorquens* PA1**

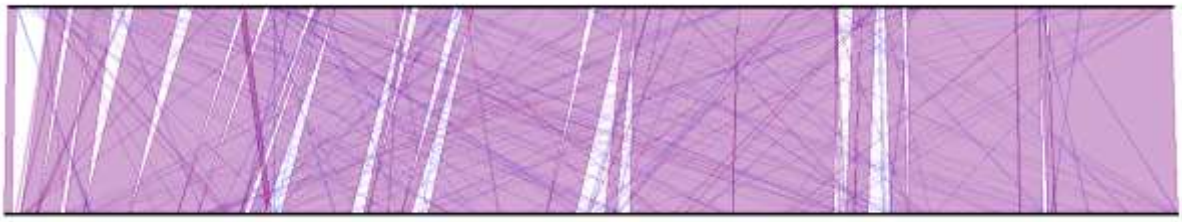

***M. extorquens* AM1**

Supplementary Figure S1.1: A line plot of strand conservation (in purple) and strand inversion (in blue) between the chromosome of *M. extroquens* PA1 (top) and the main chromosome of *M. extorquens* AM1 (bottom).

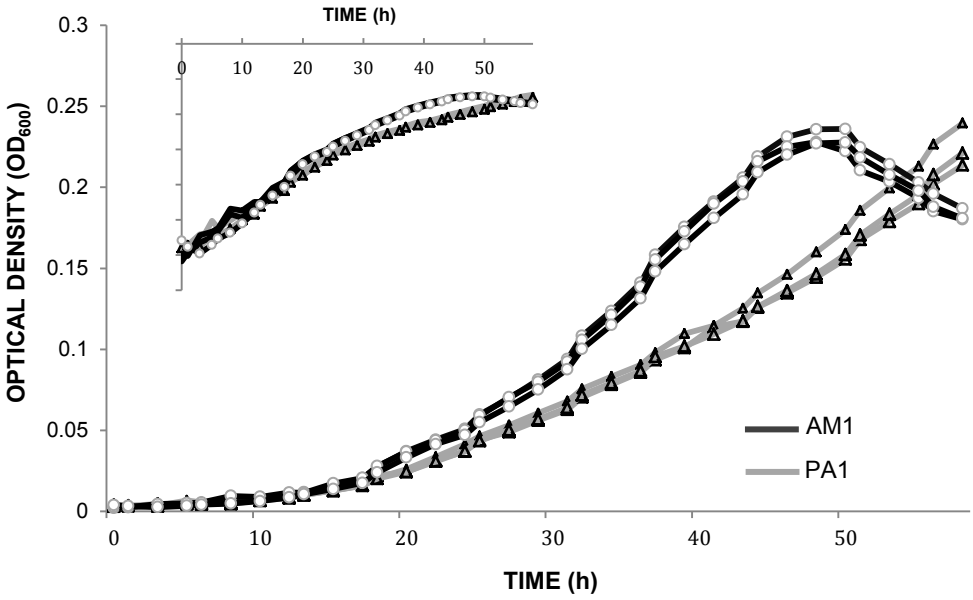

Supplementary Figure S1.2: Growth of three biological replicates of the Δ*cel* 'wild-type' strain of PA1 (gray) and the Δ*cel* 'wild-type' strain of AM1 (black) on nutrient broth. The inset shows the semi-log plot of the growth curve (s) of the Δ*cel* 'wild-type' strain of PA1 and the Δ*cel* 'wild-type' strain of AM1 on nutrient broth.

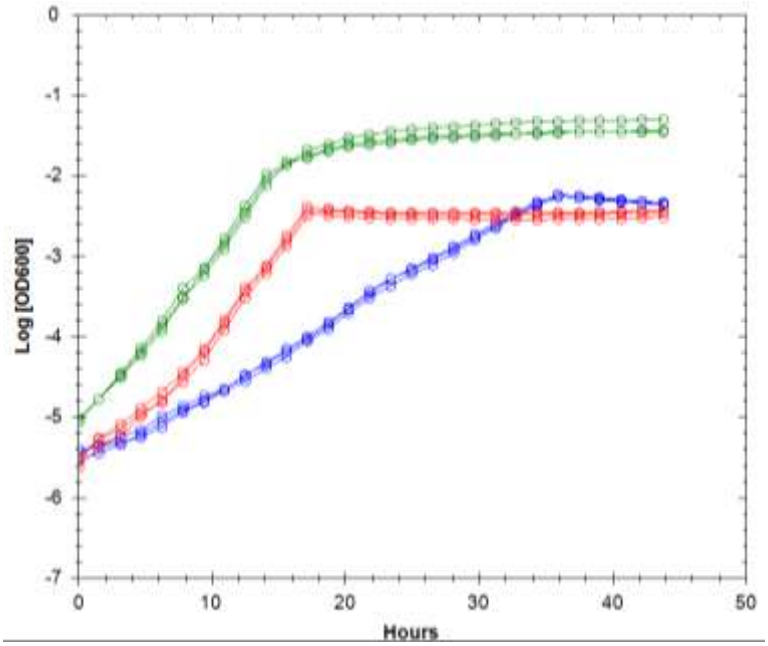

Supplementary Figure S1.3: Growth curves of three replicates of the Δ*cel* strain of PA1 (WT) (in green), the Δ*mxa* mutant of WT (in red), and the Δ*glyA* mutant of WT (in blue) on a combination of 7.5 mM methanol and 1.75 mM succinate as seen in the open-source growth curve fitter software (Clarity).

Supplementary Table S1.3: Mean growth rates (in h^{-1}) and the standard error of the mean growth rates (in h^{-1}) on single-carbon substrates M (15 mM methanol), MA (15 mM methylamine), F (15 mM formate) for *M. extorquens* strains AM1 and PA1 (both lacking the *cel* locus) as well as the following mutants in Δ*cel* PA1: Δ*fae,* Δ*mptG,* Δ*glyA,* Δ*mxa,* Δ*ftfL,* and Δ*hprA*.

Strains	M (h^{-1})	MA (h^{-1})	F (h^{-1})
AM1	0.191±0.001	0.214±0.002	0.126±0.002
PA1	0.210±0.001	0	0.150±0.004
Δ*fae*	0	0	0.163±0.004
Δ*ftfL*	0	0	0
Δ*glyA*	0	0	0
Δ*mptG*	0	0	0.161±0.002
Δ*mxa*	0	0	0.139±0.002
Δ*hprA*	0	0	0

Supplementary Table S1.4: Mean growth rates (in h^{-1}) (and the standard srror of the mean growth rates (in h^{-1}) on multi-carbon substrates S (3.5 mM succinate), P (5 mM pyruvate), E (7.5 mM ethanol) for *M. extorquens* strains AM1 and PA1 (both lacking the *cel* locus) as well as the following mutants in Δ*cel* PA1: Δ*fae,* Δ*mptG,* Δ*glyA,* Δ*mxa,* Δ*ftfL,* and Δ*hprA*

Strains	S (h^{-1})	P (h^{-1})	E (h^{-1})
AM1	0.202±0.001	0.141±0.001	0
PA1	0.213±0.002	0.192±0.002	0.158±0.001
Δ*fae*	0.212±0.001	0.178±0.002	0.166±0.001
Δ*ftfL*	0.217±0.001	0.184±0.003	0.158±0.001
Δ*glyA*	0.194±0.002	0	0
Δ*mptG*	0.184±0.002	0.144±0.003	0.155±0.001
Δ*mxa*	0.213±0.002	0.185±0.001	0
Δ*hprA*	0.203±0.001	0.192±0.001	0.160±0.001

Supplementary Table S1.5: Mean growth rates (in h^{-1}) and the standard error of the mean growth rates (in h^{-1}) on a joint single-carbon and multi-carbon substrate B (15 mM betaine) and a combination of single-carbon and multi-carbon substrates ½ M + ½ S (7.5 mM methanol and 1.75 mM succinate) for *M. extorquens* strains AM1 and PA1 (both lacking the *cel* locus) as well as the following mutants in Δ*cel* PA1: Δ*fae,* Δ*mptG,* Δ*glyA,* Δ*mxa,* Δ*ftfL,* and Δ*hprA*.

Strains	B (h^{-1})	½ M + ½ S (h^{-1})
AM1	0.160±0.001	0.207±0.001
PA1	0	0.248±0.001
Δ*fae*	0	0
Δ*ftfL*	0	0.141±0.001
Δ*glyA*	0	0.125±0.001
Δ*mptG*	0	0
Δ*mxa*	0	0.236±0.002
Δ*hprA*	0	0.184±0.001

Supplementary Table S1.6: Max OD_{600} and the standard error of the max OD_{600} on single-carbon substrates M (15 mM methanol), MA (15 mM methylamine), F (15 mM formate) for *M. extorquens* strains AM1 and PA1 (both lacking the *cel* locus) as well as the following mutants in Δ*cel* PA1: Δ*fae,* Δ*mptG,* Δ*glyA,* Δ*mxa,* Δ*ftfL,* and Δ*hprA*.

Max OD values <0.01 are reported as 0

Strains	M (h^{-1})	MA (h^{-1})	F (h^{-1})
AM1	0.165±0.009	0.227±0.005	0.046±0.001

PA1	0.288±0.02	0.021±0.002	0.069±0.0001
Δ*fae*	0	0	0.069±0.001
Δ*ftfL*	0	0	0
Δ*glyA*	0	0	0
Δ*mptG*	0	0	0.071±0.002
Δ*mxa*	0.012±0.0003	0	0.067±0.001
Δ*hprA*	0	0	0

Supplementary Table S1.7: Mean max OD_{600} and the standard error of the max OD_{600} on multi-carbon substrates S (3.5 mM succinate), P (5 mM pyruvate), E (7.5 mM ethanol) for *M. extorquens* strains AM1 and PA1(both lacking the *cel* locus) as well as the following mutants in Δ*cel* PA1: Δ*fae,* Δ*mptG,* Δ*glyA,* Δ*mxa,* Δ*ftfL,* and Δ*hprA*. **Max OD values <0.01 are reported as 0**

Strains	S (h^{-1})	P (h^{-1})	E (h^{-1})
AM1	0.162±0.002	0.188±0.002	0.012±0.001
PA1	0.182±0.003	0.231±0.002	0.252±0.003
Δ*fae*	0.189±0.001	0.232±0.0003	0.245±0.011
Δ*ftfL*	0.180±0.004	0.229±0.001	0.208±0.009
Δ*glyA*	0.178±0.006	0.048±0.0004	0
Δ*mptG*	0.194±0.001	0.230±0.001	0.259±0.008
Δ*mxa*	0.177±0.006	0.226±0.002	0.022±0.002
Δ*hprA*	0.190±0.002	0.233±0.002	0.202±0.015

Supplementary Table S1.8: Mean maxOD_{600} (Column 1) and the standard error of the Max OD_{600} (Column 2) on a joint single-carbon and multi-carbon substrate B (15 mM betaine) and a combination of single-carbon and multi-carbon substrates ½ M + ½ S (7.5 mM methanol and 1.75 mM succinate) for *M. extorquens* strains AM1 and PA1(both lacking the *cel* locus) as well as the following mutants in Δ*cel*PA1: Δ*fae,* Δ*mptG,* Δ*glyA,* Δ*mxa,* Δ*ftfL,* and Δ*hprA*. **Max OD values <0.01 are reported as 0**

Strains	B (h^{-1})	½ M + ½ S (h^{-1})
AM1	0.384±0.013	0.155±0.006
PA1	0	0.245±0.011
Δ*fae*	0	0
Δ*ftfL*	0	0.091±0.002
Δ*glyA*	0	0.103±0.001
Δ*mptG*	0	0
Δ*mxa*	0	0.087±0.002
Δ*hprA*	0	0.139±0.005

Supplementary Table S1.9: List of primers used for making null mutants in *M. extorquens* PA1

Primer	Primer Sequence	Primer Description
Δ*fae*_us_f	ATGGATGCATATGCTGCAGCTCGAGCGGC CGCCGACGTGTCCCAAACCGATG	Gibson forward linker with Not1 and 24 bp of pCM433 backbone at 5' end. Product size = 695 bp
Δ*fae*_us_r	GTCCAAGGAAGATCGAAGCCAGTCGCTG GA GGTCTCTCCCTGGATTCCTG	30 bp of ds region linker at 5'end. Product size = 695 bp
Δ*fae*_ds_f	TCCAGCGACTGGCTTCGATC	Product size = 424 bp
Δ*fae*_ds_r	GGTTAACACGCGTACGTAGGGCCCGCGGC CGC CAGCGAGAGCCAGCTTGATG	Gibson reverse linker with Not1 and 24 bp of pCM433 backbone at 5' end. Product size = 424 bp
Δ*ftfL*_us_f	GTC CCT ATG CTT CCG TGG TAG C	Product size = 617 bp
Δ*ftfL*_us_r	GGTTAACACGCGTACGTAGGGCCCGCGGC CGC CGC AGA ACG TGT GGG TGA AAC G	Gibson reverse linker with Not1 and 24 bp of pCM 433 backbone. Product size = 617 bp
Δ*ftfL*_ds_f	ATGGATGCATATGCTGCAGCTCGAGCGGC CGCCGA CAT GAC GCT GCA TCT CTC C	30 bp of us region linker at 5'end. Product size = 451 bp
Δ*ftfL*_ds_r	TTCCGTTCGCTACCACGGAAGCATAGGGA CCCT GAC TTG GGC GGA TCG TTG	Gibson forward linker with Not1 and 24 bp of pCM433 backbone at 5' end. Product size = 451 bp
Δ*mptG*_us_f	ATGGATGCATATGCTGCAGCTCGAGCGGC CGCGAT CTC GGC GAT CAG CTC ACC	Gibson forward linker with Not1 and 24 bp of pCM433 backbone at 5' end. Product size =859 bp
Δ*mptG*_us_r	GCC GTT GAG ATC GAG GAA GCC	Product size = 859 bp
Δ*mptG*_ds_f	CTGCATTTCGGCTTCCTCGATCTCAACGGC CTC GCA GAA GGA GGC GGA	Gibson forward linker from 2049230 to 2049259 on PA1 genome. Product size = 723 bp
Δ*mptG*_ds_r	GGTTAACACGCGTACGTAGGGCCCGCGGC CGCGGT GAA GGC GAT CTT CGA GAC G	Gibson reverse linker with Not1 and 24 bp of pCM433 backbone at 5' end. Product size 723 bp
Δ*glyA*_us_f	GAT CAG CTC GAT CTC GTG CTG CTG C	Product size = 497 bp
Δ*glyA*_us_r	GGTTAACACGCGTACGTAGGGCCCGCGGC CGCTGA CGC TTC CGA TCG CAC GTG	Gibson Reverse Linker with Not1 and 24 bp of pCM433 backbone at 5'end. Product size = 497 bp
Δ*glyA*-ds_f	ATGGATGCATATGCTGCAGCTCGAGCGGC CGCCGC GCA ACC TTC AGG TGA AGG ATG G	Gibson forward linker with Not1 and 24 bp of pCM 433 backbone at 5'end. Product size = 526 bp
Δ*glyA*_ds_r	GGT ACC GAC AAC CAC CTG ATG CTG G	Product size = 526 bp
Δ*mxa*_us_f	ATGGATGCATATGCTGCAGCTCGAGCGGC CGCGAT CGA GGT GCA ACT CGG CAG	Gibson forward linker with Not1 and 24 bp of pCM433 backbone at 5' end. Product size = 701bp
Δ*mxa*_us_r	TGG TCC AGA TCG CGG TCA AC	Product size = 701bp
Δ*mxa*_ds_f	CGTTGCGCCGGTTGACCGCGATCTGGACC ATCG TGA TGC TGA ACG CGC AC	Gibson linker with 4606355 through 4606384 on PA1 genome. Product size = 496bp
Δ*mxa*_ds_r	GGTTAACACGCGTACGTAGGGCCCGCGGC CGCAAC TCG ATG TCG AAG GCG TGC	Gibson reverse linker with Not1 and 24 bp of pCM433 backbone at 5' end. Product size = 496bp
Δ*hprA*_us_f	ATGGATGCATATGCTGCAGCTCGAGCGGC CGCCTC ATC GAC AAC GGC GTG AAG G	Gibson forward linker with Not1 and 24 bp of pCM433 backbone at 5' end. Product size = 344bp
Δ*hprA*_us_r	GGGCAATCGTGTCGCTCAC	Product size = 344bp
Δ*hprA*_ds_f	GCAGGGGTTTTGTGAGCGACACGATTGCC CCTCGTGGACAACGTCGAAGC	30 bp from 2016078 to 2016107 on PA1 genome at 5' end. Product size = 447bp
Δ*hprA*_ds_r	GGTTAACACGCGTACGTAGGGCCCGCGGC CGCTCT TCA CCG CCT CGA ACA CC	Gibson reverse linker with Not1 and 24 bp of pCM433 backbone at 5' end. Product size = 447bp
Δ*fhc*_us_f	ATGGATGCATATGCTGCAGCTCGAGCGGC CGCCCG AGA TGC TTG AGG CTC TG	Gibson forward linker with Not1 and 24 bp of pCM433 backbone at 5' end. Product size = 480bp
Δ*fhc*_us_r	GCT CTC GCA AGG CTC GAT CC	Product size = 480bp
Δ*fhc*_ds_f	CCCTCGACCCGGATCGAGCCTTGCGAGAG CTCC GGG TCG TAG ACG ATG AC	30 bp from 2044769 to 2044798 on PA1 genome at 5' end. Product size = 569bp
Δ*fhc*_ds_r	GGTTAACACGCGTACGTAGGGCCCGCGGC CGCTGA GGA AGC ATG GCA GCC TG	Gibson reverse linker with Not1 and 24 bp of pCM433 backbone at 5' end. Product size =569bp

Appendix 2

Supplementary Material for Chapter 3

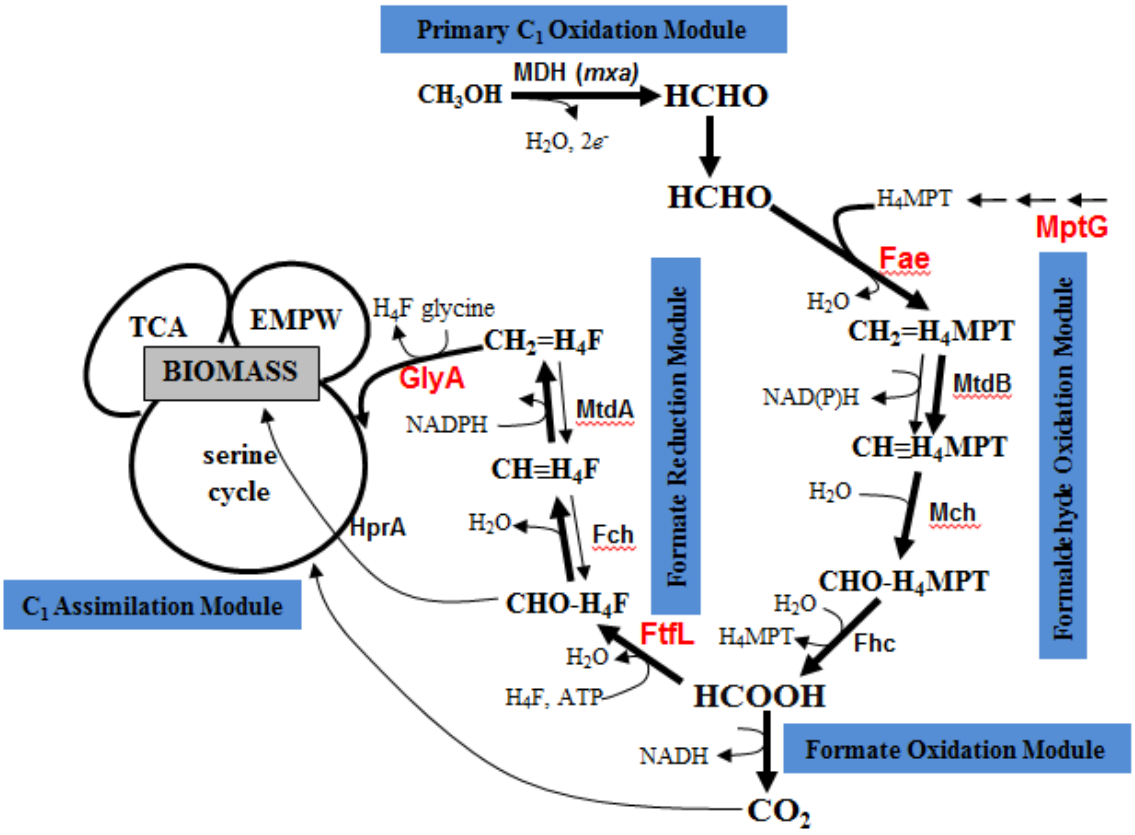

Supplementary Figure S2.1: A metabolic map illustrating metabolic modules that are involved in methanol growth in *M. extorquens* PA1. Methanol dehydrogenase serves as the primary C_1 oxidation module that oxidizes methanol to formaldehyde. Formaldehyde is further oxidized to formate by a H_4MPT mediated pathway which acts as the formaldehyde oxidation module. Formate is the branch point for metabolism - a part gets oxidized to CO_2 by formate dehydrogenases and the rest gets reduced and assimilated via a H_4F mediated pathway and serine cycle. Genes highlighted in red, representative of a particular module, were deleted to test the role of the specific module in methylamine growth via the *N*-methylglutamate pathway.

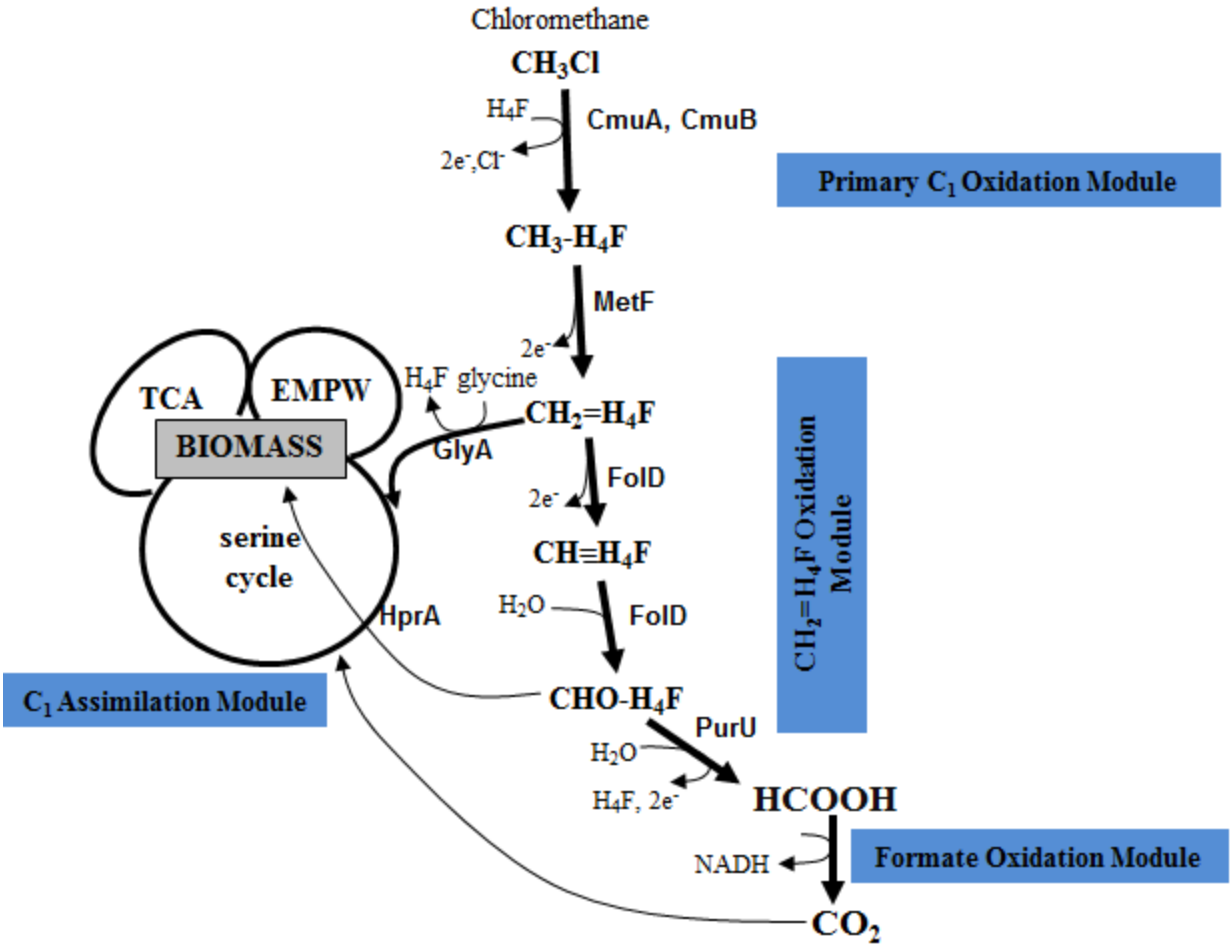

Supplementary Figure S2.2: A metabolic map illustrating the various metabolic modules that are involved in chloromethane growth in *M. extorquens* CM4. The primary C_1 oxidation module consists of CmuA and CmuB- that catalyze dehalogenation of chloromethane and subsequent methyl transfer to tetrahydrofolate (H_4F) to form methyl tetrahydrofolate (CH_3-H_4F) - and MetF that catalyzes the reduction of CH_3-H_4F to methylene tetrahydrofolate (CH_2=H_4F). CH_2=H_4F is the branch point of metabolism –a part gets oxidized by methylene tetrahydrofolate reductase (*folD*) and formyl tetrahydrofolate hydrolase (*purU*) to formate, which subsequent gets oxidized to CO_2 by a panel of formate dehydrogenases, and the rest gets assimilated via the serine cycle. ***metF, folD, and purU* are absent in *M. extorquens* PA1

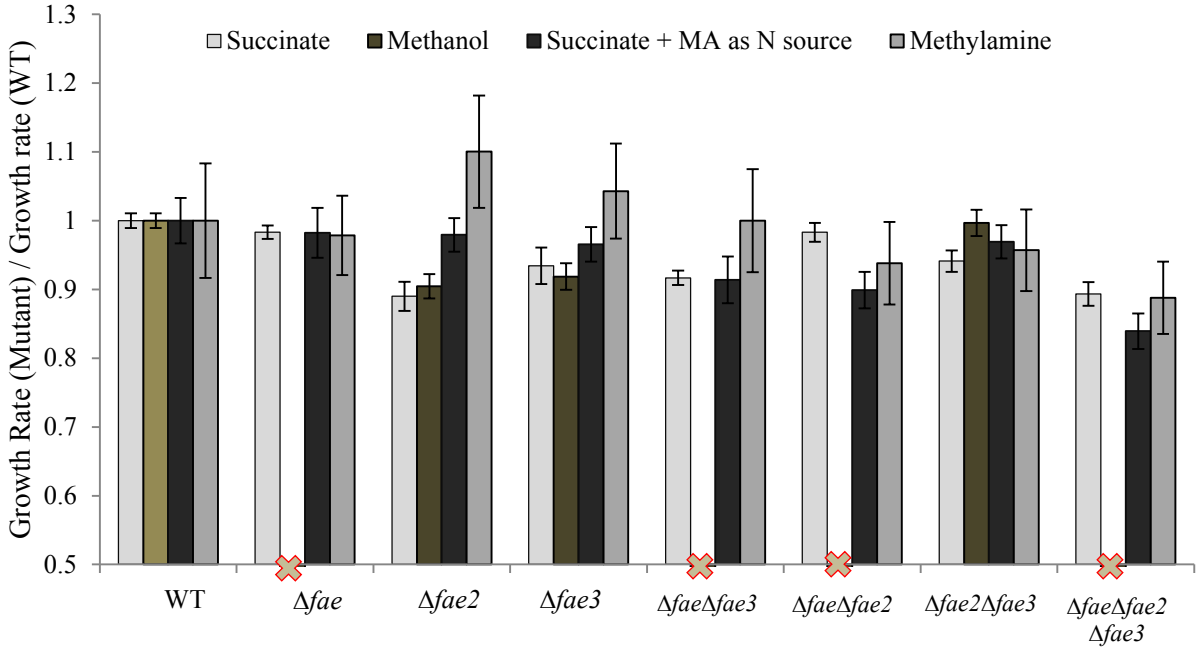

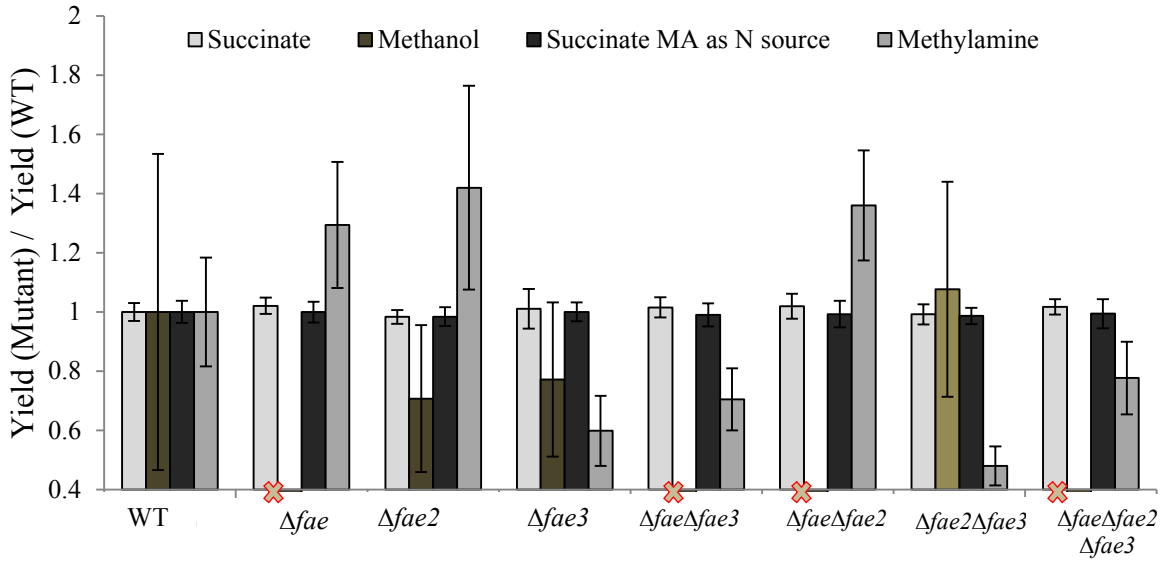

Supplementary Figure S2.3: A) Ratio of growth rates, of various knockout mutants versus the Δ*cel* 'wildtype' strain of PA1 and, in 3.5 mM succinate (white), 15mM methanol (light brown),nitrogen free media with 3.5 mM succinate and 7.66 mM methylamine (dark gray) and 15mM methylamine (blue) **B)** Ratio of yield (measured as the

maximum OD_{600} value during growth) of various knockout mutants versus Δ*cel* 'wildtype' strain of PA1, in 3.5 mM succinate (white), 15mM methanol (light brown), nitrogen free media with 3.5 mM succinate and 7.66 mM (**Supplementary Figure 2.3 Continued**) methylamine (dark gray) and 15mM methylamine (blue). Error bars represent the 95% C.I. of the average ratio of three biological replicates grown in each condition. A X indicates that the mutants did not grow in methanol. **NOTE: The y-axis doesn't start at 0.0 but at 0.5 (for growth rate ratios) and 0.4 (for yield ratios). This was done to highlight subtle changes in growth/yield for these mutants**

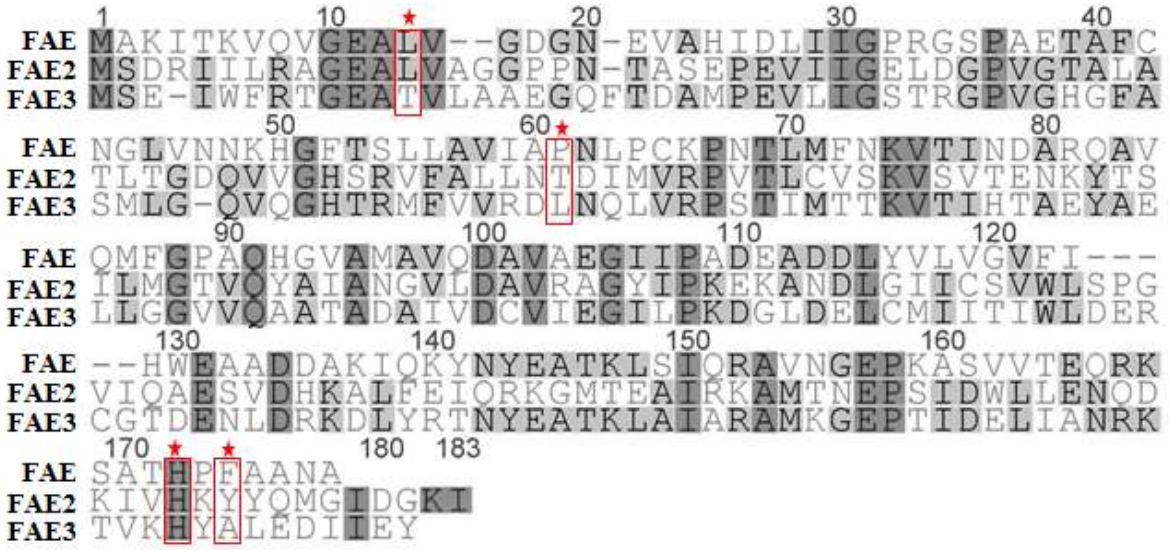

Supplementary Figure S2.4: Amino acid alignment of FAE, FAE2 and FAE3 from *M. extroquens* PA1 (using MUSCLE: https://www.ebi.ac.uk/Tools/msa/muscle/ with standard settings and 150 iterations). The highlighted residues in FAE interact with methyl groups present in tetrahydromethanopterin (H_4MPT), absent in H_4F. These interactions are responsible for the specificity of FAE to H_4MPT. Two of these residues are identical and one residue (Y173) has similar properties in FAE2. Only one residue is identical in FAE3.

Supplementary Table S2.1: Growth rates of the Δ*cel* 'wildtype' strain of PA1 and the Δ*mptG* mutant (in the WT background) in 3.5 mM succinate with either 7.66 mM NH_4^+ as the nitrogen source or 7.66 mM methylamine as the nitrogen source. S.E.M. represents the standard error of the mean growth rate for three biological replicates in each condition

Strain	Nitrogen Source	Mean Growth Rate (h^{-1})	S.E.M. (h^{-1})
WT	NH_4^+	0.213	0.002
Δ*mptG*	NH_4^+	0.184	0.002
WT	Methylamine	0.188	0.001
Δ*mptG*	Methylamine	0.148	0.002

Supplementary Table S2.2: Growth rates and maximum OD_{600} of the Δ*cel* 'wildtype' strain of PA1 and single-, double-, triple-knockout mutants (in the WT background) lacking Δ*fae, Δfae2, and/or Δfae3* in 15mM methylamine

Strain	Mean Growth Rate (h^{-1}) ± 95%C.I. (h^{-1})	Average Max. OD_{600} ± 95% C.I.
WT	0.0422±0.0018	0.712±0.071
Δ*fae*	0.0407±0.0004	1.044±0058
Δ*fae* 2	0.0476±0.0015	1.165±0.146
Δ*fae* 3	0.0427±0.0011	0.413±0.0.49
Δ*fae* -Δ*fae2*	0.0386±0.0008	1.003±0.033
Δ*fae* -Δ*fae3*	0.0406±0.0006	0.558±0.021

Δ*fae2*-Δ*fae3*	0.0409±0.0015	0.357±0.011
Δ*fae* -Δ*fae2*-Δ*fae3*	0.0375±0.0003	0.555±0.040

Supplementary Table S2.3: List of primers used to construct knockout mutants in the *N*-methylglutamate pathway as well as FAE-homologs in this study

Primer	Primer Sequence	Primer Description
Δfae2_us_f	ATGGATGCATATGCTGCAGCTCGAGCGGCCGC TCTGCATCAGGTCGTGCAGG	Gibson forward linker with Not1 and 24 bp of pCM433 backbone at 5' end. Product size = 311 bp
Δfae2_us_r	CTTTTCGACACTCAAACGCATCGAAGCGCGAG GATGATGCGGTCGCTCATGG	30 bp of ds region linker at 5'end. Product size = 311 bp
Δfae2_ds_f	CGCGCTTCGATGCGTTTGAG	Product size = 412 bp
Δfae2_ds_r	GGTTAACACGCGTACGTAGGGCCCGCGGCCGC CGACACCTCGTCGTTGCTCAAG	Gibson reverse linker with Not1 and 24 bp of pCM433 backbone at 5' end. Product size = 412 bp
Δfae3_us_f	GCGGAACCAGATCTCGGACATG	Product size = 252 bp
Δfae3_us_r	GGTTAACACGCGTACGTAGGGCCCGCGGCCGC TTCCCTCGCCTGATCCACTG	Gibson reverse linker with Not1 and 24 bp of pCM 433 backbone at 5' end. Product size = 252 bp
Δfae3_ds_f	ATGGATGCATATGCTGCAGCTCGAGCGGCCGC CGATGGTCACCCTTCAGGTG	30 bp of us region linker at 5'end. Product size = 420 bp
Δfae3_ds_r	ATGACCGACATGTCCGAGATCTGGTTCCGCGCC TCACGCGAGAAGACTAC	Gibson forward linker with Not1 and 24 bp of pCM433 backbone at 5' end. Product size = 420 bp
Δmgs1,2,3_us_f	ATGGATGCATATGCTGCAGCTCGAGCGGCCGC GGCAATGGAGGCGAATCTCG	Gibson forward linker with Not1 and 24 bp of pCM433 backbone at 5'end. Product size =433 bp
Δmgs1,2,3_us_r	TCGCGGCCCTCGTGCCAATCGTCATAGGCGCGT TCGATCACTGTCGCGAG	30 bp of ds region linker at 5'end. Product size = 433 bp
Δmgs1,2,3_ds_f	CGCCTATGACGATTGGCACG	Product size = 441 bp
Δmgs1,2,3_ds_r	GGTTAACACGCGTACGTAGGGCCCGCGGCCGC CAGATCGGTGTAGGACACGAGG	Gibson reverse linker with Not1 and 24 bp of pCM 433 backbone at 5' end. Product size = 441 bp
Δgmas_us_f	ATGGATGCATATGCTGCAGCTCGAGCGGCCGC TCGCAGTGATGACGCTGGAG	Gibson forward linker with Not1 and 24 bp of pCM433 backbone at 5'end. Product size =492 bp
Δgmas_us_r	CGCTTGACGCCCTCCACCGTGTGCCCGTCGGTG TACATGTTTCCAGGGGAGCTGGATCAG	30 bp of ds region linker at 5'end. Product size = 492 bp
Δgmas_ds_f	ACATGTACACCGACGGGCAC	Product size = 435 bp
Δgmas_ds_r	GGTTAACACGCGTACGTAGGGCCCGCGGCCGC TGGCCACGATTAGGGCGAAG	Gibson reverse linker with Not1 and 24 bp of pCM 433 backbone at 5' end. Product size = 435 bp
Δmgd1,2,3,4_us_f	GACGATCACCACGTCGTAGG	Product size = 493 bp
Δmgd1,2,3,4_us_r	GGTTAACACGCGTACGTAGGGCCCGCGGCCGC TAGAGTTCGCAGCCCGACAG	Gibson reverse linker with Not1 and 24 bp of pCM 433 backbone at 5'end. Product size = 493 bp
Δmgd1,2,3,4_ds_f	ATGGATGCATATGCTGCAGCTCGAGCGGCCGC CTCGACTCGTACGCGCATTG	30 bp of us region linker at 5'end. Product size = 607 bp
Δmgd1,2,3,4_ds_r	CCGCAGGAGGCCTACGACGTGGTGATCGTCTG ACGAGCATCGCCCATCTC	Gibson forward linker with Not1 and 24 bp of pCM433 backbone at 5' end. Product size = 607 bp

Appendix 3

Supplementary Material for Chapter 5

Supplementary Table S3.1: A list of mutations in CM1054 (A2), CM2986 (E1), and CM3014 (E2) uncovered by Illumina sequencing and alignment to the *M. extroquens* AM1 reference genome. Each of these mutations were verified by Sanger sequencing. Mutations highlighted in orange are unique to E2 relative to A2.

CM1054 (A2)	CM 2986 (E1)	CM3014 (E2)
G420551C (R73P) Meta_0397	G2837255A(Q446*) *kefB*	G420551C (R73P) Meta1_0397
2308994 (+T) Meta1_2237	Deletion (28679 bp-30272 bp) Meta1_2751-Meta1_2783	G1617391A(W173*) Meta1_1544
G3724230A(intergenic) Meta1_3582/Meta1_3583	New Junction Position 162893 (Meta1_1554) and Position 1616982 (Meta1_1544)	2308994 (+T) Meta1_2237
A4125088G (intergenic) Meta1_4038/*rffH*		G3724230A(intergenic) Meta1_3582/Meta1_3583
A11165G(R31R) Meta2_1054		A4125088G (intergenic) Meta1_4038/*rffH*
T144186G(Q24H) Meta2_0154		A11165G(R31R) Meta2_1054
C5903G (intergenic) p2meta_006/p2meta_007		T144186G(Q24H) Meta2_0154
Deletion (28679bp -30281 bp) (Meta1_2751 -Meta1_2783)		C5903G (intergenic) p2meta_006/p2meta_007
Deletion (61658bp -61678bp) (Meta1_3749-Meta1_tRNA33)		Deletion (28679bp -30281bp) (Meta1_2751 -Meta1_2783)
Deletion (~0.6Mb Meta2_0933 – Meta1_0277)		Deletion (61658bp-61678bp) (Meta1_3749-Meta1_tRNA33)
ISmex4 insertion (Meta1_2101/Meta1_2102)		Deletion (~0.6Mb Meta2_0933 – Meta1_0277)
ISmex4 insertion *glnE*		ISmex4 insertion (Meta1_2101/Meta1_2102)
ISmex4 insertion (Meta1_4102/*proV)*		ISmex4 insertion *glnE*

ISmex4 insertion *ureA/icuA*		ISmex4 insertion (Meta1_4102/*proV)*
		ISmex4 insertion *ureA*/*icuA*

Supplementary Table S3.2: *N*-methylglutamate dehydrogenase (NMGDH) activity (measured as nmol formaldehyde production/ mg protein. min) in CM2986 (E1), CM4149 (a Δ*mgd* mutant of E1) and CM4189 (a Δ*mgd- Δmgd'* mutant of E1). The values represent the mean ±95% CI of the NMGDH activity of three biological replicates

Strain	NMGDH Activity (nmolHCHO/mg protein.min)
CM2986	76.2 ± 8.4
CM4149	19.9 ± 5.1
CM4189	5.5 ± 2.0

Supplementary Table S33: Growth rate (h^{-1}) of CM2720 (WT), CM2986 (E1) and CM3014 (E2) on 3.5 mM succinate with 7.66 mM ammonia as a nitrogen source and in nitrogen-free hypho with 35 mM succinate as the carbon source and 7.66 mM methylamine as the nitrogen source. The values indicate the mean of three replicate growth measurements and the 95% CI of the mean

Strain	**k(**succinate, ammonia**)**	**k(**succinate, methylamine**)**	**Ratio** **k(**succinate, methylamine**)** **k(**succinate, ammonia**)**
CM2720	0.207±0.001	0.220±0.001	1.059±0.013

CM2986	0.251±0.004	0.222±0.001	0.884±0.021
CM3014	0.271±0.001	0.245±0.001	0.906±0.011

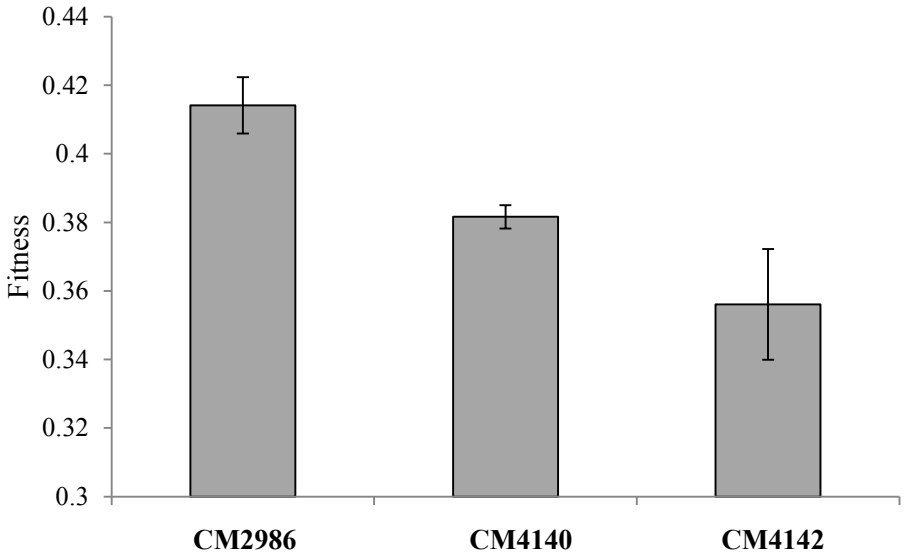

Supplementary Figure S3.1: Competitive fitness of CM2986 (E1), CM4140 (Δ*kefB* E1) and CM4142 ($kefB^{Ancestral}$ E1) on 15 mM methylamine hydrochloride. The error bars indicate the 95% CI of the mean fitness value of three replicate competition assays.

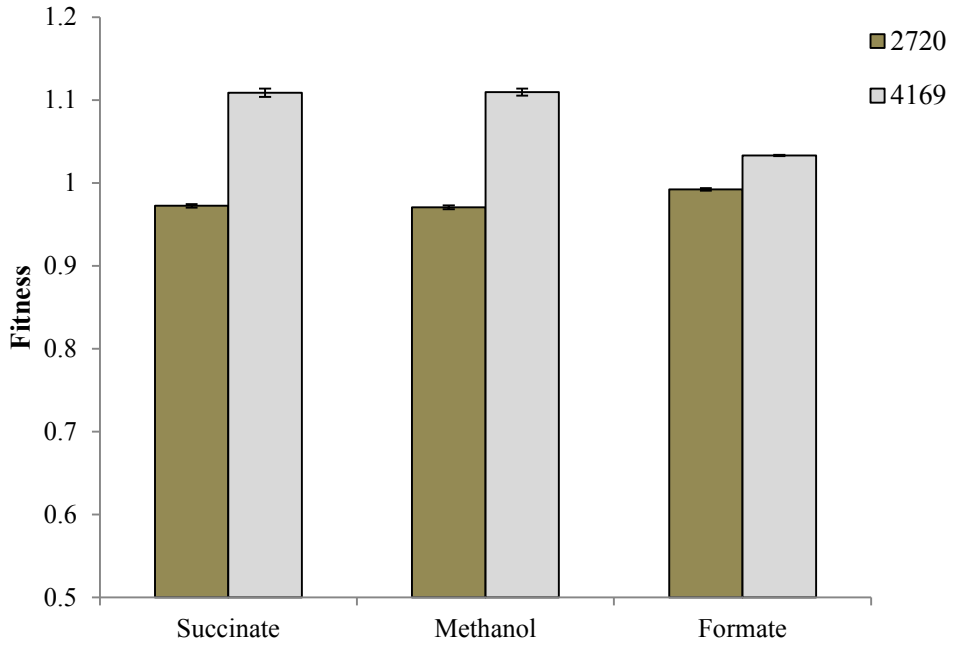

Supplementary Figure S3.2: Competitive fitness of CM2720 (WT) CM4169 (*kefB*^{Evolved} in WT) relative to the fluorescent mCherry WT(CM3120) on 3.5mm succinate, 15mM methanol and 15mM sodium formate. The error bars indicate the 95% CI of the mean fitness value of three replicate competition assays.